

NAVAL POSTGRADUATE SCHOOL

Monterey, California



19980210 128

THESIS

**COMPARING TIME-BASED AND HYBRID
TIME-BASED/FREQUENCY BASED
MULTI-PLATFORM GEO-LOCATION SYSTEMS**

by
Andrew D. Stewart

September, 1997

Thesis Advisor:
Second Reader:

Arnold H. Buss
Carl R. Jones

Approved for public release; distribution is unlimited.

REPORT DOCUMENTATION PAGE

Form Approved
OMB No. 0704-0188

Public reporting burden for this collection of information is estimated to average 1 hour per response, including the time for reviewing instruction, searching existing data sources, gathering and maintaining the data needed, and completing and reviewing the collection of information. Send comments regarding this burden estimate or any other aspect of this collection of information, including suggestions for reducing this burden, to Washington headquarters Services, Directorate for Information Operations and Reports, 1215 Jefferson Davis Highway, Suite 1204, Arlington, VA 22202-4302, and to the Office of Management and Budget, Paperwork Reduction Project (0704-0188) Washington DC 20503.

1. AGENCY USE ONLY (Leave blank)		2. REPORT DATE September 1997	3. REPORT TYPE AND DATES COVERED Master's Thesis
4. TITLE AND SUBTITLE COMPARING TIME-BASED AND HYBRID TIME-BASED/FREQUENCY BASED MULTI-PLATFORM GEO-LOCATION SYSTEMS		5. FUNDING NUMBERS	
6. AUTHOR(S) Stewart, Andrew D.			
7. PERFORMING ORGANIZATION NAME(S) AND ADDRESS(ES) Naval Postgraduate School Monterey, CA 93943-5000		8. PERFORMING ORGANIZATION REPORT NUMBER	
9. SPONSORING / MONITORING AGENCY NAME(S) AND ADDRESS(ES)		10. SPONSORING / MONITORING AGENCY REPORT NUMBER	
11. SUPPLEMENTARY NOTES The views expressed in this thesis are those of the author and do not reflect the official policy or position of the Department of Defense or the U.S. Government.			
12a. DISTRIBUTION / AVAILABILITY STATEMENT Approved for public release; distribution unlimited.		12b. DISTRIBUTION CODE	
13. ABSTRACT (maximum 200 words) While time difference of arrival (TDOA) information is sufficient to passively solve for the location of a radio frequency transmitter, frequency difference of arrival (FDOA) information may be added to the TDOA information to solve for both the position and velocity of the transmitter. This analysis implements a stochastic discrete event simulation, written in Java, to compare and stochastically describe, under a variety of conditions, the differences between a mixed TDOA/FDOA Multi-platform Global Positioning System (GPS) Assisted Geo-location System and that of the same system which uses TDOA information only. The presented analysis compares both solution types for two- and three-dimensional fixes across: various measurement error distributions and correlation values, sensor network geometry, and sensor platform selection. The simulation results show first order stochastic dominance in the accuracy of the TDOA/FDOA solution in the two-dimensional scenarios. In the three-dimensional scenarios, sensor network to target geometry dominates both solutions' accuracy. While solution accuracy is used as the primary method of effectiveness, the distribution of each solution's uncertainty is also compared. Finally, the simulation itself remains a useful tool for further system design experimentation, performance indication, and as a means to describe system capabilities to the war fighter.			
14. SUBJECT TERMS Time Difference of Arrival, Frequency Difference of Arrival, Discrete Event Simulation, Square Root Information Filter, Java, Global Positioning System, Geo-location, TDOA, FDOA, GPS, SRIF		15. NUMBER OF PAGES 114	16. PRICE CODE
17. SECURITY CLASSIFICATION OF REPORT Unclassified	18. SECURITY CLASSIFICATION OF THIS PAGE Unclassified	19. SECURITY CLASSIFICATION OF ABSTRACT Unclassified	20. LIMITATION OF ABSTRACT UL

NSN 7540-01-280-5500

Standard Form 298 (Rev. 2-89)
Prescribed by ANSI Std. Z39-18

Approved for public release; distribution is unlimited

**COMPARING TIME-BASED AND HYBRID
TIME-BASED/FREQUENCY BASED
MULTI-PLATFORM GEO-LOCATION SYSTEMS**

Andrew D. Stewart
Lieutenant, United States Navy
B.S., United States Naval Academy, 1991

Submitted in partial fulfillment of the
requirements for the degree of

MASTER OF SCIENCE IN OPERATIONS RESEARCH

from the

NAVAL POSTGRADUATE SCHOOL
September 1997

Author:



Andrew D. Stewart

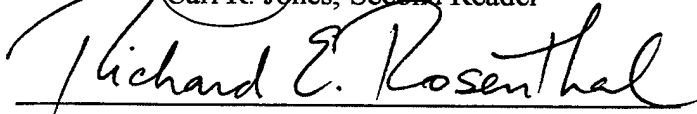
Approved by:



Arnold H. Buss, Thesis Advisor



Carl R. Jones, Second Reader



Richard E. Rosenthal, Chairman
Department of Operations Research

ABSTRACT

While time difference of arrival (TDOA) information is sufficient to passively solve for the location of a radio frequency transmitter, frequency difference of arrival (FDOA) information may be added to the TDOA information to solve for both the position and velocity of the transmitter. This analysis implements a stochastic discrete event simulation, written in Java, to compare and stochastically describe, under a variety of conditions, the differences between a mixed TDOA/FDOA Multi-platform Global Positioning System (GPS) Assisted Geo-location System and that of the same system which uses TDOA information only. The presented analysis compares both solution types for two- and three-dimensional fixes across: various measurement error distributions and correlation values, sensor network geometry, and sensor platform selection. The simulation results show first order stochastic dominance in the accuracy of the TDOA/FDOA solution in the two-dimensional scenarios. In the three-dimensional scenarios, sensor network to target geometry dominates both solutions' accuracy. While solution accuracy is used as the primary method of effectiveness, the distribution of each solution's uncertainty is also compared. Finally, the simulation itself remains a useful tool for further system design experimentation, performance indication, and as a means to describe system capabilities to the war fighter.

THESIS DISCLAIMER

The reader is cautioned that computer programs developed in this research may not have been exercised for all cases of interest. While every effort has been made, within the time available, to ensure that the programs are free of computational and logic errors, they cannot be considered validated. Any application of these programs without additional verification is at the risk of the user.

TABLE OF CONTENTS

I.	INTRODUCTION	1
	A. BACKGROUND	1
	B. PURPOSE.....	4
	C. ORGANIZATION	5
II.	ARL:UT SYSTEM OVERVIEW	7
III.	TDOA AND FDOA MEASUREMENTS.....	9
	A. BACKGROUND AND PURPOSE.....	9
	B. BASIC MODEL AND THE GENERALIZED CROSS CORRELATION	10
	C. COMPLEX AMBIGUITY FUNCTION	11
	D. CYCLOSTATIONARY DETERMINATION	13
	E. IMPLICATIONS OF SIGNAL PROCESSING TO GEOLOCATION.....	15
IV.	EMITTER GEOLOCATION.....	17
	A. BACKGROUND	17
	B. DIRECT GEOLOCATION SOLUTION	19
	C. LINEARIZED LEAST SQUARES APPROACH.....	22
V.	JAVA-BASED STOCHASTIC TDOA AND FDOA SIMULATION (JBSTAFSIM)	27
	A. BACKGROUND	27
	B. DISCRETE EVENT SIMULATION IN JBSTAFSIM.....	27
	C. MODEL ASSUMPTIONS	29
	D. MODEL DATA PROCESSING.....	36
	E. STATISTICAL RESULT ESTIMATION AND CALCULATIONS.....	38
	F. MODEL INPUT AND OUTPUT	39
VI.	JBSTAFSIM AND THE WORLD WIDE WEB	41
VII.	SIMULATION ANALYSIS.....	45
	A. BACKGROUND	45
	B. TWO DIMENSIONAL GEO-LOCATION SCENARIO RESULTS.....	45
	C. THREE DIMENSIONAL GEO-LOCATION SCENARIO RESULTS	59
VIII.	CONCLUSIONS AND RECOMMENDATIONS.....	69
	A. CONCLUSIONS	69
	B. RECOMMENDATIONS.....	71
APPENDIX A.	SEQUENTIAL SQUARE ROOT DATA PROCESSING ALGORITHM AND THEORY	75

A. CONTEXT OF THE PROBLEM AND REVIEW OF LEAST SQUARES [REF. 16, 14-16].....	75
B. A PRIORI INFORMATION [REF. 16, 16-17].....	78
C. A PRIORI INFORMATION AS ADDITIONAL OBSERVATIONS [REF. 16, 17-18].....	79
D. HOUSEHOLDER ORTHOGONAL TRANSFORMATIONS [REF. 16, 57-62]	79
E. THE SRIF DATA PROCESSING ALGORITHM [REF. 16, 69-72].....	83
F. WHITENING OBSERVATION ERRORS [REF. 16, 47-49]	85
APPENDIX B. MIXED TDOA/FDOA SCALING	87
APPENDIX C. RELATIVE PRECISON	93
LIST OF REFERENCES.....	95
INITIAL DISTRIBUTION LIST	97

ACKNOWLEDGEMENT

The author would like to acknowledge the help and support of the members of the ARL:UT project team for their time and support. In particular, most profound thanks to Dr. Brian Tolman for his patient guidance and mentoring in numerical computations and the TDOA/FDOA solution formulation. His work and notes permeate this thesis along with Bierman's work to which he introduced me. Also, thanks to Mark Leach, Barbara Kozel, Lisa Julianelli, Petre Rusu, Miguel Cardoza, David Feurstein, Cary Logan, and Anabelle Colestock for numerous hours of tutoring, encouragement, and taking time out of their schedules to provide the resources necessary to produce this thesis.

In addition, many thanks to Rosemary Wenchel and LT Kevin Steck whose sponsorship made all of this happen.

Of course, many profound thanks to Commander Gus K. Lott whose guidance, continuous availability, and interest were crucial to the production of this thesis.

I am also greatly indebted to my advisors, Arnold H. Buss and Carl R. Jones. Their guidance in all aspects of this thesis kept me within the proper bounds, ensured I produced something of which I would be proud, and forged my analytic and modeling capabilities beyond the bounds I thought possible.

Finally, I am deeply grateful to my family. To my parents-in-law, Bryan and Luise Gray, thank you for your loving support and the gifts of your presence and time when we all most needed it. For my Mother and Father, Don and Anne Stewart, thank you for a lifetime of encouragement, guidance, and help, I am proud to be your son. To Charlie and Wil, thanks for taking me away from the computer when I needed some play time. Lastly and most importantly, to my wife Katharine—this is as much your achievement as it is mine. Without your infinite love, patience and support, none of this would have been possible. As such, you worked harder and bore more burdens than could ever be expected by anyone. Thank you.

EXECUTIVE SUMMARY

The passive location of both hostile and friendly electromagnetic emitters has been an important capability for the war-fighter, for law enforcement, and in search and rescue operations. The characteristics of an emitted signal once received by several sensors in an operating environment can be exploited to passively locate an emitter. Two of the characteristics that can be measured by separate receivers of such a signal are: (1) the differences in Doppler shifts (if any) in the signal's frequency and (2) the difference in the time that the signal arrived at the sensors. These measurements are known as Frequency Difference of Arrival (FDOA) and Time Difference of Arrival (TDOA). In the presence of moving sensors, the sensors' receivers measure the frequency of arrival (FOA) of the signal. The difference of two FOA's provides an FDOA which yields a surface called an isodop, in this case meaning equally differenced Doppler data, which contains the locus of all points on which the emitter could lie given the Doppler information. Similarly, the difference of a single receiver's time of arrival (TOA) with another TOA yields a TDOA which describes a surface known as an isochron, in this case meaning equally differenced time, which contains the locus of all points on which the emitter could lie given the TDOA information.

In the past, the measurement of such quantities in the tactical environment has been difficult due to their sensitivities to timing errors between any two sensors. Further, when trying to use these measurements for the geolocation of an emitter, errors in the sensor's own location and velocity measurements compound with the signal processing errors to provide unreliable emitter fixes. Historically, the Navy has relied upon long range, shore-based High Frequency Direction Finding (HFDF) networks. These networks use large antennas to measure the angle of arrival of a signal and cross these bearings over long distances to triangularize the emitter's location. Given the recent losses of Navy overseas assets and that more and more emitters in the tactical environment operate in the Very High Frequency (VHF) and Ultra High Frequency (UHF) range, the ability to perform emitter geolocation is diminishing. As a result, the Naval Security Group Support Activity (NSGSA) contracted with the Applied Research Lab at the University of Texas at Austin (ARL:UT) to develop an affordable, low-risk TDOA geolocation system using commercial off the shelf (COTS) and government off the shelf (GOTS) technologies.

ARL:UT responded by the development of the Carry-On Multi-Platform Global Positioning System Assisted TDOA System.

When using TDOA techniques, errors in the emitter geolocation problem is essentially related to three components: the location of the observer relative to the emitter (the “geometry”), signal timing, and observer position measurement. The emergence of Global Positioning System (GPS) technology offers capabilities which can greatly enhance TDOA applications by reducing measurement error components. Specifically, GPS allows for dramatic reductions in the observer position error and sample timing between observers. In addition, the advantages of using such commercially available and government “off-the-shelf” technology allows the system to be placed on a variety of platforms and, thus, could make the GPS-Assisted TDOA Geolocation System a highly desirable Multi-Platform tool in the “Joint Warfare” environment.

The measurement of the FDOA is done simultaneously when measuring the TDOA in the formulation used by the ARL:UT Test System. While the initial test and development of the ARL:UT system focused on the use of only TDOA measurements for geolocation, the combined use of TDOA and FDOA measurements for geolocation has become possible due to the GPS technology in the ARL:UT system. By providing more information to the geolocation solution, combined TDOA and FDOA measurements can expand the size of the state of the observer—providing velocity information as well as the emitter’s location. In addition to providing velocity information, it has been postulated that when poor geometry exists between observers, FDOA can more tightly resolve the solution of the geolocation fix than TDOA alone. Further, when the emitter is believed to have zero velocity, FDOA can provide the emitter’s three dimensional location using only three observers instead of four by fixing the solution’s velocity state to zero.

Regardless of which method or algorithm is used, the measurement of the TDOA and the FDOA is a statistical process, built upon standard estimation assumptions. As such, any measurement of either component can be viewed as a random variable related to the signal, the environment, and the accuracy and precision of the whole system that performs the measurement. Through the use of a Java-based, Stochastic TDOA and FDOA Simulation (JBSTAFSim), this thesis explores the impact on the geolocation of an emitter in the presence of such measurement errors. Given an estimate of the distribution of these measurement errors, JBSTAFSim can simulate the impact on a TDOA or mixed TDOA/FDOA geolocation solution within a given “Joint Warfare” scenario of observers. In particular, JBSTAFSim allows the user to: adjust the magnitude and correlation of

measurement error variance; adjust the believed measurement error variance used by the geolocator; dictate the network geometry and types of observers; and elect to choose a batch processed geolocator which incorporates previous geolocation information into the current solution to solve for the emitter's state.

Through simulation, this thesis shows that the mixed T/FDOA solution stochastically dominates the TDOA solution in two-dimensional fix scenarios. While no stochastic dominance of either solution is shown in the three-dimensional fix case, the author shows that the accuracy of the three-dimensional problem is related to the sensor network geometry. Further, if a three-dimensional fix is required, it is shown that robust sensors like satellites should be used to improve the sensor network to target geometry. Finally, since the location of the target relative to the sensors is generally not known, the author demonstrates the need to define a method to rate the sensor network geometry given possible target locations.

These results can be viewed from three perspectives. The first view is from the perspective of the designer of the system who wishes to understand the sensitivities of measurement errors and wishes to improve upon these measurements by the system or take them into account in the geolocation process. The next view is from the warrior, or user of the system, who would be employing this system to localize a hostile or friendly emitter. The warrior is concerned with the quality of the information provided by the system. As such, the warrior needs to know how well the system can perform and what he or she can do with respect to the sensor network to improve the fix of the target. Finally, the last perspective is from that of the activities which fund the designer to create such systems for the warrior. This activity is concerned with system performance for the amount invested. Given several functional areas that system designers could pursue to develop or improve, the simulation can rate the impact of this additional or improved information on the system's performance and describe how this impacts the warfare commander's utility for such information.

I. INTRODUCTION

A. BACKGROUND

The passive location of both hostile and friendly electromagnetic emitters has been an important capability for the war-fighter, for law enforcement, and in search and rescue operations. The characteristics of an emitted signal once received by several sensors in an operating environment can be exploited to passively locate an emitter. Two of the characteristics that can be measured by separate receivers of such a signal are: (1) the differences in Doppler shifts (if any) in the signal's frequency and (2) the difference in the time that the signal arrived at the sensors. These measurements are known as Frequency Difference of Arrival (FDOA) and Time Difference of Arrival (TDOA). In the presence of moving sensors, the sensors' receivers measure the frequency of arrival (FOA) of the signal. The difference of two FOA's provides an FDOA which yields a surface called an isodop, in this case meaning equally differenced Doppler data, which contains the locus of all points on which the emitter could lie given the Doppler information (see Figure 1-1). Similarly, the difference of a single receiver's time of arrival (TOA) with another TOA yields a TDOA which describes a surface known as an isochron, in this case meaning equally differenced time, which contains the locus of all points on which the emitter could lie given the TDOA information (see Figure 1-2).

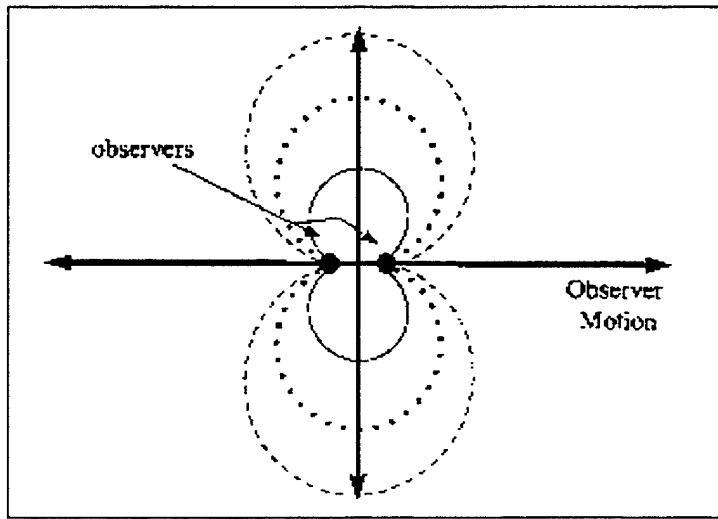


Figure 1-1 FDOA Isodops (From Ref. 1)

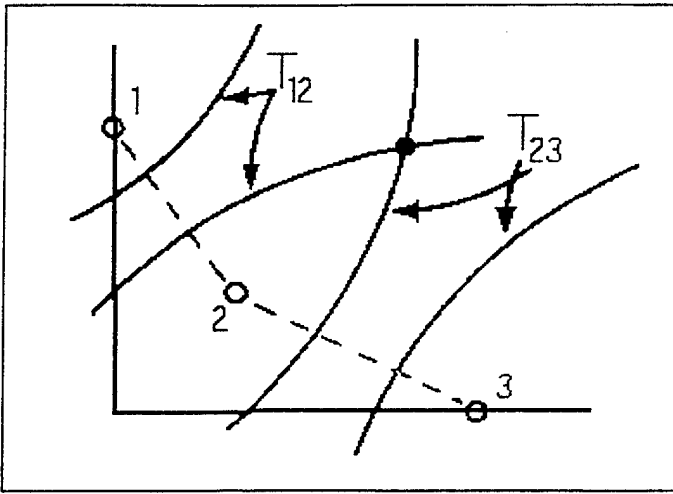


Figure 1-2 TDOA's of Three Observers (From Ref. 3)

In the past, the measurement of such quantities in the tactical environment has been difficult due to their sensitivities to timing errors between any two sensors. Further, when trying to use these measurements for the geolocation of an emitter, errors in the sensor's own location and velocity measurements compound with the signal processing errors to provide unreliable emitter fixes. Historically, the Navy has relied upon long range, shore-based High Frequency Direction Finding (HFDF) networks. These networks use large antennas to measure the angle of arrival of a signal and cross these bearings over long distances to triangularize the emitter's location. Given the recent losses of Navy overseas assets and that more and more emitters in the tactical environment operate in the Very High Frequency (VHF) and Ultra High Frequency (UHF) range, the ability to perform emitter geolocation is diminishing. As a result, "the Naval Security Group Support Activity (NSGSA) contracted with the Applied Research Lab at the University of Texas at Austin (ARL:UT) to develop an affordable, low-risk TDOA geolocation system using commercial off the shelf (COTS) and government off the shelf (GOTS) technologies" [Ref. 1]. ARL:UT responded by the development of the Carry-On Multi-Platform Global Positioning System Assisted TDOA System.

When using TDOA techniques, errors in the emitter geolocation problem is essentially related to three components: the location of the observer relative to the emitter (the "geometry"), signal timing, and observer position measurement. The emergence of Global Positioning System (GPS) technology offers capabilities which can greatly enhance TDOA applications by reducing measurement error components. Specifically, GPS allows for dramatic reductions in the observer position error and sample timing between

observers. In addition, the advantages of using such commercially available and government "off-the-shelf" technology allows the system to be placed on a variety of platforms and, thus, could make the GPS-Assisted TDOA Geolocation System a highly desirable Multi-Platform tool in the "Joint Warfare" environment as illustrated in Figure 1-3.

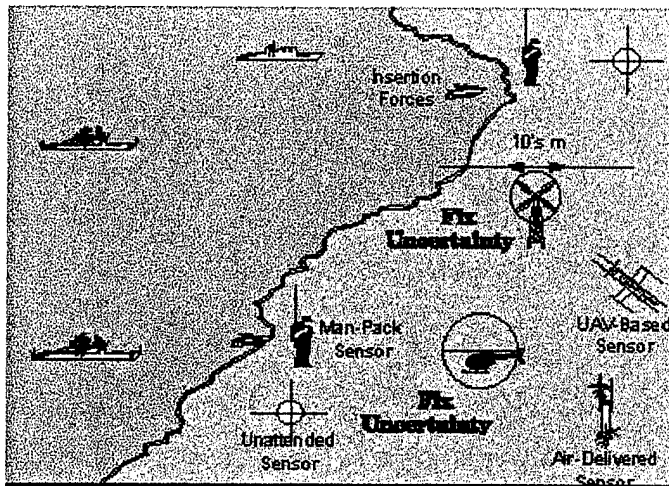


Figure 1-3 GPS Assisted Geolocation System in Joint Warfare (From Ref. 2)

Through the use of GPS technology and differential techniques combined with Rubidium standard oscillators, the total theoretical signal timing error is approximately 25 nanoseconds which, when multiplied by the speed of light, converts to 7.5 meters in distance.[Ref. 1]

The measurement of the FDOA is done simultaneously when measuring the TDOA in the formulation used by the ARL:UT Test System. While the initial test and development of the ARL:UT system focused on the use of only TDOA measurements for geolocation, the combined use of TDOA and FDOA measurements for geolocation has become possible due to the GPS technology in the ARL:UT system. By providing more information to the geolocation solution, combined TDOA and FDOA measurements can expand the size of the state of the observer—providing velocity information as well as the emitter's location. In addition to providing velocity information, it has been postulated that when poor geometry exists between observers, FDOA can more tightly resolve the solution of the geolocation fix than TDOA alone. Further, when the emitter is believed to

have zero velocity, FDOA can provide the emitter's three dimensional location using only three observers instead of four by fixing the solution's velocity state to zero.

B. PURPOSE

Regardless what method or algorithm used, the measurement of the TDOA and the FDOA is a statistical process, built upon standard estimation assumptions. As such, any measurement of either component can be viewed as a random variable related to the signal, the signal's environment, and the accuracy and precision of the whole system that performs the measurement. Through the use of a Java-based, Stochastic TDOA and FDOA Simulation (JBSTAFSim), the author explores the impact on the geolocation of an emitter in the presence of such measurement noise. Given an estimate of the variance of these measurement errors, JBSTAFSim can simulate the impact on a TDOA or mixed TDOA/FDOA geolocation solution within a given "Joint Warfare" scenario of observers. In particular, JBSTAFSim allows the user to: adjust the magnitude and correlation of measurement error variance; adjust the believed measurement error variance used by the geolocator; dictate the network geometry and types of observers; and elect to choose a batch processed geolocator which incorporates previous geolocation information into the current solution to solve for the emitter's state.

These results can be viewed from three perspectives. The first view is from the perspective of the designer of the system and wishes to understand the sensitivities of measurement errors and wishes to improve upon these measurements by the system or take them into account in the geolocation process. The next view is from the warrior, or user of the system, who would be employing this system to localize a hostile or friendly emitter. The warrior is concerned with the quality of the information provided by the system. As such, the warrior needs to know how well the system can perform and what he or she can do with respect to the sensor network to improve the fix of the target. Finally, the last perspective is from that of the activities which fund the designer to create such systems for the warrior. This activity is concerned with system performance for the amount invested. Given several functional areas that system designers could pursue to develop or improve, the simulation can rate the impact of this additional or improved information on the system's performance and describe how this impacts the warfare commander's utility for such information.

C. ORGANIZATION

The next chapters discuss briefly: the configuration of the ARL:UT test system, how the TDOA and FDOA measurements are made, and how these measurements enter into the geolocation process. Some of the detailed theory and methods that JBSTAFSim uses can be found in Appendixes A-C. Chapters V and VI provide an overview of JBSTAFSim and a description of the simulated environment. Chapter VII presents the results of the simulation of TDOA and mixed TDOA/FDOA geolocation methods. Chapter VIII offers recommendations based on the results presented in the previous chapter.

II. ARL:UT SYSTEM OVERVIEW

The ARL:UT system is capable of receiving a frequency in the HF, VHF, or UHF frequency bands. Only one voice grade channel compatible with existing Navy hardware for communication between sensors is required. Further, the system is designed to be compatible with the Unified Build (UB) environment and interface with and display its results graphically on the Joint Maritime Command and Information System (JMCIS). Each observer updates its location with a GPS receiver. The receivers have a one pulse-per-second (pps) output which is used to trigger sampling of the incoming signal of interest. The accuracy of the GPS clocks drives each receivers' output of the one pps pulse to be within 20 nano seconds of each other. The sampler at each observer, then, is phase-locked to the one pps pulse to within five nano seconds making the samples between observers to be within 25 nano seconds [Ref. 20]. As depicted in Figure 2-1, the system network consists of one master sensor and a few slave sensors. In the evenly

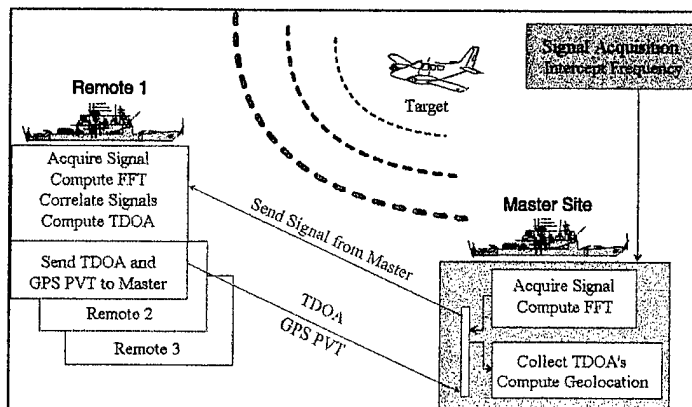


Figure 2-1 System Overview (From Ref. 20)

determined case, three sensors are required for a two-dimensional geolocation and four for a three-dimensional fix. Once given the frequency of interest from traditional detection means, the master tunes its receiver to that frequency and orders the slaves to tune to the same frequency. Each observer stores the incoming signal as buffered data. Since only one communications channel is required to be available, the ARL:UT system uses a distributed processing system to make the most efficient use of the single communications link. The master determines a 400 milli second portion that contains the most energy and computes the Fast Fourier Transform (FFT) of this sample. This FFT is then sent to the

slaves with a GPS time stamp. The slaves search their buffers for the 400 millisecond sample that corresponds to the master's time stamped FFT. The slaves then FFT their own data and correlate these samples using a Complex Ambiguity Function (CAF) to determine the TDOA. The TDOA, FDOA, GPS position of the observer, velocity of the observer, and timestamp are returned to the master. The master collects the information and sends the package to a standard Navy TAC3/4 workstation which calculates the geolocation. A detailed reference of the preliminary hardware configuration and specifications of the ARL:UT system can be found in Reference 20.

Like any system that depends on the Global Positioning System, this system is very vulnerable if GPS were lost or significantly degraded. While relatively reliable sensor information such as position and velocity might be available from inertial systems on the sensor's platform, the need for a reliable, common time standard between sensors so that data can be buffered and retrieved at common times would still be required. While the vulnerabilities of GPS is an issue well beyond the scope of this discussion, it must be considered when weighing the value, limitations, and capabilities of such a system.

III. TDOA AND FDOA MEASUREMENTS

A. BACKGROUND AND PURPOSE

The main purpose of this chapter is to describe how the TDOA and FDOA measurements are made and the assumptions behind those measurements. Much of the next section is a basic summary of several signal processing theories and methods. If the reader is not interested in these details, the first three sections of this chapter may be omitted with the following in mind. *The main importance of this chapter is to present the measurement of TDOA's and FDOA's from a stochastic RF reception as a statistical process* and to get an understanding of the assumptions required to formulate these processes. The measurement errors in any TDOA or FDOA are multivariate functions of *many* parameters—many of which are random variables themselves. Measurements are further confounded by the sensitivity and accuracy of the method employed to determine the TDOA or FDOA measurement.

JBSTAFSim does not assume any one particular method to measure the TDOA or FDOA; nor does JBSTAFSim assume any properties with respect to the signal, the noise in the signal, or the noise in the environment—the random variables which have been shown in the works listed below to function as parameters which describe the measurement error estimate. Rather, JBSTAFSim allows the user to set the measurement error variance estimate and correlation of the measurements. Since these measurements are modeled statistically, it is reasonable to assume that regardless of the method used to obtain them or the many parameters which might describe them, the error in their measurement can also be described statistically. By doing this, JBSTAFSim can simulate these measurements and indicate their effect on the geolocation process with minimal information provided with respect to: the system performing the measurements, the signal of interest, and the many random variables describing the received signal and its environment. Viewed this way, the model maintains integrity while also allowing it to serve in the most general sense.

The following discussion is based on Reference 1, an NPS thesis by LT David A. Streight who applies Cyclostationary techniques to measure the TDOA of an emitter. In describing the advantages of this particular method LT Streight provides an excellent overview of the basic statistical properties and assumptions of the signal involved in

determining the TDOA and FDOA measurement using traditional methods. More information about these process can be found in detail in References 4, 5, and 6.

B. BASIC MODEL AND THE GENERALIZED CROSS CORRELATION

Most TDOA models assume a stationary signal which is received by two sensors in the presence of white Gaussian noise. These signals have been mathematically modeled as a function in the time domain:

$$x(t) = s(t) + n_1(t) \quad 2-1$$

$$y(t) = A \cdot s(t - D) + n_2(t) \quad 2-2$$

where $s(t)$ is assumed to be statistically independent and uncorrelated with independent noises $n_1(t)$ and $n_2(t)$. A is the complex valued relative magnitude and phase mismatch between the receivers; D represents the TDOA between the signals.[Ref. 1] The autocorrelation and cross-correlation functions are given by:

$$R_x(\tau) = R_s(\tau) + R_{n_1}(\tau) \quad 2-3$$

$$R_y(\tau) = |A|^2 R_s(\tau) + R_{n_2}(\tau) \quad 2-4$$

$$R_{yx}(\tau) = A \cdot R_s(\tau - D) + R_{n_1 n_2}(\tau) \quad 2-5$$

and the spectral density functions are:

$$S_x(f) = S_s(f) + S_{n_1}(f) \quad 2-6$$

$$S_y(f) = |A|^2 S_s(f) + S_{n_2}(f) \quad 2-7$$

$$S_{yx}(f) = A \cdot S_s(f) \cdot e^{-j2\pi f D} + S_{n_1 n_2}(f) \quad 2-8$$

Using these relationships and assumptions, the parameter D , the TDOA, can be obtained by using correlation techniques. The most basic technique is the Generalized Cross Correlation method. First, note that (by 2-5) $R_{yx}(\tau)$ peaks when $\tau = D$. Next assuming that f of the received signal is within a finite Bandwidth B around the carrier frequency f_0 , the ratio of $S_{yx}(f)$ to $S_x(f)$ is:

$$\frac{S_{yx}(f)}{S_x(f)} = \begin{cases} A \cdot e^{-j2\pi f D} & f_0 - \frac{B}{2} \leq f \leq f_0 + \frac{B}{2} \\ 0 & \text{otherwise} \end{cases} \quad 2-9$$

The inverse Fourier transform of this ratio is equal to:

$$h_0(\tau) = \int_{f_0-B/2}^{f_0+B/2} \frac{S_{yx}(f)}{S_x(f)} e^{+j2\pi f \tau} df \quad 2-10$$

which peaks at $\tau = D$ and provides the TDOA measurement.[Ref. 1]

C. COMPLEX AMBIGUITY FUNCTION

The Generalized Cross Correlation method as described above works well in the case of static transmitters and receivers. However, as shown in Reference 5, in order to determine the TDOA when there exists a Doppler shift, the spectrum of one of the signals must be translated in frequency equal to the FDOA measured between the observers. This can be shown by rewriting the generalized model above so that:

$$x(t) = s(t) + n_1(t) \quad 2-11$$

$$y(t) = A \cdot s(t - D) e^{-j2\pi f_d t} + n_2(t) \quad 2-12$$

where f_d is the Doppler difference measured between the two observers. This requires the maximization over the two parameters D and f_d which leads to:

$$A(D, f_d) = \int_0^T x(t)y^*(t-D)e^{-j2\pi f_d t} dt \quad 2-13$$

Notice that at $f_d = 0$, the CAF reduces to the Generalized Cross Correlation method. In Reference 5, Stein shows, given these assumptions, the variance of the estimates for the TDOA and FDOA can be related to the signal integration time, the signal bandwidth, and the noise bandwidth:

$$\sigma_{TDOA} = \frac{1}{\beta} \frac{1}{\sqrt{BT\gamma}} \quad 2-14$$

$$\sigma_{FDOA} = \frac{1}{T_e} \frac{1}{\sqrt{BT\gamma}} \quad 2-15$$

where:

B = the noise bandwidth at the input of both receivers,

$$\beta \stackrel{\Delta}{=} 2\pi \left[\frac{\int_{-\infty}^{+\infty} f^2 W_s(f) df}{\int W_s(f) df} \right]^{1/2} \quad 2-16$$

with $W_s(f)$ = the spectral density of the signal as shaped by the receiver,

T_e = rms. integration time and,

$$\frac{1}{\gamma} = \frac{1}{2} \left[\frac{1}{\gamma_1} + \frac{1}{\gamma_2} + \frac{1}{\gamma_1 \gamma_2} \right] \quad 2-17$$

with $\frac{1}{\gamma_i}$ = the signal to noise ratio (SNR) for each receiver. [Ref. 1]

With a little sensitivity analysis of the above equations, it can be seen that the driving component in the standard deviation of the TDOA measurement is SNR. In an idealized case, below 10dB SNR and with a 400 ms integration time of the ARL:UT system, the standard deviation of a single TDOA measurement exceeds 100 meters. "With three measurements to provide a fix, all within this idealized case, the geolocation would have a standard deviation of 173 meters" [Ref. 1], a large best-case error.

D. CYCLOSTATIONARY DETERMINATION

LT Streight's thesis applies Cyclostationary techniques to measure the TDOA. This is a robust approach which is able to perform well despite both low SNR and the presence signals which may or may not intentionally seek to jam the observers' receivers. By taking advantage of the cyclic—time periodic—nature of most signals, a three dimensional correlation in the frequency and cyclic frequency domains can be performed. Thus, where the signal of interest and noise may have appeared overlapping in the traditional models, they can still be separated by a cyclic autocorrelation function which can be thought of as a special autocorrelation function which produces spectral lines at frequencies indicative of the signal's periodic nature. In the frequency domain, the cyclic autocorrelation function is replaced by the spectral correlation function. The Spectral Correlation Function (SCF) is a correlation in the frequency domain which peaks at the nominal spectral frequency and cyclic frequency in what is called a bi-frequency plane. See Figure 2-1.

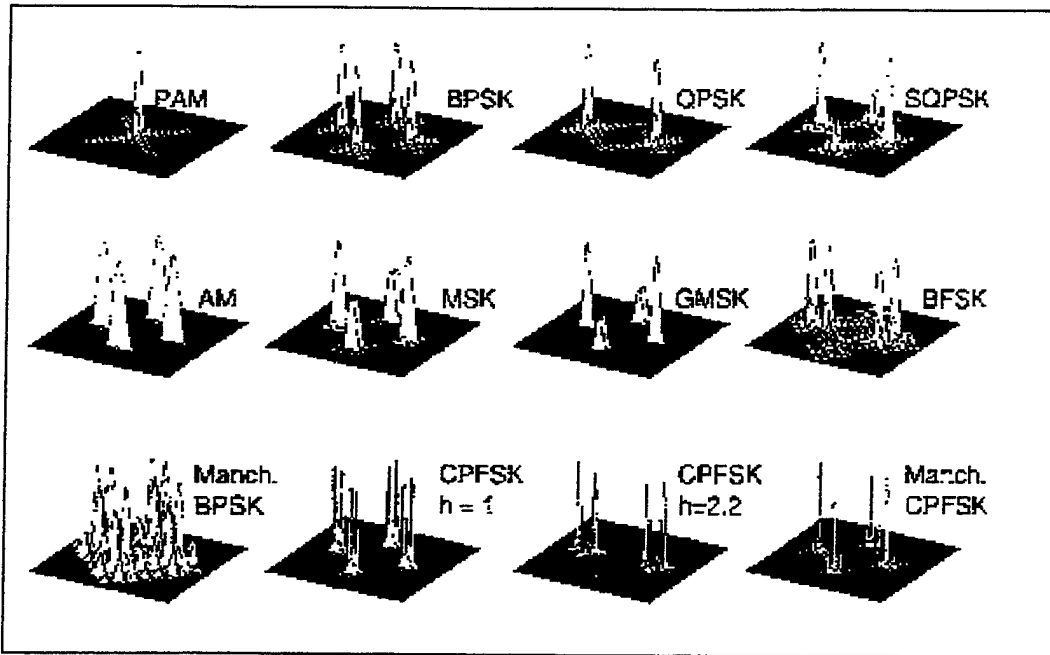


Figure 3-1 Signals plotted in the Bi-frequency Plane (From Ref. 1)

This method allows for dramatically better results in the presence of greater interference and, as seen above, can provide a classification of the modulation type. The model of the signal at any pair of receivers remains as in 2-1 and 2-2,

$$x(t) = s(t) + n_1(t)$$

$$y(t) = A \cdot s(t - D) + n_2(t),$$

and assumes the same statistical assumptions with respect to the properties of the signal and noise *except* that now the noise may now contain co-channel interference which could spectrally mask the signal. As before, auto and cross-correlation functions are used in conjunction with the spectral density functions to measure the TDOA; however, now these correlated values are *aligned* by the cyclic frequency characteristic of the desired signal. While highly accurate in the presence of interference, this method is computationally expensive. LT Streight employs a computationally efficient cyclostationary TDOA algorithm, SPECCOA, "which may not be as accurate as others but is the best choice for the efficiency required in a tactical system." [Ref. 1] While not implemented by the ARL:UT test system, this method could be implemented as the

algorithm of choice in the next system or in future systems. It is presented here in detail, along with the GCC and CAF, to point out the multitude of processes, parameters, and assumptions required to estimate the TDOA or FDOA measurement error variance. Regardless of the method used to obtain them, the TDOA and FDOA measurement errors can be represented as a stochastic process.

E. IMPLICATIONS OF SIGNAL PROCESSING TO GEOLOCATION

Throughout this chapter, discussion has focused on the signal models and their assumptions. As noted previously Stein, in Reference 5, gives the TDOA and FDOA estimate measurement errors based on a few parameters and several assumed conditions. Dr. Petre Rusu and Dr. Lisa Julianelli of ARL:UT, in References 7 and 8, follow the work of Azaria and Hertz, in Reference 4, to find the solution for the correlation between TDOA measurements as a function of SNR, observation interval length, and noise and signal bandwidths. Unfortunately, many of these parameters that go into these formulations are in fact stochastic themselves. Further, in Reference 7, the enabling assumptions with regard to the estimation of the measurement error correlation begin with those of equations 2-1 and 2-2, namely, that the signal received at any observer can be described as the summation of two parts—a deterministic signal plus Gaussian noise. The noises are considered “uncorrelated with the signal and with each other across observers”[Ref. 7]. While these assumptions like these are critical for the necessary mathematical formulations like those in sections B through D above and in works such as Reference 7, in an operating environment, these models will fail to represent the one stochastic, and most important, variable present at the observers’ receivers—the actual, “real world” signal itself. Viewing each signal received at each of the observers as a stochastic process, the TDOA and FDOA measurement process should not be thought of as that which can parameterize the measurement errors; rather, it is the randomness nascent in each observer’s received signal that introduces the measurement errors.

Since quantifying the impacts of the estimate covariance and correlation of TDOA and FDOA measurement errors on the geolocation process is the goal of these analyses, this discussion might seem to be disputing a fine point. However, it demonstrates the evaluative value of JBSTAFSim as a tool for assessing the impact of *any* assumption or model of the TDOA and FDOA measurement errors on the geolocation process.

JBSTAFSim, then, functions as an “If—Then” tool. The “If—Then” portion of the simulation is remarkably simple: given a network and allocation of observers, *if* measurement errors are introduced with a given probabilistic description; *then*, the expected Geolocation results are as follows. JBSTAFSim, then, exploits one of the greatest advantages of simulation; rather than redefine our mathematical models or simulate only the equations of our models, let us instead violate our own assumptions, stochastically, and examine the results within an empirical simulation space. The results of such an investigation are useful for anyone who: is designing a system such as this and wishes to evaluate or improve its effectiveness; using a system such as this for tactical decisions and wishes to know its capabilities and limitations; and for anyone sponsoring the development of such a system and wishes to know how added capabilities or improvements might improve the warrior’s use of such a system.

IV. Emitter Geolocation

A. BACKGROUND

The TDOA and FDOA measurements computed by the signal processing methods described in the previous chapter form the basis for the measurement data required to solve for the emitter's location. These quantities measured in seconds and in Hertz can be represented formally in terms of length (meters) and velocity (meters/second) by the following algebraic equations:

$$TDOA_{ij} = c(t_i - t_j) \quad 4-1$$

$$TDOA_{ij} = \sqrt{(x_i - x_s)^2 + (y_i - y_s)^2 + (z_i - z_s)^2} - \sqrt{(x_j - x_s)^2 + (y_j - y_s)^2 + (z_j - z_s)^2}$$

$$FDOA_{ij} = -f_s \left[\left(\frac{(\vec{v}_i - \vec{v}_s) \cdot (\vec{r}_i - \vec{r}_s)}{c} \right) - \left(\frac{(\vec{v}_j - \vec{v}_s) \cdot (\vec{r}_j - \vec{r}_s)}{c} \right) \right] \quad 4-2$$

Where the subscripts i and j represent the observer pair forming the differences and s denotes the signal's source. An observer's three dimensional location in space is defined by (x,y,z) , and r and v represent the radial and velocity vectors of the target or observers. Therefore, the TDOA and FDOA can be thought of as spatial differences and relative velocity differences, rather than in time and frequency units.

Much has been written and theorized about the best way to solve for the state of an emitter given TDOA information. While the TDOA measurement is non-linear in the emitter's state, solutions can be formulated to directly solve for the location of the target as linear models which satisfy non-linear constraints. These solutions usually involve squaring the TOA equation which results in two locations which satisfy the TDOA data. References 9, 10, and 12 all show different, but mathematically equivalent *algebraic* methods to *directly* solve for the state of an emitter. In particular, in Reference 10, Dr. Petre Rusu, of ARL:UT, goes through great work to linearly propagate the estimate errors through his solution to provide an uncertainty estimate for his solution to the emitter's state. In Reference 11, Dr. Rusu further proves, given consistent weighting matrices, the theoretical equivalence of the TOA direct solution and least squares

formulation. References 9 and 13 are specifically geared to the algebraic solution of GPS equations; however, their techniques can be applied to any TDOA geolocation problem.

In JBSTAFSim, the method of Reference 13, by Chaffee and Abel, is used to provide an initial starting position for the linearized least squares approach. This method is very elegant and numerically robust. Further, it provides a useful understanding of the solution ambiguity by not immediately squaring the TOA equation. Thus, this method was chosen for its numerical superiority and for its elegant resolution of the ambiguity of emitter location. The linearized least squares solution uses this direct solution as its starting point from which it seeks a solution to minimize the sum of squared errors. After a fix is computed, the solver then uses the previous solution as the starting position for the subsequent solutions until a request is made for another direct solution to update the current solution. The periodicity of these updates may be set by the user. In an actual geo-location system, direct solution updates might be requested as a function of many complex variables and parameters, for instance: quality of the previous fix, the dimensionless shock, time since the last fix, by request of the system user, or quality of the received signal. JBSTAFSim seeks to minimize the sum of squared errors by implementing a Square Root Information Filter (SRIF). The SRIF was chosen for its numerical superiority and its ability easily include a priori statistics and function as a numerically stable extended Kalman filter. The SRIF in JBSTAFSim can perform either as a single epoch state solver or as an extended Kalman Filter, “batch”, processor. JBSTAFSim’s SRIF does not, however, incorporate a movement model that considers a target which moves with time. While a movement model would no doubt provide the most robust approach, given limited communications between observers, the complexity of such a model, the non-linearity of the measurements, and the purpose of the system to act as a locator and not as a fire control system, the batch process mode without a movement model should be considered adequate for those targets with zero, or near zero, velocities. The development of movement models for particular classes of targets would be a large undertaking; however, their design could be facilitated through empirical simulation by extending the JBSTAFSim solver.

Finally, and as will be discussed in the next chapter, JBSTAFSim’s simulation results should not be viewed as a measure of the ARL:UT system. In particular, ARL:UT’s system is currently in the test and development phase in which its Engineers and Scientists are considering a multitude of design issues like the ones presented in this thesis. Therefore, JBSTAFSim’s results are not necessarily identical with that of the

ARL:UT system, but should be viewed as representative of that of a generic, though robust, multi-platform, GPS assisted TDOA/FDOA system.

B. DIRECT GEOLOCATION SOLUTION

This method was introduced in Reference 13 in order to provide a description of the exact solution for the GPS pseudorange equations. This method provides a greater understanding of the geometry involved in the TDOA equations and can be applied in a numerically stable fashion. Dr. Tolman of ARL:UT provides a simple explanation of Chaffee and Abel's formulation in Reference 14. This section provides a quick summary of this direct solution method based on both of these references.

Following the notation and example of Dr. Tolman's notes in Reference 14, let the emitter be located at position \vec{r} and define an observer to be located at position \vec{r}_i . The range between one observer and the emitter is defined by:

$$R_i = \|\vec{r}_i - \vec{r}\| \quad 4-3$$

The TOA equation is defined as:

$$TOA_i = ct_i = \|\vec{r}_i - \vec{r}\| + ct_0 = R_i + ct_0 \quad 4-4$$

where t_0 is the unknown time of transmission of the signal. This equation holds for any change in the origin of time. The TDOA is simply the difference of two TOA's:

$$TDOA_{ij} = \frac{1}{c} (R_i - R_j) \quad 4-5$$

Algorithms in References 9 and 10 begin by squaring the TOA equation above. Chaffee and Abel do not. Instead, label one receiver I, the master. Let all other receivers be denoted with $i \in 1, \dots, M-1$.

$$ct_i - ct_I - (ct_0 - ct_I) = \|\vec{r}_i - \vec{r}_I - (\vec{r} - \vec{r}_I)\| \quad 4-6$$

Further, define:

$$\Delta_i = ct_i - ct_I$$

$$\vec{r}'_i = \vec{r}_i - \vec{r}_I$$

$$\vec{r}' = \vec{r} - \vec{r}_I$$

This makes the TOA equation:

$$\Delta_i + \|\vec{r}'\| = \|\vec{r}'_i - \vec{r}'\| \quad 4-7$$

Square this equation and note $\|\vec{r}'\|^2$ cancels:

$$\|\vec{r}'_i\|^2 + 2\vec{r}'_i \cdot \vec{r}' = \Delta_i^2 + 2\|\vec{r}'\|\Delta_i \quad 4-8$$

Stack this equation for M-1 differences yields:

$$\begin{bmatrix} \vec{r}'_i & \Delta_i \\ \vdots & \vdots \end{bmatrix} \begin{bmatrix} \vec{r}' \\ \|\vec{r}'\| \end{bmatrix} = \frac{1}{2} \begin{bmatrix} \vec{r}'_i \cdot \vec{r}'_i - \Delta_i^2 \\ \vdots \end{bmatrix} \quad 4-9$$

For continuity, Chaffee and Abel describe this set of equations as:

$$\begin{bmatrix} S_i \\ \Delta_i \end{bmatrix}, Z \begin{bmatrix} u \\ \|u\| \end{bmatrix} \rangle = \frac{1}{2} \begin{bmatrix} S_i \\ \Delta_i \end{bmatrix} \begin{bmatrix} S_i \\ \Delta_i \end{bmatrix} \quad 4-10$$

Where $\langle v, w \rangle$ represents the Lorentz inner product on \mathbb{R}^4 defined as: if $v = (x', a)$ and $w = (y', c)$ are vectors, then $\langle v, w \rangle = x'y - ac$. In addition, also note $Z \begin{bmatrix} u \\ b \end{bmatrix} = \begin{bmatrix} u \\ -b \end{bmatrix}$, $S_i \equiv \vec{r}'_i$, and $u \equiv \vec{r}'$. [Ref. 13]

Note that these two equations, 4-9 and 4-10, are both of the form $AX = B$. Thus, this appears to be a linear problem in X , but the emitter location solved by TDOA techniques is not linear. In this case, the fourth component of X is non-linear; this non-

linearity will act as a separate constraint on the solution of the linear problem. In the overdetermined case when there are four equations ($M=5$ observers), the non-linear constraint is automatically satisfied; however, we rarely expect to be in an overdetermined case. Therefore, the matrix A is singular, but still can be inverted as a generalized inverse: $A^{-g} = A^T (AA^T)^{-1}$. The best way to obtain A^{-g} , however, is by the singular value decomposition (SVD) algorithm. More compelling, the SVD algorithm directly provides the null space, a^\perp , required to satisfy the non-linear constraint. Since A is 3×4 , and we assume rank 3, then the null space of A is one dimensional and the complete solution for X is:

$$X = A^{-g}B + \lambda a^\perp \quad 4-11$$

Where a^\perp is a unit vector spanning the null space of A and λ is a real variable. To prove this is the solution to $AX = B$, multiply both sides of the solution by A and recall $Aa^\perp = 0$,

$$AX = AA^T (AA^T)^{-1}B + \lambda Aa^\perp = AX = B \quad 4-12$$

Given the above equation, it is evident that the constant λ is arbitrary with respect to the linear equation; however, from equation 4-9, the non-linear constraint requires the fourth component of X be equal to the magnitude of the vector of its first three components: $\|\vec{r}\|^2 - (X_4)^2 = 0$.

Now, consider the first three dimensions or components of the solution for X —Chaffee and Abel call this vector: $u_A = A^T (AA^T)^{-1}u = A^{-g}B$. The solution to the linear equation has given us this vector which describes the emitter's location uniquely in a three-dimensional subspace orthogonal to a^\perp , but cannot provide any information to the ambiguous component normal to this subspace, i.e. along a^\perp . The non-linear constraint must be used to determine this component defined by λ . Substituting the four dimensional solution to the linear equation, Chaffee and Abel label w_A , plus λa^\perp back into the Lorentz functional, yields a quadratic equation for λ :

$$\langle a^\perp, a^\perp \rangle \lambda^2 + 2\lambda \langle w_A, a^\perp \rangle + \langle w_A, w_A \rangle = 0 \quad 4-13$$

which provides a direct solution for λ .

Thus, to summarize the result and combining the two notations:

$$Z \begin{bmatrix} \vec{r} \\ b \end{bmatrix} = w_A + \lambda a^\perp + Z \begin{bmatrix} \vec{r}_I \\ t_I \end{bmatrix}, \quad 4-14$$

where $(w_A + \lambda a^\perp) \geq 0$ which is from the constraint on the solution vector $w_A + \lambda a^\perp = \begin{bmatrix} \vec{r}' \\ \|\vec{r}'\| \end{bmatrix}$. The quantity b in Equation 4-14 is called the bias which, used in GPS equations, represents the offset of time between the master's and emitter's time reference. The vector \vec{r} gives the emitter's location.

Like all direct solutions, the impact of squaring the TOA equation results in two possible solutions for the emitter location. For GPS, this is not a problem since one solution is on the face of the earth and the other lies opposite to the satellite plane in space. In a tactical environment, however, this problem must be solved with some prior knowledge of the target of interest or with some common sense with respect to the components which describe the target's location.

C. LINEARIZED LEAST SQUARES APPROACH

The linearized least squares approach to the geolocation of an emitter provides a statistically robust estimate of the emitter's state and covariance uncertainty estimate. While the method does require an initial guess with respect to the location of the emitter, in many cases this can be provided by picking a point in the area of observers or by first solving for the state via one of the direct methods mentioned above. Certainly, the performance of linear least squares algorithms is well-known and stable given that care is taken into their formulation. In this regard, JBSTAFSim utilizes a Square Root Information Filter (SRIF), see Appendix A for a detailed description, which has been proven to be more numerically stable and accurate than other methods. In addition, the SRIF allows for elegantly simple inclusion of prior estimates to be included with the current state estimate for batch processing as an extended Kalman Filter. Further a hybrid linearized least squares solution aided by a direct solution will most likely be the geolocation method of choice by the ARL:UT system. In the mixed TDOA/FDOA case,

JBSTAFSim also enhances the numerical accuracy of the SRIF solution by scaling the partials matrix and TDOA and FDOA data so that every equation is dimensionless and on unity order. Appendix B contains a detailed description of the scaling of mixed TDOA/FDOA data in order to improve the numerical accuracy and stability of a linearized least squares solution.

Consider in detail the mixed TDOA/FDOA problem as described in Reference 19:

Observation equations:

$$c \cdot TDOA_{ij}(\vec{r}) = R^{(i)} - R^{(j)} \quad 4-15$$

$$f_T^{-1} \cdot FDOA_{ij}(\vec{r}, \vec{v}) = \frac{\Delta\vec{v}_{\varphi}^{(i)}}{c} - \frac{\Delta\vec{v}_{\varphi}^{(j)}}{c} \quad 4-16$$

Measurement covariance matrix:

$$M = \begin{bmatrix} c^2 \sigma_{TDOA}^2 & 0 \\ 0 & f_T^{-2} c^2 \sigma_{FDOA}^2 \end{bmatrix} \quad 4-17$$

Linearized least squares equation:

$$\left[\begin{pmatrix} (\alpha^{(j)} - \alpha^{(i)}) \\ \left(\frac{\Delta\vec{v}_{\perp}^{(j)}}{R^{(j)}} - \frac{\Delta\vec{v}_{\perp}^{(i)}}{R^{(i)}} \right) \end{pmatrix} \quad \begin{pmatrix} 0 \\ (\alpha^{(j)} - \alpha^{(i)}) \end{pmatrix} \right]_{X_0} \begin{pmatrix} d\vec{x} \\ d\vec{v} \end{pmatrix} = \left[\begin{pmatrix} c \cdot TDOA_{ij} \\ \frac{c}{f_T} \cdot FDOA_{ij} \end{pmatrix} - \begin{pmatrix} R^{(i)} - R^{(j)} \\ \Delta\vec{v}_{\varphi}^{(i)} - \Delta\vec{v}_{\varphi}^{(j)} \end{pmatrix} \right]_{X_0} \quad 4-18$$

Direction cosines are denoted by α , and R is the observer-target separation. In the state vector, $d\vec{x}$ and $d\vec{v}$ refer to the offset from the position and velocity, respectively, of the nominal state, and the subscripts φ and \perp refer to components parallel and perpendicular, respectively, to the line of sight. Thus, for mixed T/FDOA, the above partials matrix is $2(M - 1) \times N$, where M equals the number of observers and N is the size of the unknown emitter's state. When only TDOA information is used for geolocation, the partials matrix is reduced to $(M - 1) \times N$, where $N \leq 3$, and, thus, no information with respect to the target's velocity can be given. For the purposes of this thesis, only cases which are evenly determined are considered. The overdetermined solutions will most

likely always dominate the evenly determined ones; further, this method of analysis assumes that resources are typically scarce and, thus, the overdetermined case event is unlikely to occur. With this philosophy in mind, JBSTAFSim is designed to produce two- or three-dimensional fixes in the TDOA only case and four- or six-dimensional fixes in the mixed T/FDOA mode.

In addition to the solution to the state of the target, the linearized least squares approach also provides an estimate of the error covariance of the state estimate. Viewing 4-18 as the set of equations $Ax = b$, the estimate of the state vector takes on the form $(A^T M^{-1} A)^{-1} = P$. If we are interested in only the first n components of the solution vector and take the first $n \times n$ components of P correspondingly; then, given the implicit assumptions of Normality in the least squares and extended Kalman filter, it can be shown that:

$$(x_n - \mu)^T P_n^{-1} (x_n - \mu) \sim \chi_n^2 \quad 4-19$$

where μ represents the true location of the target. Since this covariance matrix parameterized by n is always positive definite, it can be said that its column vectors form the basis of the eigenspace P_n and the corresponding eigenvalues are: $\alpha_1 \dots \alpha_n$. Thus a hyperellipsoid defined by:

$$\frac{y_1^2}{\alpha_1} + \frac{y_2^2}{\alpha_2} + \dots + \frac{y_n^2}{\alpha_n} = \ell^2 \quad 4-20$$

forms surfaces of equal probability densities. Therefore, for a certain ℓ , the probability that a point will lie inside the ellipsoid can be computed. For example, if an $n=2$ dimensional fix with an $\ell = 3$ sigma error ellipse is desired, the ellipse defined by the covariance matrix would yield an ellipse for which there would be a 99.7% probability that the target lies inside the ellipse. Thus, the size of the ellipsoid created by the covariance matrix can be thought of as a measure of the uncertainty of the solution.

In addition to generating error ellipsoids, the covariance matrix also provides a means to measure the amount by which the observer geometry is degrading the fix. This measurement is often referred to as the geometric dilution of precision (GDOP). Again, given that the residuals of the state vector are Normally distributed, the covariance matrix

is a measure of their statistical properties. If these errors are small, a linear approximation which relates them to the observations may be considered satisfactory. "Moreover, if the observation residuals are Normally distributed, the fix residual residuals computed via the linear approximation are automatically Normally distributed." [Ref. 15] In this case the linear error propagation may be defined from Reference 15 as:

$$C_y = AMA^T. \quad 4-21$$

The total error on the fix as the root-mean-square deviation is

$$\sqrt{Tr(C_y)} = \sqrt{Tr(AMA^T)} \quad 4-22$$

which provides the "total fix position error." Dividing this quantity, as suggested above, by the total measurement error provides an estimate of the relative dilution of precision:

$$\frac{\sqrt{Tr(AMA^T)}}{\sqrt{Tr(M)}} \quad 4-23$$

While there is nothing geometric about 4-23, it places all the geometric errors in the (AA^T) factor separately from the stochastic contribution of C_y . The relationship between GDOP, measurement error, and fix error has been described as:

$$\sigma_{position} \approx GDOP \cdot \sigma_{measurement} \quad 4-24$$

Therefore, the GDOP is not truly geometric, but depends on the stochastic portion of the model. It is, however, "accurate for quantitative predictions within a class of stochastic models defined by covariance matrices that are not too different from each other" [Ref. 15]. Further, it appears that based on the numerical experience of the ARL:UT test system, that it is a good tool for quantitative prediction. [Ref. 20] As will be shown in Chapter VII, while GDOP provides a good relative measure of the geometry, a better means to measure the degree to which the geometry of the observers is needed.

V. JAVA-BASED STOCHASTIC TDOA AND FDOA SIMULATION (JBSTAFSIM)

A. BACKGROUND

JBSTAFSim was written to stochastically explore the differences and similarities of TDOA and TDOA/FDOA GPS-assisted geo-location solutions. It assumes a Multi-platform, GPS-assisted architecture similar to that being developed by ARL:UT as described in the previous chapters. JBSTAFSim allows the user to: create scenarios of various types of sensors and targets defined by straight-forward parameters; distribute these platforms in a simulated operating environment; dictate solver characteristics for the linear-least squares formulation; and adjust the measurement error distribution and correlation. While the purpose of JBSTAFSim was to mainly explore the differences between the two types of solutions in the evenly determined case, it could also be used a tool to investigate and experiment with various solver properties, solution methods, or algorithms in a variety of cases. Further, it could simply be used to experiment with various platform combinations, characteristics, or allocations to provide an understanding of the system's strengths, weaknesses, and limitations. Finally, JBSTAFSim is an object-oriented program which has been written to be extendible. Given an understanding of the model as described in the following sections, the simulation can be extended to satisfy any of the areas of study discussed above or modified to include more complex sensor or target models.

B. DISCRETE EVENT SIMULATION IN JBSTAFSIM

If geo-location of an RF transmitter using TDOA and FDOA techniques was a straight-forward analytical problem, then a simple closed-form solution could be produced on paper. Yet, the signal processing techniques and assumptions presented in Chapter III, show that any realistic geo-location system is a “system” built on highly complex models so complex that any one analytic model designed to mathematically represent the whole system will fail to realistically describe the real-world system. Simulation, on the other hand, provides a means to “evaluate a model numerically, and ... [gather data] to estimate the desired true characteristics of the model” [Ref. 23]. Therefore, simulation provides a means to examine the output measures of effectiveness by numerically exercising the model with inputs that would violate the assumptions of the analytic model and, thus,

provide estimates that are more characteristic of the real-world system. Given this complex mathematical model which acts dynamically and is influenced by stochastic components, JBSTAFSim, then, provides an evaluative, numeric tool which can evaluate and/or estimate the performance of a Multi-platform GPS-assisted geo-location system as it would perform in a realistic environment—an analysis well outside and beyond the bounds of that provided by any mathematical formula, theorem, or set of equations.

In Discrete Event Simulation (DES), simulated time only passes when events are not occurring. “In mathematical terms, we might say that the system can change [state] at only a *countable* number of points in time” [Ref. 23]. Events are listed on a master schedule in time and priority order. The entity which passes simulated time and ensures that events are executed in simulated time is often referred to as the Time Master. When no events are occurring, the Time Master simply advances the simulation clock to the scheduled time for the next event on the event list. The Time Master then allows that event to execute; this event may cause other events to execute or be scheduled with the Time Master. When the event is complete, the Time Master takes control again and executes the next event on the event list, advancing time as appropriate. When there are no more events left to schedule or execute, the simulation is finished.

While Java is not strictly a simulation language, as Java gains popularity, new packages are being developed for many Java-based applications, including simulation. JBSTAFSim utilizes a simulation package named SIMKIT which was developed at Naval Postgraduate School by LT Kirk Stork, USN, in conjunction with Professor Arnold H. Buss. SIMKIT is a package designed to facilitate Discrete Event Simulation (DES). The version of SIMKIT used in JBSTAFSim is a development release written in the JDK 1.0.2 and utilizes the version of Object Space’s Java Generic Library (JGL) written for the JDK 1.0.2. Since SIMKIT is under development, further references to SIMKIT shall refer to the development release version of SIMKIT used in JBSTAFSim. Detailed information about the JGL and SIMKIT can be found at www.objectspace.com and http://131.120.142.115/~stork/simkit_home.html, respectively.

In addition to providing the DES mechanization, SIMKIT also provides a “RandomStream” class to produce psuedorandom variables. While Java does implement a psuedorandom number generator, SIMKIT’s RandomStream class not only provides more suitably random numbers, but also provides the user a library of random variate distributions. JBSTAFSim employs several of these psuedorandom number generators for

platform movement and makes use of SIMKIT's random uniform [0,1] generator to produce the random distributions for TDOA and FDOA measurement errors.

C. MODEL ASSUMPTIONS

Before going too deeply into model assumptions and sensor models, it is important to understand that JBSTAFSim was designed to provide a stochastic simulation for the comparison of TDOA and TDOA/FDOA geolocation systems. Like any good model, the model strives for simplicity wherever possible. As described below, platforms which move in the simulated environment are fairly simple yet retain their basic qualities which differentiate them from each other. Further, the logic of the solver is a very limited to solving for a target's position given the data provided by the sensors. The solver expects an evenly determined case and it does not accept user guidance during the simulation nor does it make decisions using a complex algorithm or neural network. Functions such as these are those which are assumed to be in place in an operational system. In addition to assuming a geo-location system which is properly functioning and that the master has good communications with its slave sensors, the following sections describe the clarifying assumptions made in JBSTAFSim.

1. GPS Data

First, JBSTAFSim assumes that the platform GPS positions and velocities represent truth. For the model, this is a necessary condition since the model must establish some representation of ground truth. In reality, this is also a fairly good assumption given that a survey-grade GPS unit, which is fully Precise Positioning Service (PPS) and precision (p-code) capable, is implemented in the ARL:UT test platform. With this type of equipment, GPS fixes are considered to be accurate to within 10 meters. With respect to velocities, the manufacturer of the GPS receiver in the ARL:UT prototype system asserts velocity measurements accuracy of 0.01 meters per second. [Ref. 24]

As a consequence of using GPS information, the coordinate system used by JBSTAFSim and the ARL:UT system is the earth-centered-earth-fixed coordinate system as established by the World Geodetic System of 1984 (WGS84 ellipsoid). This system places all platforms in an ellipsoid defined by three coordinates (X, Y, Z) in units of meters. In order to assist the user in inputting data and for graphically displaying results,

JBSTAFSim receives and displays data in coordinates Latitude, Longitude, and Height. All calculations and results, however, are measured in meters in the WGS84 ellipsoid.

2. Platform Models

The platform models which function in the JBSTAFSim simulated environment require some clarifying assumptions for each platform's movement within this simulated space. In order to understand how the JBSTAFSim platform models function in the DES environment, Figures 5-1 through 5-4 depict event graphs for each platform.

a. *Ship Model*

The ship model retains the most common features of all five platform models. Like all platform models, the ship keeps track of its current position and velocity in earth centered earth fixed coordinates. The event graph for a ship's movement is shown in Figure 5-1. Upon creation, any ship in JBSTAFSim is provided by the user an operating box in which to steam. Also at creation, the ship chooses independent random uniform X and Y coordinates in this box as its destination. The ship calculates the amount of time it will take to arrive at its destination based on its current speed and distance to the destination. The ship then schedules an event to create a new destination when it arrives at the current destination. In addition to destination events, ships schedule their own change speed events. New ship speeds are selected randomly from a uniform distribution defined by the low and high speed bounds provided by the user. Occurrences of speed change events are modeled as events with an exponential distribution with input parameter provided by the user. The first speed change event is scheduled upon initialization. When a speed change event occurs, in addition to changing the speed of the ship, the waiting change destination event is canceled and a revised arrival time is computed based on the new speed of the ship. A new change destination event is then scheduled for this revised time. Finally, the speed change event schedules a new speed change event to occur at a random time provided by the exponential distribution.

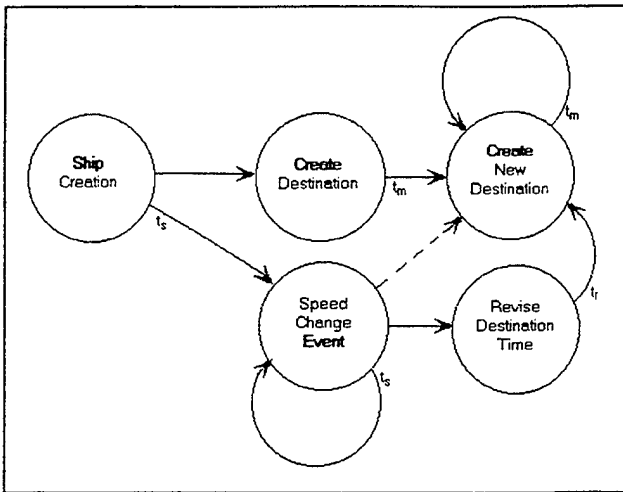


Figure 5-1. Ship Model Event Graph.

b. *Ground Unit Model*

The ground unit model is slightly more complex than the ship model. The event graph for the ground unit model is provided in Figure 5-2. Like the ship model the ground unit keeps track of its position and velocity and schedules change destination events and change speed events. The difference with the ground unit is that it occasionally ceases to move, or does what is called a “take break event.” Break events are scheduled as a random process with an exponential distribution with input parameter provided by the user. The length of such take break events are also modeled randomly by an exponential distribution with input parameter provided by the user. When a take break event occurs, in addition to zeroing the speed of the ground unit, the waiting change speed event and change destination event are canceled. A revised change destination event is scheduled for the remaining transit time to the current destination but only after the amount of break time has elapsed. Similarly a change speed event is scheduled in an amount of time provided by the random distribution plus the amount of rest time for the break. Finally, after the rest period has elapsed, a take break event schedules another take break event in a random amount of time provided from the exponential distribution.

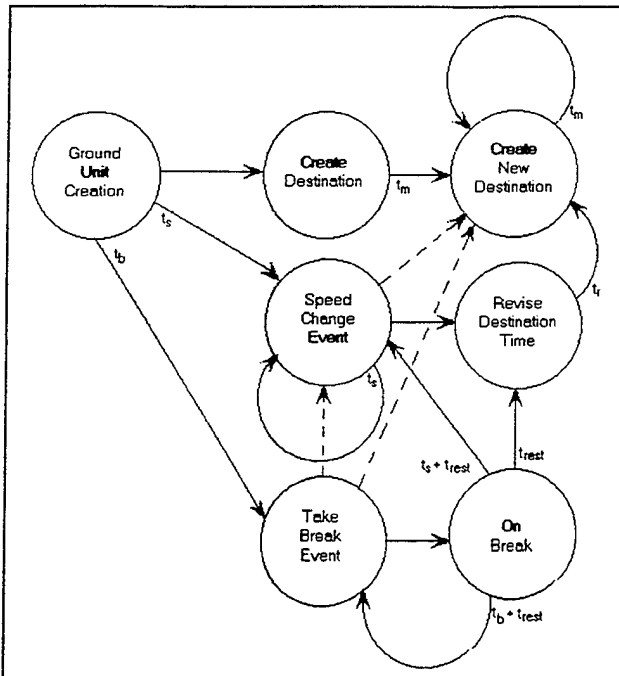


Figure 5-2. Ground Unit Model Event Graph.

c. Aircraft Model

The aircraft model is more simple. Each aircraft patrols a circular “orbit” defined by the circle’s center and radius. In addition to these parameters, the user also defines the aircraft’s base height and how much the aircraft deviates from this base. Since the aircraft moves around its center in a fixed two-dimensional circle, the aircraft’s speed is vital to determining where on the circle the aircraft lies. For any circle with radius r the angle θ at the center of the circle swept by an aircraft traveling along an arc length s is simply defined as $\theta = \frac{s}{r}$. The rate at which this angle changes can be simply defined by

the first derivative: $\frac{d\theta}{dt} = \frac{1}{r} \frac{ds}{dt} = \omega$. Since $\frac{ds}{dt}$ is a measure of the magnitude of the aircraft’s velocity, $|v|$, ω can be computed as $\frac{|v|}{r}$. With this value of ω , the aircraft’s

position on the circle can be computed as a function of time. Thus, the aircraft model need only keep track of ω and update its value when $|v|$ changes. In order to prevent two aircraft from having the same or near similar values for θ , each aircraft is given its own offset angle chosen randomly over the interval $[0, 2\pi]$. With this model, an aircraft need

only update its position on its circular track when polled and then pick a random height adjustment to make to its base height. However, when polled, the aircraft must also update its current velocity state. In order to compute the current velocity of an aircraft, the aircraft need only look a very short amount of time into the future and draw a straight line to this point to set its velocity vector. With this construct in mind, the event graph below is simple to understand. The aircraft need only update positions and velocity when polled or when a speed change event changes $|v|$. As before, speed change events occur randomly; are modeled with an exponential distribution; and cause a new speed change event to be scheduled.

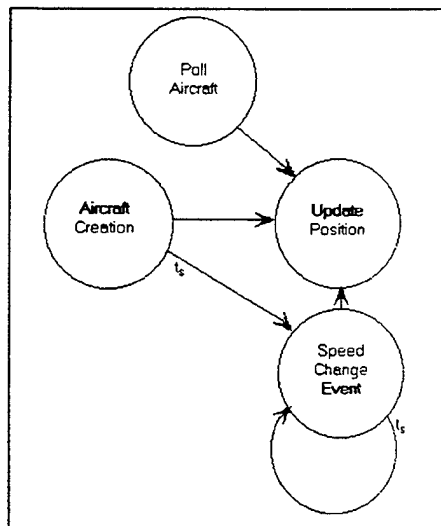


Figure 5-3. Aircraft Model Event Graph.

d. Satellite Model

While much could be done to model satellites of different orbital characteristics, the satellite model in JBSTAFSim is remarkably simple. The reason for this simplicity is for the model to serve its purpose as an evaluative simulation. Certainly, more complex orbits could be included by extending the current model. JBSTAFSim's satellite model assumes a satellite, or satellites, in a circular orbit with no gap in coverage. The model only requires the orbit height, starting and ending footprints of the region of coverage. Simulating continuous coverage, the satellite flies starting point to endpoint and returns back to the starting point. Velocity information need not be entered since, for

satellites in a circular orbit, the magnitude of the satellite's velocity is determined by the height of its orbit: $|v| = \sqrt{\frac{GM}{r + R}}$, where G is the Gravitational Constant in $\text{N}\cdot\text{m}^2/\text{kg}^2$, M is the mass of the earth, r is the radius (height) of the orbit, and R is the radius of the earth. Since the satellite's movement is deterministic, like the aircraft model, satellite position and velocity are updated only when polled. Otherwise, the satellite continues across the sky and returns to its starting point when it reaches the ending footprint point.

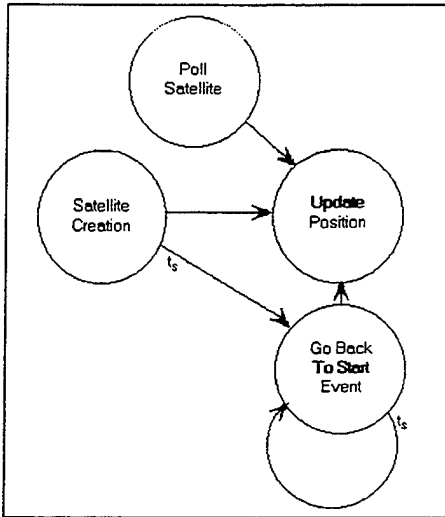


Figure 5-4. Satellite Model Event Graph.

e. Fixed Model

The simplest of all models is the fixed sensor. The fixed model's position never changes and its velocity is set to zero. A call to update a fixed object's position literally results in nothing happening. Simply, the fixed model sends its information on whenever polled and requires no discrete event mechanization.

3. Solver

By using a square root information filter (SRIF) in a linearized least-squares formulation, JBSTAFSim's solver assumes that measurement errors are statistically independent and distributed Normal with mean zero and input covariance. With some modification, a weighting matrix that assumes some correlation could be implemented;

however, since little is known about the true distribution of TDOA and FDOA measurement errors, an estimate of the correlation seems even more unlikely.

In order to have an initial estimate of the target's position, the linearized least squares geo-location solution is started with the results provided by a direct solution. JBSTAFSim solves this set of equations as described in Chapter IV using a Singular Value Decomposition routine adapted from Reference 21. As discussed in Chapter IV, after a fix is computed, the solver then uses the previous solution as the starting position for the subsequent solutions until a request is made for another direct solution to update the current solution. The periodicity of these updates may be set by the user. In an actual Geo-location System, direct solution updates might be requested as a function of many complex variables and parameters, for instance: quality of the previous fix, the dimensionless shock, time since the last fix, by request of the system user, or quality of the received signal. While having a set doctrine for computing direct solutions leaves little room for qualitative decision making algorithms that would exist in the ARL:UT system, it is a simple abstraction for the simulation given the assumptions already made. In addition, by updating the target's initial "guess" position, the direct solution prevents the model from losing track of the target if the previous linearized least squares solution was too great in error. The difficulty with any direct solution lies in the dual solutions provided as a result of squaring the TOA equations. As described earlier in Chapter IV, this ambiguity is generally resolved with some knowledge of where the target is in relation to the observers or by simply comparing the two solutions and throwing out the one that is obviously too distant from the observers. JBSTAFSim assumes that the operational system will have several algorithms for resolving this ambiguity, and, thus, always picks the correct starting point.

4. Measurement Errors

Related to the solver error assumptions, is the actual error mechanization itself. JBSTAFSim measures precise TOA's and FOA's in meters and meters per second. These values are differenced from those of the platform designated as the master. Thus, these differences are the true TDOA's and FDOA's that any sensor would measure in the absence of measurement noise. In order to simulate measurement noise, the truth values are then corrupted by Normal, zero mean random values generated from a distribution

defined by the user. The user is free to define the standard deviation of errors across each TDOA/FDOA measurement. In addition, the user is allowed to correlate the errors between TDOA/FDOA measurements.

The production of measurement errors begins by first producing a covariance matrix using the data provided by the user. While the user is only concerned with the correlation of measurement errors between those differences which include the master as a sensor and not the correlation between slaves, for the three dimensional case, this correlation must nevertheless be supplied in order to build a covariance matrix from which to generate random errors. Further, JBSTAFSim checks this value against the partial correlation with those errors associated with the master to ensure that the given correlation vector generates a positive-definite symmetric covariance matrix from which to generate errors. The covariance matrix is then factored into a lower triangular matrix using the Cholesky decomposition routine. Next, JBSTAFSim uses SIMKIT's uniform [0,1] generator to produce Normal (0,1) variables using the Box and Muller method. Calling the Normal (0,1) variables Z_i , the correlated errors X_i , and the lower triangular matrix C , the measurement errors are produced from the following algorithm (Scheuer and Stoller's method) from Reference 23:

$$\text{For } i = 1 \dots n, \quad X_i = \sum_{j=1}^i C_{ij} Z_j \quad 5-1$$

Equation 5-1 could be changed to produce non-zero mean random numbers by simply adding the mean, μ_i , to the sum on the right hand side. Equation 5-1 also makes clear the need for a positive definite covariance matrix since any other matrix could not be factored into the matrix C .

D. MODEL DATA PROCESSING

As discussed above, JBSTAFSim assumes a GPS-assisted geo-location system that is functioning nominally with good communications between all sensors. JBSTAFSim sensors are polled and fixes are computed every 10 seconds of simulation time. While this poll frequency is not set permanently, it was chosen to correspond in value to that in some initial tests of the ARL:UT system. JBSTAFSim never misses a fix or loses

communication between sensors since these are not characteristics that JBSTAFSim is endeavoring to simulate.

The polling, fix, and result comparison process are depicted in the flow-chart in Figure 5-5 below.

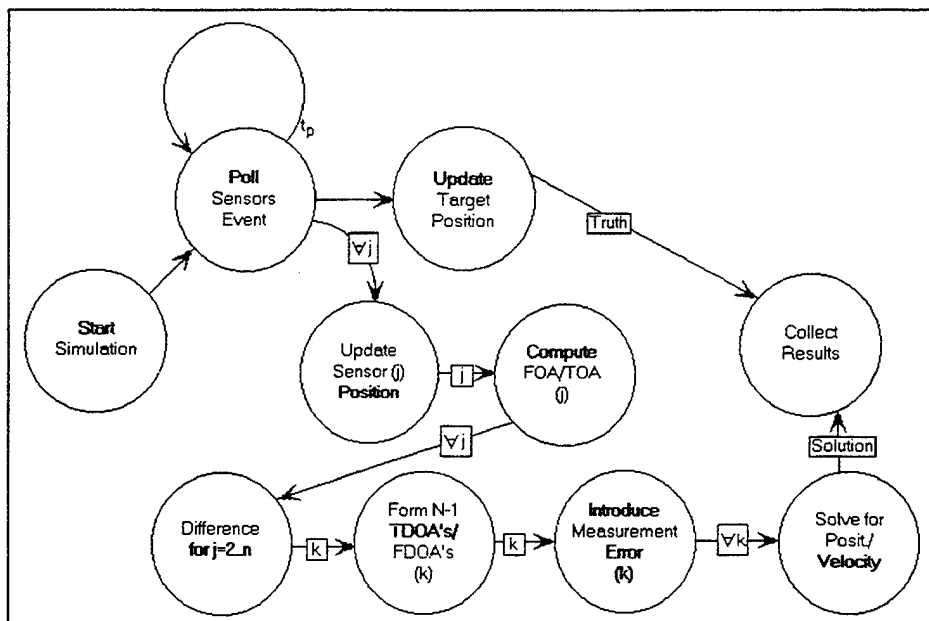


Figure 5-5. JBSTAFSim Flow Chart.

In addition to scheduling the next poll sensors event, the poll sensors event causes the target and all sensors to update their positions and velocities. Sensors, who maintain a reference to the target, compute their TOA (distance to target measured in meters) and FOA (line of sight velocity measured in meters per second) to the target. The slave measurements are then differenced from the master to form N-1 TDOA's/FDOA's. This "truth" data is then corrupted by inducing measurement errors that are modeled by a Normal distribution with zero mean and standard deviation and cross-correlation input by the user. This data and the sensor positions are then passed to the solver. The solver uses the sensor positions and the current guess of the target's position to form the partials matrix for the square root information filter (SRIF). The SRIF then performs the required iterations to solve for the target's position. These results are sent to a data collector that compares the solution to the truth position. The data collector keeps running statistics—mean, variance, 95% confidence interval half-width, largest and smallest extremes—of the miss distance, geometric dilution of precision (GDOP), and size of the area of uncertainty.

Finally, the solver need not be a SRIF. Due to JBSTAFSim's object oriented design, the data returned by all sensors to the master is itself an object which could be processed by any solver. This data object consists of a collection of objects which hold each sensor's position, velocity, TOA data, FOA data, and has methods to evaluate the numerical quantities which make up the partials matrix. The master's data is stored in the first location of this data object vector. In order to form the "DOA's" from the data, the remaining data objects difference their information from the master's. Of course, in a linearized least squares formulation, the partials matrix must be evaluated at some point; this point is supplied by an object which contains the current target estimate position and velocity. When the solver finishes its iterations, it returns its solution as this type of an object. Thus, any solver coupled to JBSTAFSim need only accept the basic objects in JBSTAFSim which define position and velocity for any platform.

E. STATISTICAL RESULT ESTIMATION AND CALCULTAIONS

Since the focus of analysis is centered on the miss distance of the geo-location fix, JBSTAFSim uses this parameter's precision for the terminating condition. Miss distance is simply the Euclidean distance between two points—the truth position and the solution. Since both of these points are represented as objects in Java, the calculation of the miss distance is merely a matter of asking one object the distance to the other.

Thus, JBSTAFSim seeks a precise estimate for the mean of the miss distance. However, since JBSTAFSim runs for no fixed sample size, the model has no control over the confidence-interval half-length which directly impacts the precision of the estimate. Therefore, in order to produce a precise estimate for the mean miss distance and provide a terminating condition, JBSTAFSim employs relative precision. Using relative precision as a terminating condition for the estimation of the mean of a random variable is discussed in Appendix C and in detail in Reference 23. The advantage of using relative precision lies in its ability to provide a precise estimate of the mean miss distance when the sample size is beyond the analyst's control.

In addition to fix miss distance, JBSTAFSim keeps statistical information on the geometric dilution of precision (GDOP) and uncertainty ellipsoid area or volume. Ellipsoid volume is calculated using the eigenspace as described in Chapter IV, Equations 4-19 and 4-20. JBSTAFSim employs a Jacobi Transformation algorithm which consists of a sequence of orthogonal similarity transformations. Each transformation is a plane

rotation designed to annihilate one of the off-diagonal matrix elements. While each transformation may undo previously zeroed elements, each element continues to get smaller and smaller until the matrix is diagonal to machine precision.[Ref. 21] With the eigenvalues of the estimate covariance matrix, the area or volume of the ellipsoid of uncertainty can be calculated as described in Chapter IV. GDOP information is accumulated to rate the quality and consistency of the geometry of the simulation. GDOP calculation is a straightforward application of Equation 4-23.

These statistical results and accumulated data are provided to the user through the model output selections provided by the user at the simulation's initialization.

F. MODEL INPUT AND OUTPUT

1. Input

For any simulation run, JBSTAFSim requires a large amount of initialization data. The solver needs to know how many dimensions and how many sensors with which it will be dealing. In addition the user must set the weights for the TDOA and FDOA data. In practice, these weights would be computed on-line by the system using a hybrid of both equations and algorithms similar to those in Chapter 3 and from experience of the system's performance. The solver can also be set to "batch" mode in which it combines the information of the previous fixes with the current data to produce a fix. In addition to solver information, the user must set the initialization data for each sensor and target—up to five total platforms. As discussed above, by inputting the error standard deviation and error cross-correlation between sensor measurements, the user must also create a distribution for the measurement errors.

While this amount of input is extensive, once it is entered, the model takes over and requires no further guidance by the user. In order to make the model initialization process easier, JBSTAFSim allows the user to save the input data to a file specified by the user. With this file of initialization data, the JBSTAFSim simulation run may be immediately started by simply selecting the input file. With this construct, any initialization need only be entered once; further the data stored in the input file is relatively easy to edit and could be changed in any text editor.

2. Output

As the user chooses, JBSTAFSim outputs simulation results to the screen and/or a data file. If output to a file is selected, JBSTAFSim returns the results of its simulation to a file designated by the user. This file contains the statistical results of three data accumulators for each solution type. As described above, the statistical accumulators keep track of the fix miss distance, GDOP, and size of the uncertainty ellipsoid. At simulation termination, the number of data points, mean, variance, standard deviation, largest and smallest extremes of the data for each accumulator are written to the output file.

If a graphical display has been requested by the user, JBSTAFSim animates the simulated movement of sensors and the target while displaying the TDOA and TDOA/FDOA fixes. In addition a small summary at the bottom of the animation provides the current fix miss distance, an updated average miss distance, and GDOP of the current fix. As previously mentioned, the graphical display is in the latitude, longitude, height coordinate system—although height is not displayed in the animation. The latitude scale on the left of the screen provides a quick reference for the scale of the display. Each tenth of a degree of latitude represents six nautical miles or 12,000 yards. Thus, given that the coordinates of each sensor in the simulation is represented by WGS84 Ellipsoid coordinates on the order of 10^6 - 10^7 meters which translates to order 10^1 latitude and longitude degrees, and is then translated into integer screen pixels displayed on a small scale (large area) chart, it should come as no surprise that most platforms in the display do not tend to move with great speed, especially when fixes are being taken every 10 seconds of simulated time.

Despite these facts and the fact that the screen images provide little analytical information, the graphical display does provide a very effective and quick means to ascertain what is actually happening in the model for both the analyst and for any audience of the analysis. Further, the ability to provide such an animated stochastic simulation across a variety of computer platforms must be considered a true asset for analyst who must present the analysis to an (any) audience. Yet, Java is able to deliver not only on this ability, but also allows the analyst and audience to be separated by thousands of miles with only the Internet and a Web browser between the two. Accordingly, the ability for JBSTAFSim to function as an applet is described in the next chapter.

VI. JBSTAFSIM AND THE WORLD WIDE WEB

As its name implies, JBSTAFSim is written in Java—specifically, the first release of the Java Development Kit (JDK 1.0.2). Java is an object-oriented programming language which is currently gaining increased popularity in the programming world. One of the reasons Java has become so popular is its run time library which gives Java bytecode platform independence. The same code (without recompiling) can be used on Windows 95, Solaris, UNIX, Macintosh, and so on. Given the exponential growth of the Internet, this is a true advantage, if not necessity, for any programming language. As a result of this portability, JBSTAFSim can not only run on any of the machines listed above as an application, but also can run as an applet on any machine using a Java enabled Web browser. The JBSTAFSim applet requires no special programming, code, recompilation, or platform. It only requires a Web browser, nothing else. Therefore, due to Java's portability, JBSTAFSim can be run and its results examined instantly from anywhere and on any machine with little overhead. Thus, Java is a full featured programming language that provides the ability to be run from the Internet on any machine via a Web browser. There are many more advantages to programming in Java, but simply stated, it is a simple, robust, portable, high performance, and dynamic language which allows for efficient, object-oriented, distributed code. For a detailed explanation of Java's design and accomplishments, Sun has published a "White Paper" which can be found at "<http://java.sun.com/whitePaper/java~whitepaper-1.html>."

Java programs that work within a Web browser are called applets. The idea behind an applet is simple: "users download bytecodes from the Internet and run them on their own machines" [Ref. 22]. Some might ask why use a Java applet on a Web page to run programs? Since Java is a full programming language, it has all the power of any "true" programming language with the ability to run dynamically on the host computer via the Internet. Without Java, if you were to design a "dynamic" Web page that could respond to a user or a stochastic simulation, each change in the Web page would require that data be sent to a CGI script on the server. The script would need to process the data and send the results back to the browser—probably requiring the creation of a new Web page on the fly. This is a horror to program and without a doubt will be slow. With Java, once the applet's bytecodes are downloaded, the power of the programming language is available to run without updates from the server. In order to protect the host computer system from malicious bytecodes, Java implements a "sandbox" that restricts the applet

from corrupting memory outside the applet's process space. In addition, secure Web browsers, like Netscape Navigator, or browsers that have their security features enabled by the user (Microsoft Internet Explorer) will prevent applets from writing or reading local files. Applets can include graphical user interfaces, can catch mouse movements and clicks, and can interpret text inputs. Further, all processing is performed by the user's system; thus, the originating server is not continually bombarded with hits for information and number crunching. In addition, the user is not hampered by bandwidth when running an applet (although, bandwidth could be an issue *downloading* the applet). [Ref. 22]

The power of Java and the applet concept above can be realized within the nature and abilities of the JBSTAFSim applet itself. Quite simply, the only difference between the JBSTAFSim applet and JBSTAFSim application is *one* Java class which declares that it is an applet and will oversee the events which occur in the JBSTAFSim simulation. With no revisions or recompilations, every bit of code that the simulation uses as an application is used by the applet. Thus, the full power and stochastic nature of the JBSTAFSim application can be delivered anywhere to a Web browser via the Internet with precisely the same code. An illustration of the JBSTAFSim applet running in Netscape Navigator is shown in Figure 6-1.

As an example of the power, flexibility and utility of this design, consider how the JBSTAFSim applet is currently configured to run from the World Wide Web. A user, somewhere on some operating system with a Java enabled Web browser starts the JBSTAFSim applet by visiting the appropriate Web page. This Web page currently exists on a server which is running on a SPARC clone with NEXT as its operating system. The JBSTAFSim bytecodes are retrieved by the server from another SPARC clone which uses SOLARIS as its operating system. The JBSTAFSim bytecodes consist of bytecodes compiled on a Windows-95 system. This code implements SIMKIT bytecodes which were compiled on a Macintosh. Further, the SIMKIT bytecodes implement bytecodes from the Java Generic Library that were compiled on some system unknown to the author of JBSTAFSim. The server, ignorant to all of this, delivers all these bytecodes to the user's system for execution in the user's Web browser. The point is: it is irrelevant from what system the code originated; from where the code is coming; and to where the code is going for execution. The bytecodes need only be delivered to the user's machine which will locally process the bytecodes' information quickly and efficiently—all bytecodes run the same everywhere.

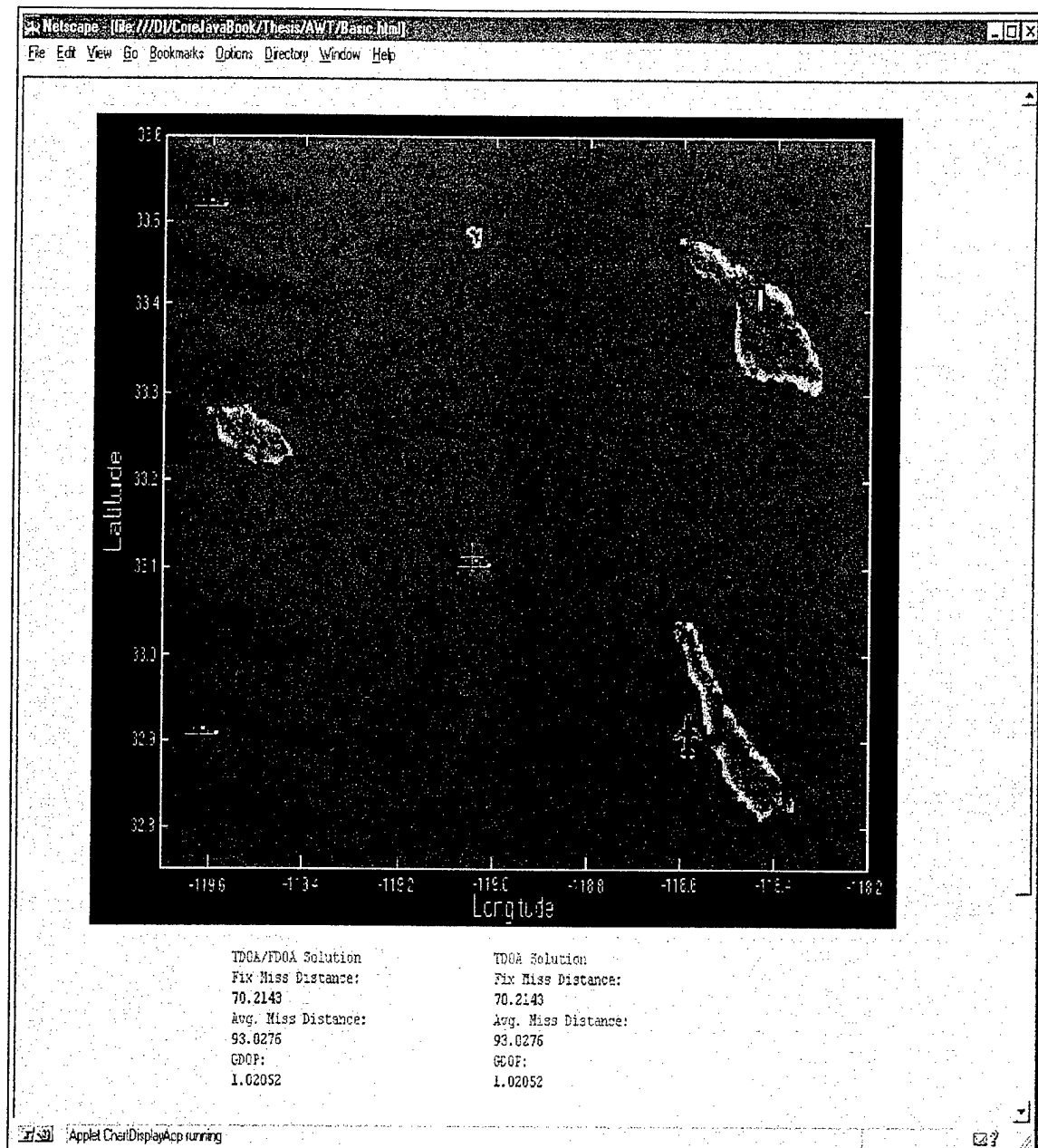


Figure 6-1 JBSTAFSim Applet in Netscape Navigator

For both the analyst and the audience, this is a powerful tool. The analyst's sponsors can quickly inspect a product or proposal without special software, hardware, or large investments of time and money. Further, the tool is extendible and can be coupled with other models regardless of the operating system or environment in which they were originally created. In the case of JBSTAFSim, in addition to ARL:UT and faculty at

Naval Postgraduate School, the applet's audience quickly included the Naval Information Warfare Activity and other Commander, Naval Security Group offices and activities. Each activity only requiring a Web browser and a connection to the Internet. Certainly, in this light, JBSTAFSim could represent one small component in what has the potential to be a robust, high-performance, and distributed modeling architecture for the DOD and its community.

VII. SIMULATION ANALYSIS

A. BACKGROUND

Several simulation scenarios were conducted to evaluate and compare the performance of both the TDOA and mixed TDOA/FDOA solutions. Both two dimensional and three dimensional fix scenarios were conducted. Within these two cases, several parameters were varied to quantify their effect on both solution types, including: measurement error variance, the correlation between measurement errors, geometry of the sensor network, and the frequency that the SRIF requests direct solution updates.

B. TWO DIMENSIONAL GEO-LOCATION SCENARIO RESULTS

The two dimensional case consisted of a sensor network of two ships and a satellite geo-locating a ship, as depicted in Figure 7-1. This scenario was run seven times each for four measurement error correlation values. The seven runs varied: the frequency—continuous, every 10 fixes, and every 20 fixes—of direct solution updates; the TDOA measurement error variance; and the FDOA measurement error variance. The measurement correlation values were: 0.0, 0.1, 0.5, and 0.9 error correlation between all measurements. The TDOA measurement error variance was examined for the values of 60^2 and 30^2 meters. The FDOA measurement error variance was examined for the values of 0.2^2 meters per second and 0.1^2 meters per second. Sensor to target geometry was mediocre with GDOP averaging 1.5 with minimum and maximum values of 1.3 and 2.6, respectively. For reference, the values of 60^2 meters and 0.2^2 meters per second for the respective TDOA and FDOA measurement error variances are approximately equivalent to those empirically experienced in the ARL:UT system.

1. Geo-Location Accuracy

Results from these simulation runs are depicted in Figure 7-2 through Figure 7-17 with some summarized information provided Table 7-1. The distance from the solution's position to the target's actual position—the miss distance—is the primary measure of effectiveness (MOE), while the area of the 2-sigma uncertainty ellipse is a secondary MOE. Thus, the primary MOE is a measure of the solution's accuracy while the

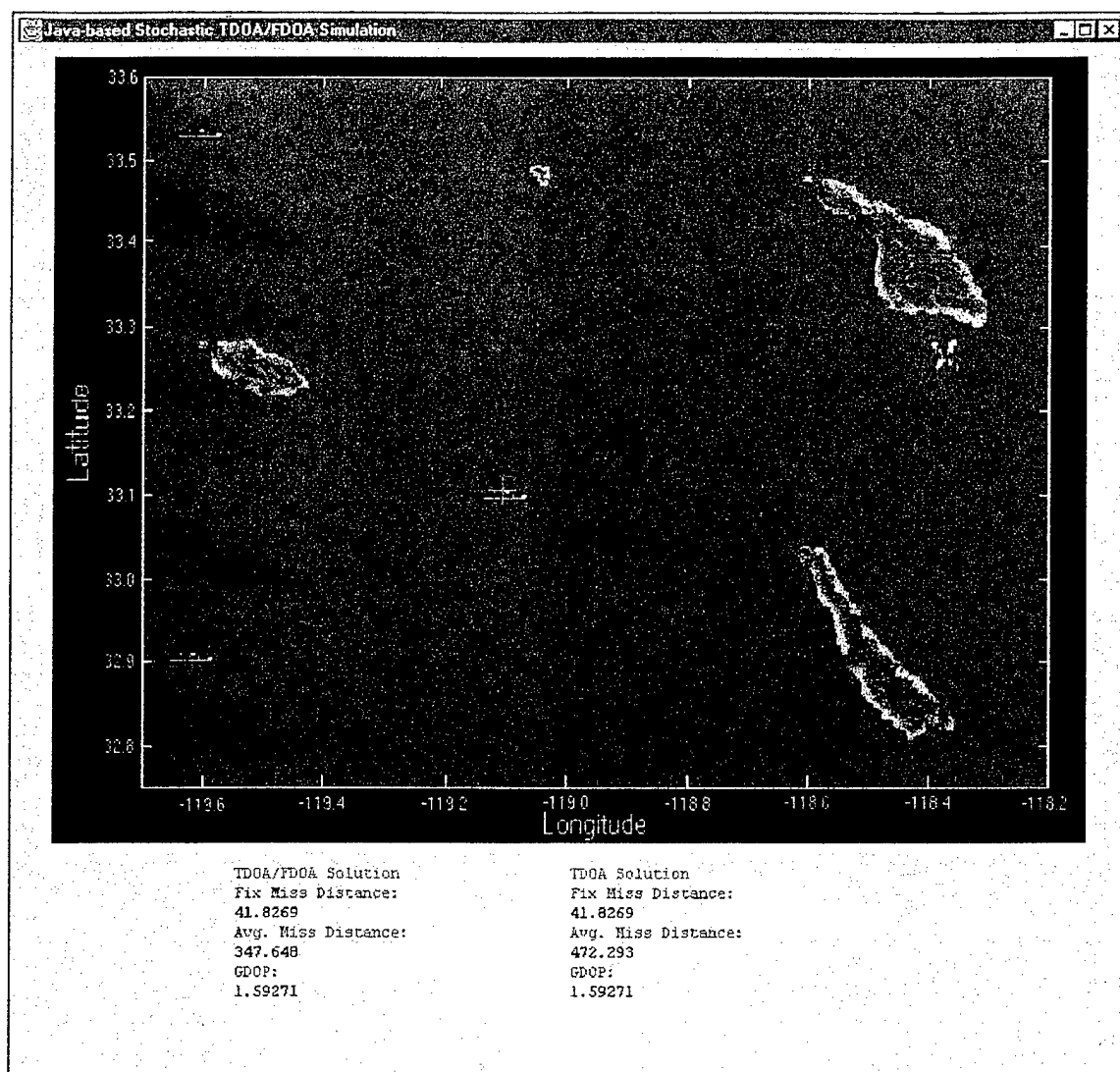


Figure 7-1 Two Dimensional Scenario Sensor Allocation

secondary MOE is a measure of the solution's ability to rate its precision. In terms of the miss distance, the primary MOE, Figures 7-2 through 7-8 show that the mixed TDOA/FDOA solution maintains first order stochastic dominance for each simulation run which varied the fix update frequency in addition to the cases where the TDOA and FDOA measurement error variances were contrasted.

a. Fix Updates

In order to prevent JBSTAFSim's solution from diverging due to a poor target estimate, direct solutions are provided at a regular update interval. This interval

was varied from continuous updates, to updates after every ten fixes, and for updates after every 20 fixes. Clearly, as seen in Figure 7-2, the continuous direct solution updates are degrading the accuracy of both solutions, but particularly so for the TDOA solution. These continuous update distributions are so poor, they are dismissed from further analysis. Notice that while the TDOA solution and mixed T/FDOA solution are more similar in the "10 fix update" and "20 fix update" cases, the "10 fix update" scenario offers the best shape to this distribution. This can be seen in the relative location of the point in the distribution where the curve makes its "right hand turn" in the upper quantiles. Notice that this location tends to be higher and more to the left in the "10 fix update" scenario.

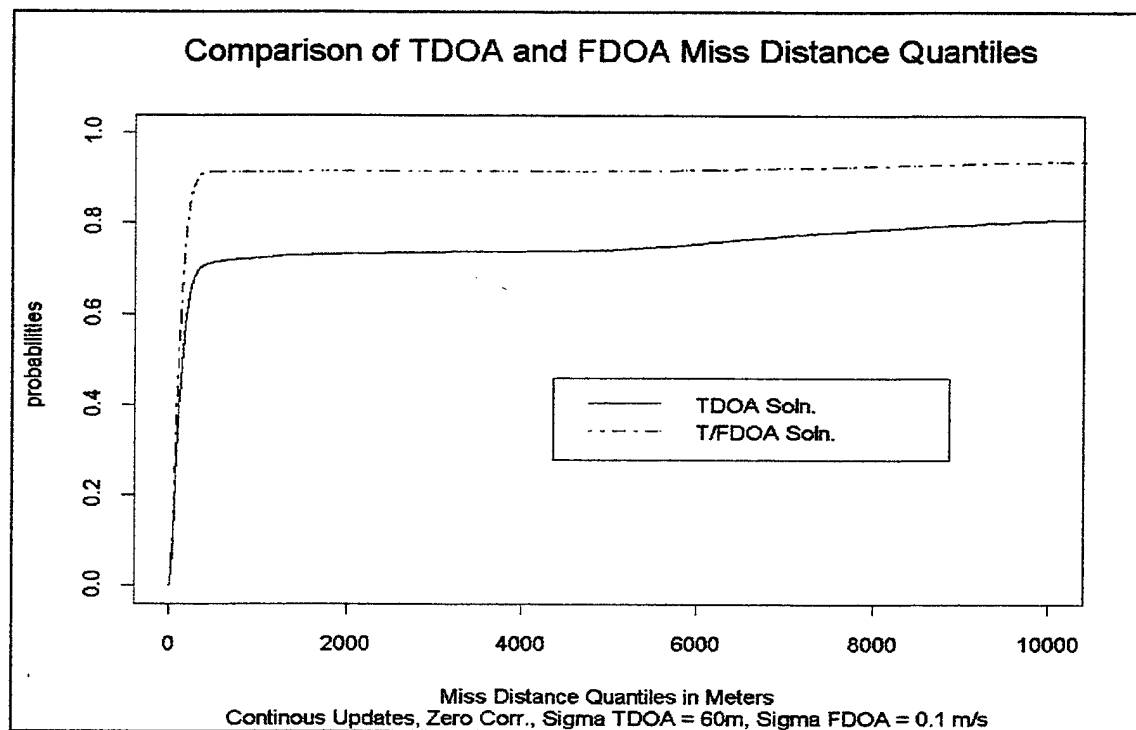


Figure 7-2 Comparison of TDOA and T/FDOA Miss Distance Quantiles

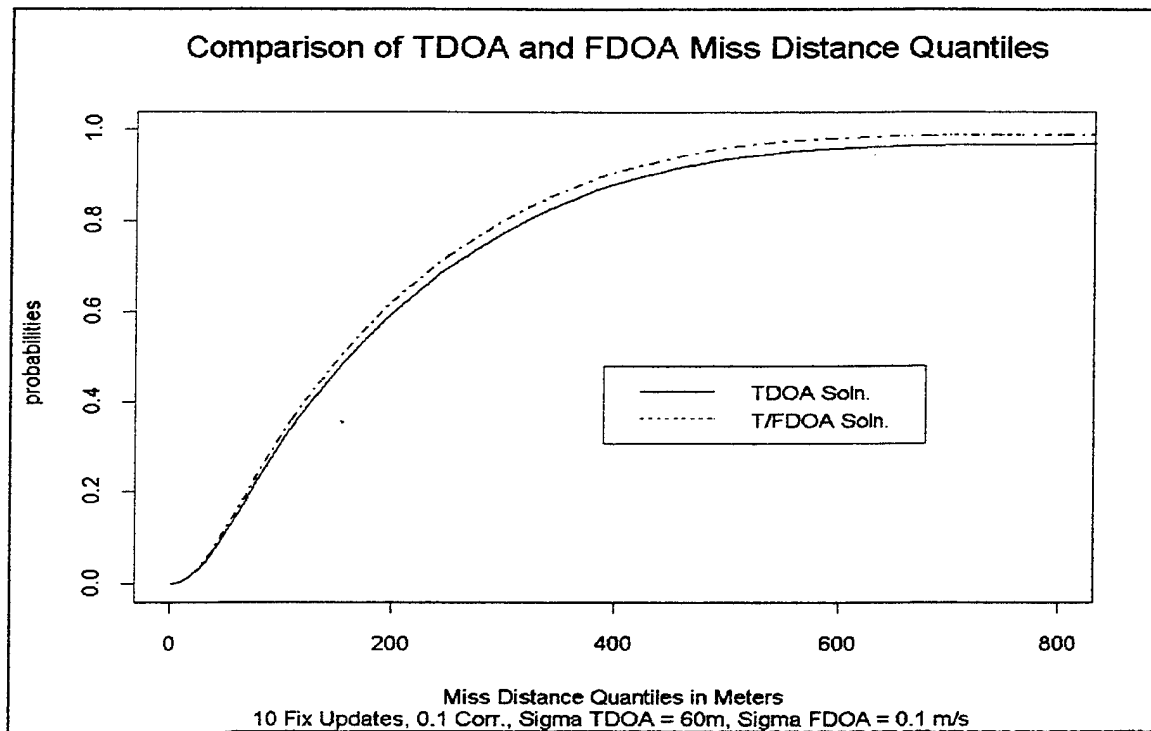


Figure 7-3 Comparison of TDOA and T/FDOA Miss Distance Quantiles

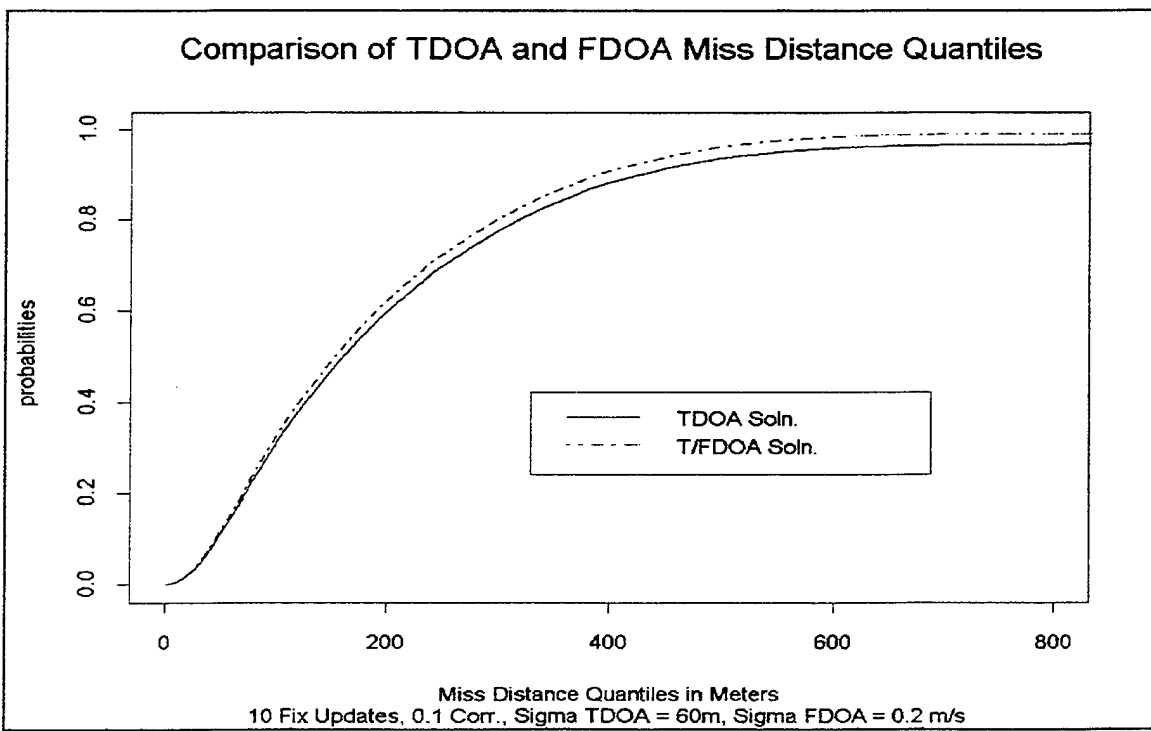


Figure 7-4 Comparison of TDOA and T/FDOA Miss Distance Quantiles

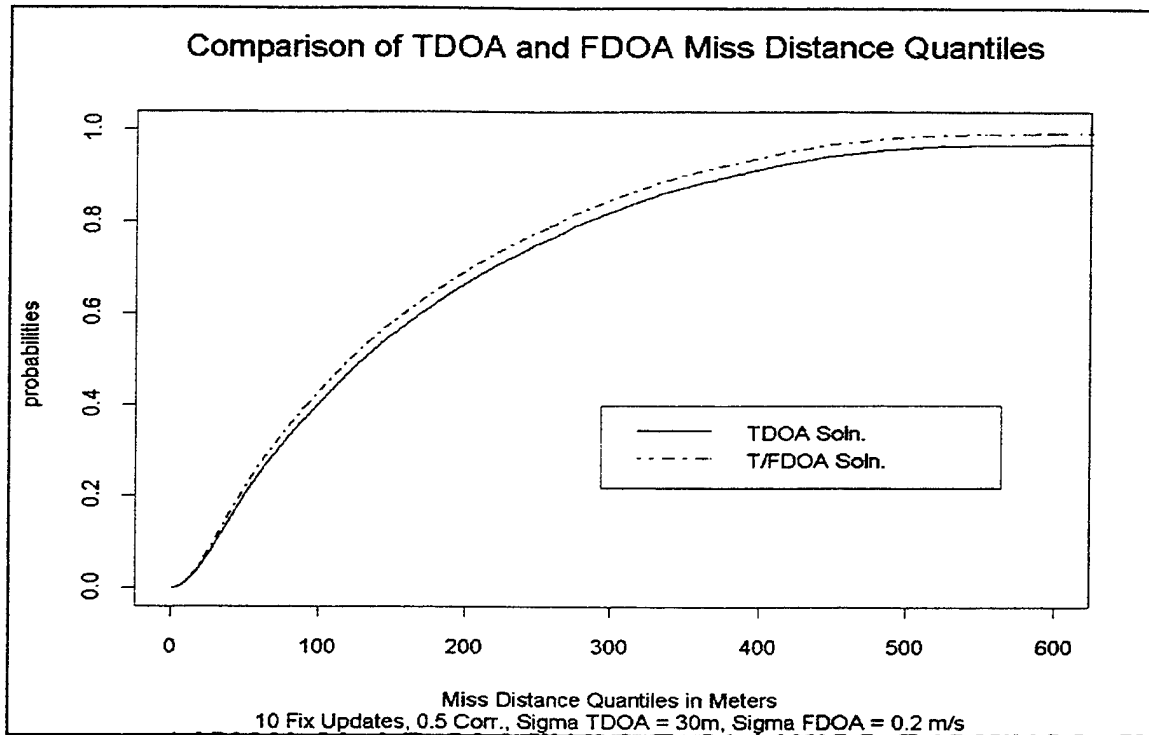


Figure 7-5 Comparison of TDOA and T/FDOA Miss Distance Quantiles

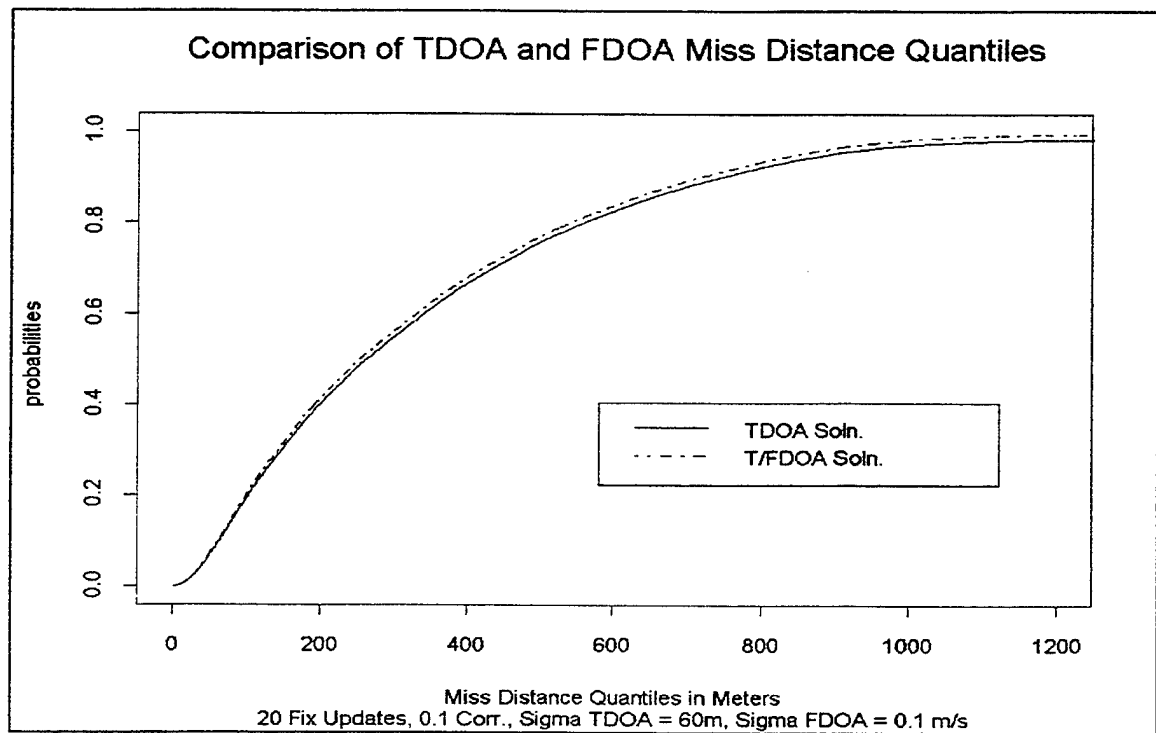


Figure 7-6 Comparison of TDOA and T/FDOA Miss Distance Quantiles

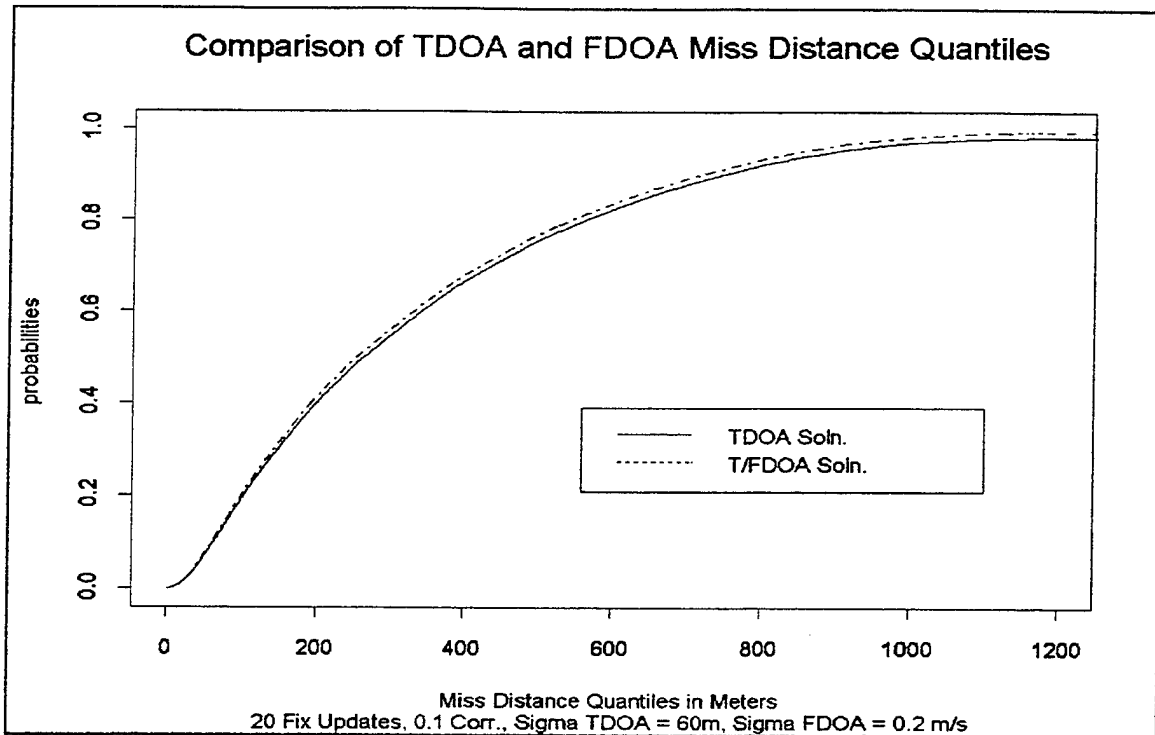


Figure 7-7 Comparison of TDOA and T/FDOA Miss Distance Quantiles

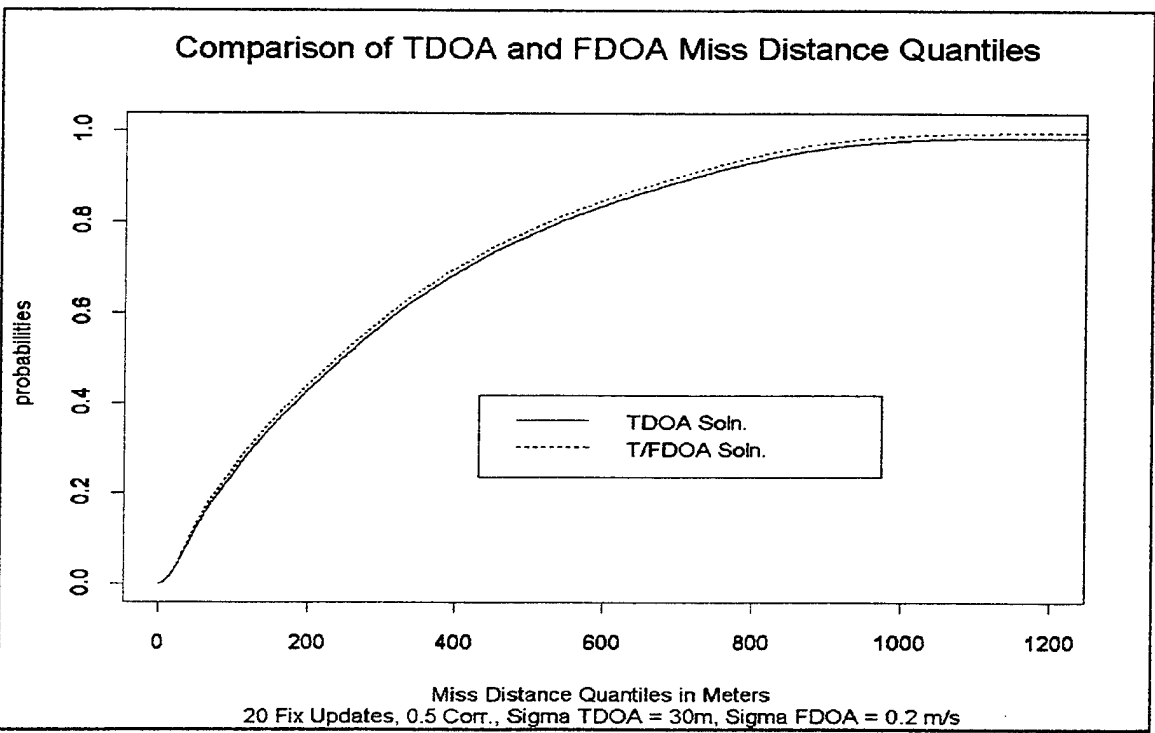


Figure 7-8 Comparison of TDOA and T/FDOA Miss Distance Quantiles

b. Solution Type Performance

In each scenario above, the mixed T/FDOA case dominates the TDOA solution. The T/FDOA solution's dominance is largest in the upper portion of the distribution after the characteristic curve as noted above. In order to show these contrasts more clearly, Figure 7-9, below, plots some of the scenario results together. In this figure, a horizontal line representing the 0.95th quantile is drawn to intersect the solution distribution curves. This line intersects the mixed T/FDOA solution, with measurement error variances of 30^2 m and 0.2^2 m/s, 100 meters to the left of the TDOA solution with a measurement error variance of 30^2 m. Thus, there is a significant difference between the two solution types in the upper areas of their distributions.

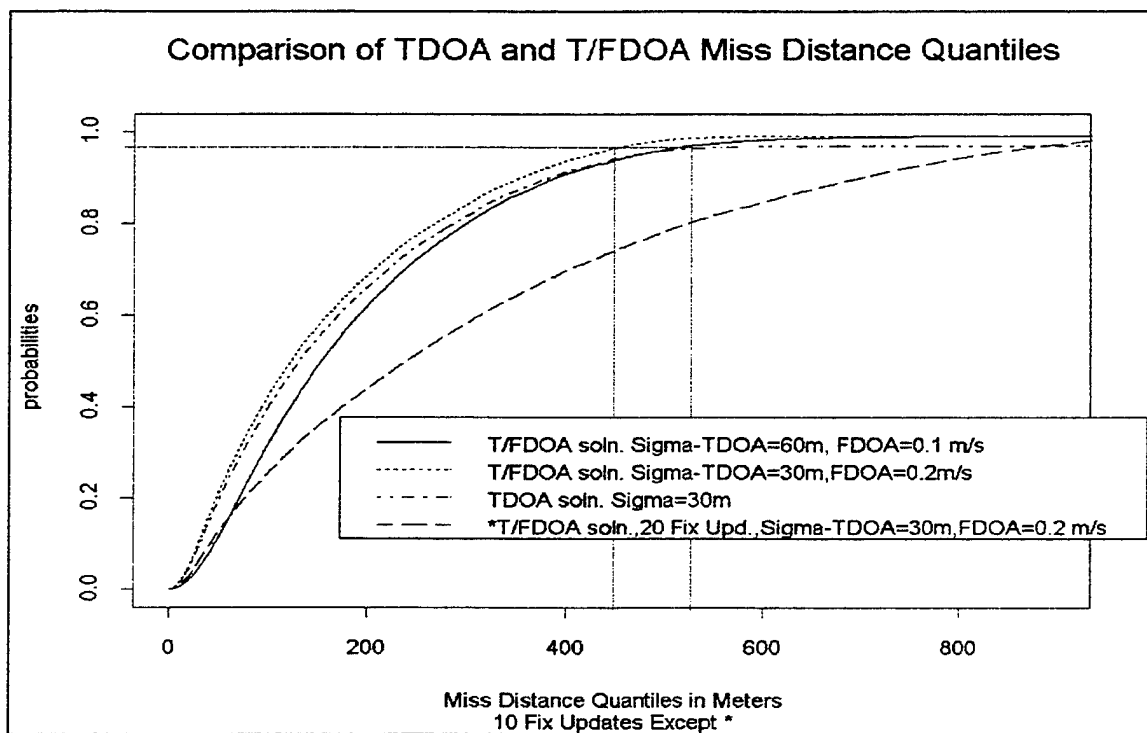


Figure 7-9 Comparison of Several TDOA and T/FDOA Miss Distance Quantiles

Even more interesting, notice that the mixed solution curve identified above (error variances of 30^2 m and 0.2^2 m/s) outperforms a mixed solution with an improved FDOA error variance of 0.1^2 m/s and a degraded TDOA measurement error variance of 60^2 m. Further, note that at this quantile, this second mixed solution curve (error variances of 60^2 m and 0.1^2 m/s) has started to dominate the TDOA solution with

an improved TDOA measurement error variance of 30^2 m. Thus, this T/FDOA solution outperforms that of the TDOA solution in the upper quantiles where either measurement error or geometry is degrading the accuracy of the fix. Therefore, despite a larger error variance in the TDOA measurement errors, a mixed T/FDOA solution provides more accurate fixes when facing situations that are more difficult for the TDOA solution to solve by itself. Thus, the designers or users of a system such as this would desire a larger reduction the TDOA measurement error variance as compared to that in the FDOA measurement even though it is the FDOA information which will improve the accuracy of the fix.

c. Upper Quantile Performance

The most striking feature of these curves is the sharp, near right-angle turn that the distributions take at the upper quantiles. The effect of rotating any of the quantile plots 90 degrees to the left so that the actual quantiles are on the X -axis make the “right-angle turn” feature of the distribution appear even more pronounced. With this understanding of the shape of the distribution, gaining an intuition of the difference between the two solutions that transcends first order stochastic dominance can be gleaned. As pointed out, the area in which the two solution distributions differ the most can be seen in the separation between the curves in the higher quantiles. In this light, the mixed T/FDOA solution’s dominance can be applied to the outliers of the distribution. In the cases where noise or geometry degrade the TDOA solution, the additional information from the FDOA measurements increases the accuracy of the T/FDOA solution over that of TDOA solution. Thus, it is especially in these cases of bad geometry or large noise that the mixed solution outperforms the TDOA only solution. Unfortunately, at each individual data point, it is unclear from these results whether it is the geometry or the measurement error which causes the size of the error in the location of the target. Two interesting plots of the mixed T/FDOA performance distribution are shown in Figures 7-10 and 7-11 below. Notice in Figure 7-10 that the lower FDOA measurement error variance leads to better results as would be expected. In addition, holding the FDOA measurement error variance at 0.2^2 m/s and decreasing the TDOA measurement error variance leads to a distribution which dominates the other two distributions. These are not unexpected results; however, Figure 7-11 turns these results around. The distribution with the worst measurement error variance dominates. Notice that Figure 7-10 displays

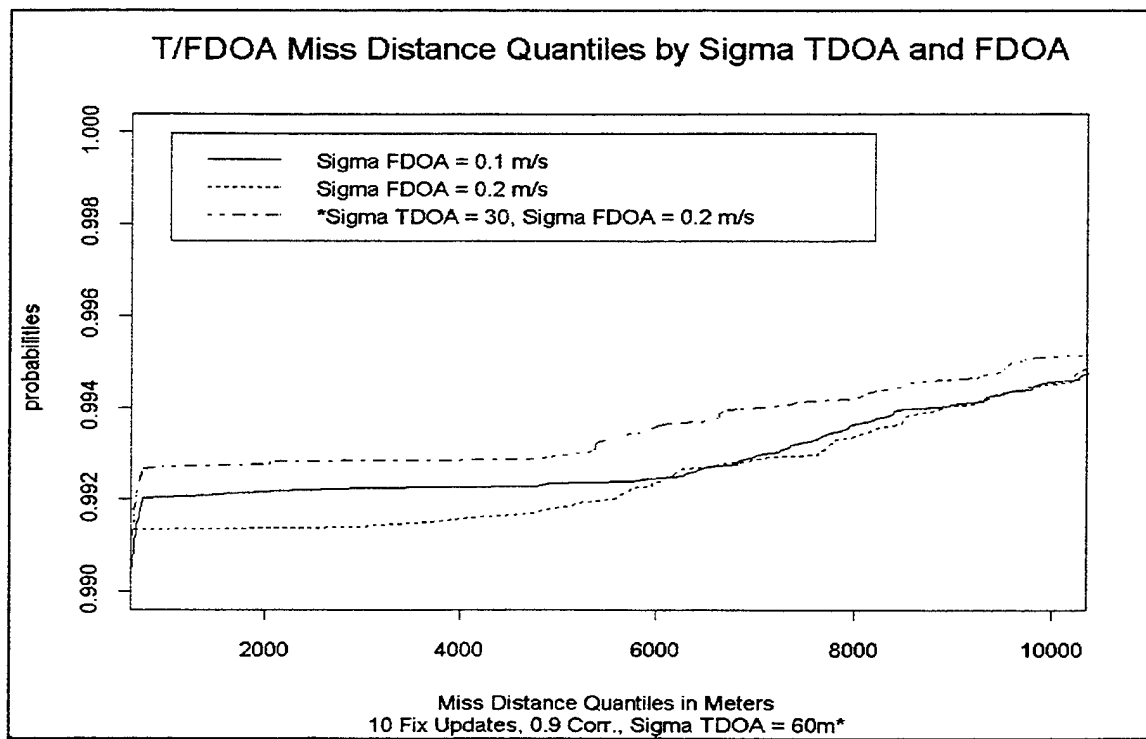


Figure 7-10 Comparison of TDOA and T/FDOA Miss Distance Quantiles

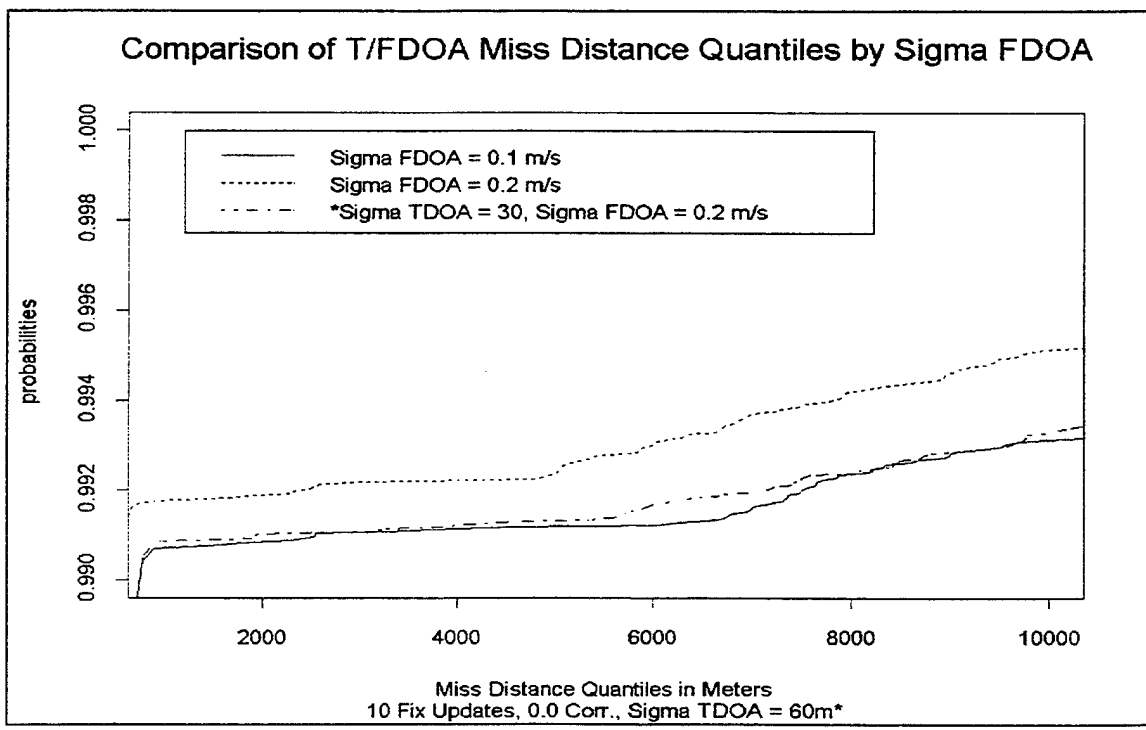


Figure 7-11 Comparison of TDOA and T/FDOA Miss Distance Quantiles

distributions where the measurement error correlation is high—0.9; yet, Figure 7-11 portrays the results from 0.0 measurement error correlation. It is difficult to describe why measurements with higher error correlation should outperform those with no correlation. Further, it is not obvious that measurements with a larger error distribution should outperform those with better measurement data. Yet, this is exactly what these figures indicate. These results lead to two avenues of discussion—geometry and uncertainty.

If the results of Figure 7-10 and 7-11 were functions of geometry, it is not clear from the GDOP measurements the degree to which geometry is degrading the accuracy of the fix. Recall from Chapter IV that GDOP is not really a measure of geometry but a description of the diagonal elements of the estimate covariance and weighting matrices. It is more a measure related to what the system thinks *might happen* versus that of what is *actually happening* in the system. In Reference 13, Chaffee and Abel, the authors of JBSTAFSim’s direct solution theory, discuss how the null space of the direct solution relates to the two roots of the direct solution. Perhaps, the null space could provide some information with regard to the geometry of the observers and their target; however this type of analysis might only describe the geometry of the TDOA surfaces. It is more than conceivable that the ability of the mixed T/FDOA solution to be more accurate in the highest quantiles of the miss distance distribution—the outliers—can be attributed to cases where the geometry of the TDOA surfaces is poor yet the geometry of the FDOA surfaces is sufficient enough to improve the mixed solution. In view of the shape of the miss distance distributions in the upper quantiles, this theory could describe the sharp “right hand turn” as described above. The solution to rating the geometry of a network of observers in relation to their target is beyond the scope of this thesis; however, JBSTAFSim would be the perfect tool to empirically experiment with this theme of geometry. The second issue, fix uncertainty, deserves a section unto itself to describe.

2. Uncertainty of Geo-locations

If geometry is not all or only part of the answer to the unexplained improvement in the accuracy of the solution in the presence of correlation, then, perhaps, the uncertainty of the estimate may provide another avenue to help explore this issue. Figures 7-12 through 7-17 display the distribution of the area of the two-sigma uncertainty ellipse

associated with both solution types for the continuous, 10 fix, and 20 fix update scenarios. In these graphs, the standard span (the area inside the “whiskers”) of the distribution is drawn at 1.5 times the Inter-Quartile Range beyond the quartiles. All points outside the standard span are drawn individually. With this construction, it is easy to view the density of the outliers.

When the TDOA solution is compared with that of the mixed T/FDOA solution, the main difference between the two plots is the density of the outliers. Another way of indicating the larger spread of the T/FDOA uncertainty ellipse size is through the comparison of the standard deviation of this area. These quantities are summarized in Table 7-1 below.

Error Correla- tion.	Continuous Update		10 Fix Update		20 Fix Update	
	Sigma	Sigma	Sigma	Sigma	Sigma	Sigma
	TDOA	T/FDOA	TDOA	T/FDOA	TDOA	T/FDOA
0.0	13571.4	56457.7	5618.3	13197.1	4711	10962
0.1	13175.6	55483.4	5875.9	12765.0	4901	9659
0.5	13389.5	55616.6	5643.1	14718.5	4703	9658
0.9	13708.7	55613.3	5576.7	14228.6	4610	11007

Table 7-1 Distribution of TDOA and T/FDOA Ellipse Size Standard Deviations

First, notice that the ellipse size standard deviations for the mixed T/FDOA solutions are much larger than those of the TDOA solutions in all cases. This is confirmed by the outlier spread and densities in the graphs below. Second, notice that in the 10 Fix Update scenario (where the accuracy of the 0.0 correlation was compared to that of the 0.9 correlation in Figures 7-10 and 7-11 above) the solution which produced more accurate results—0.9 correlation—has a larger standard deviation of ellipse area.

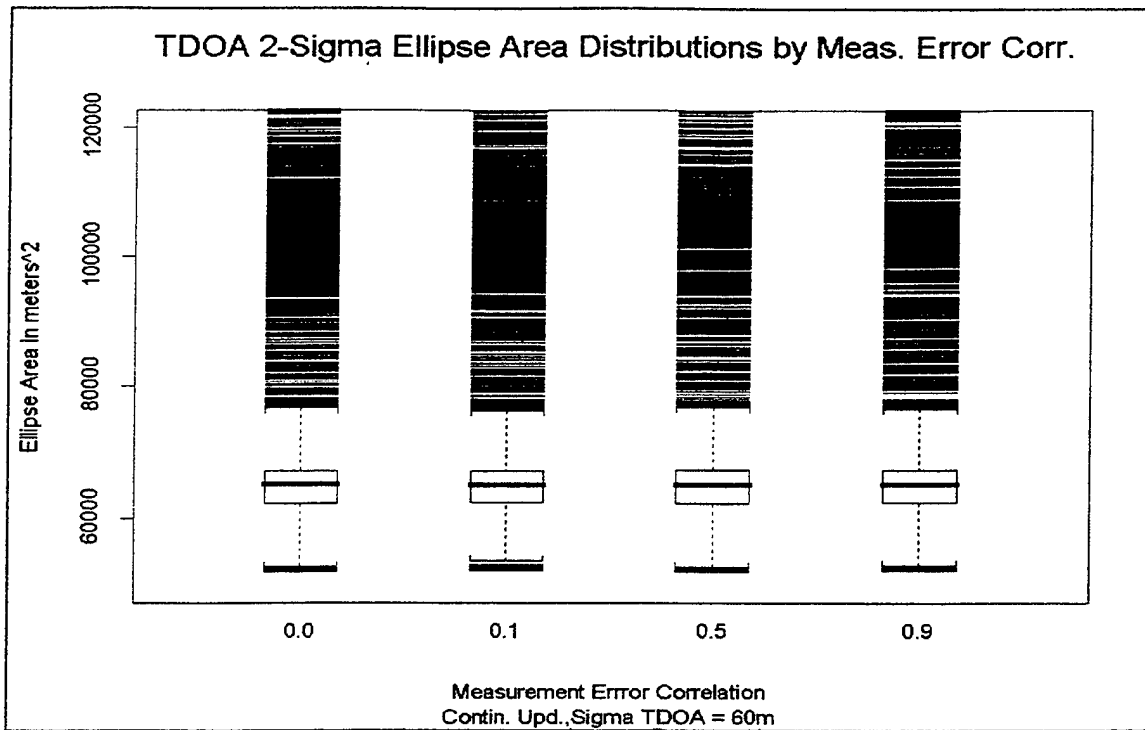


Figure 7-12 Comparison of TDOA Ellipse Areas by Correlation

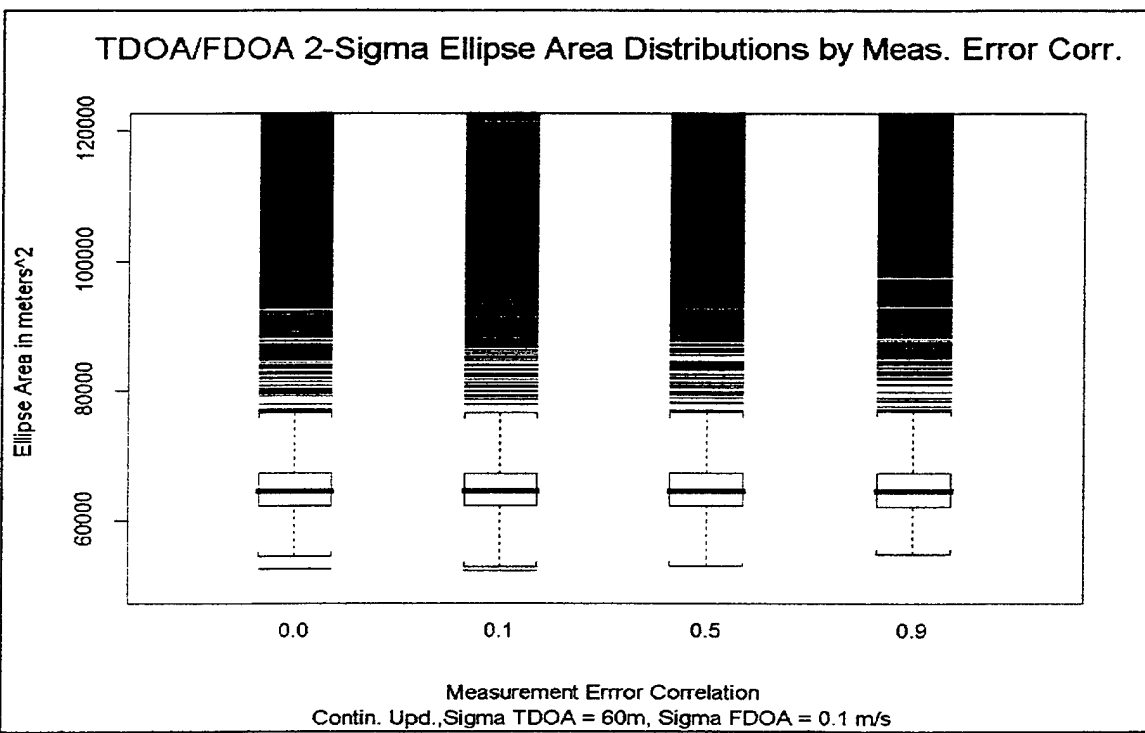


Figure 7-13 Comparison of T/FDOA Ellipse Areas by Correlation

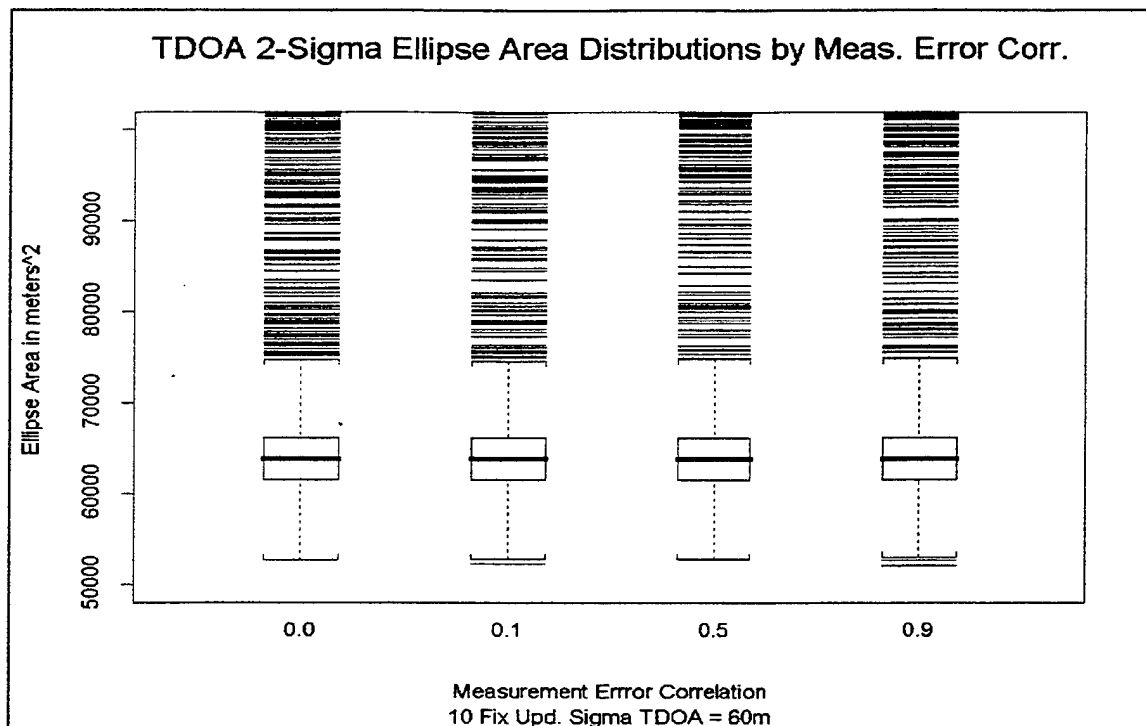


Figure 7-14 Comparison of TDOA Ellipse Areas by Correlation

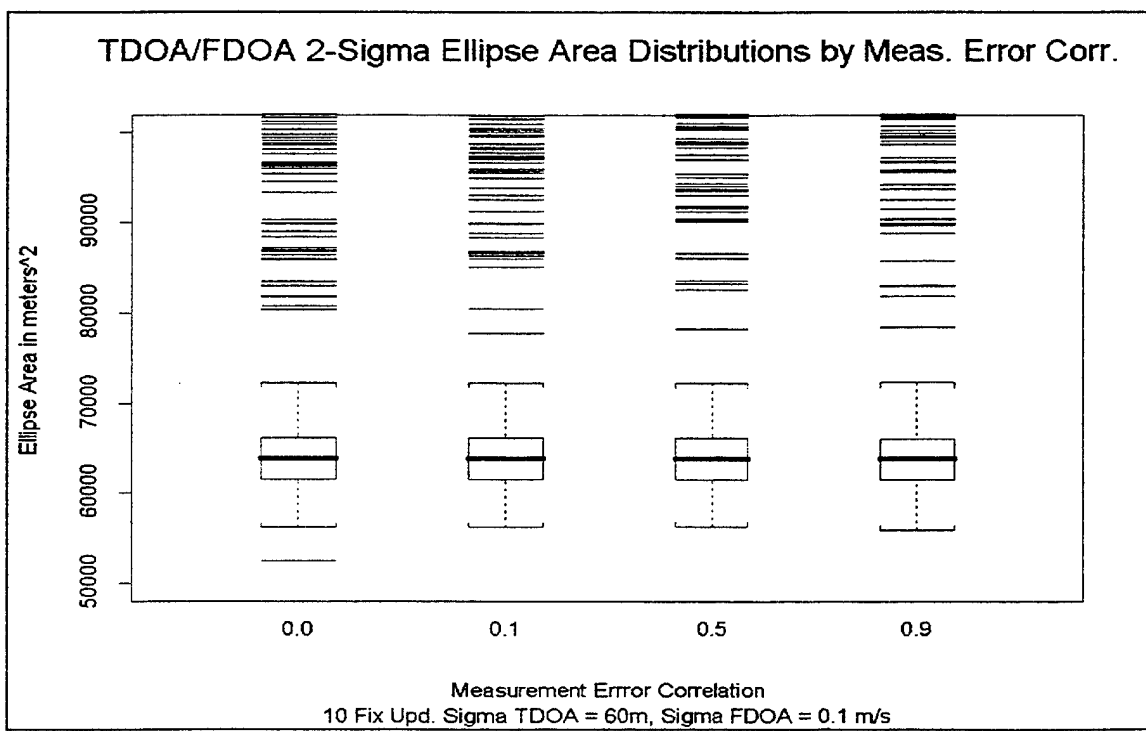


Figure 7-15 Comparison of T/FDOA Ellipse Areas by Correlation

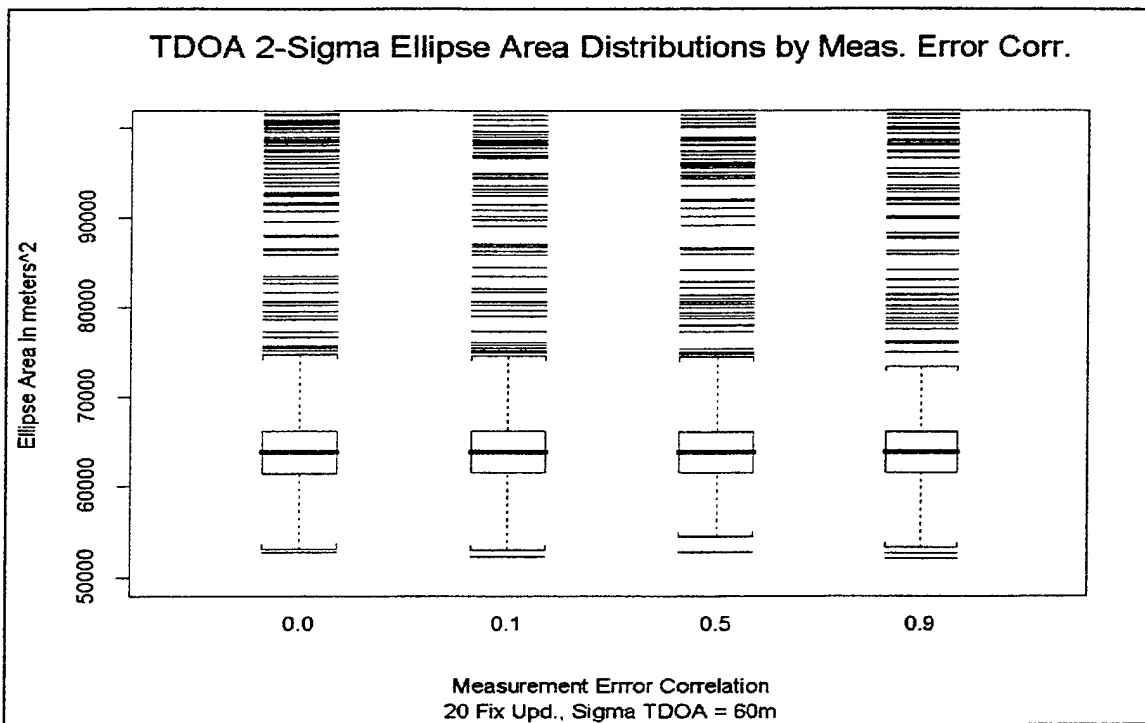


Figure 7-16 Comparison of TDOA Ellipse Areas by Correlation

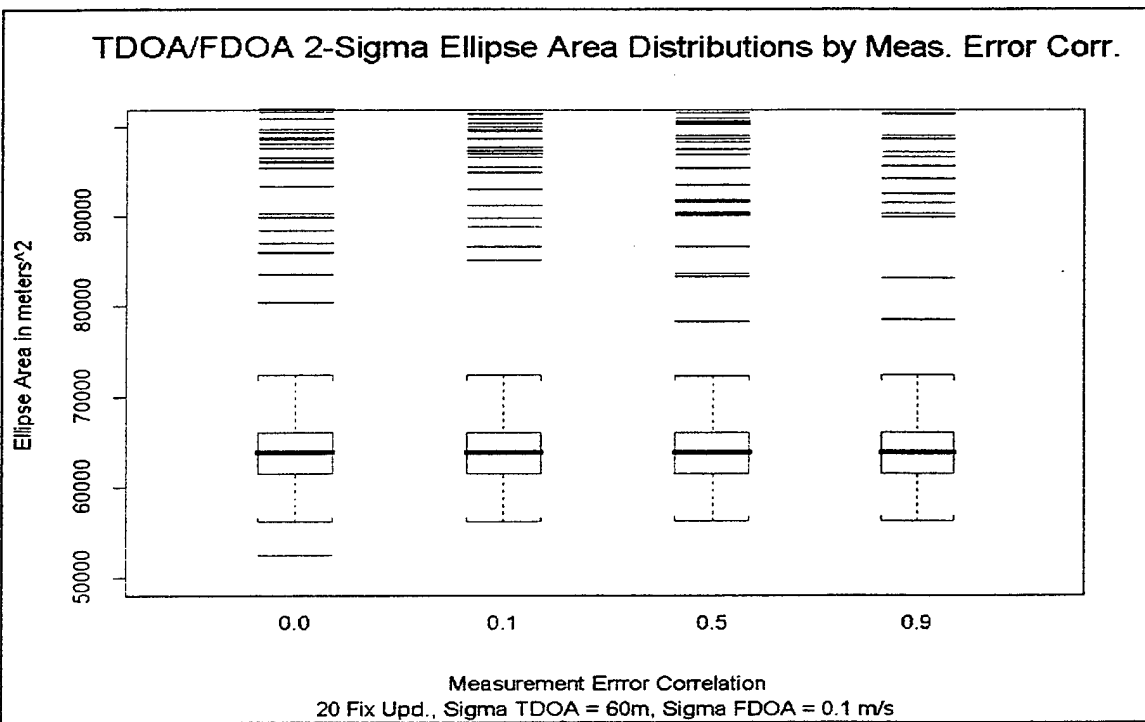


Figure 7-17 Comparison of T/FDOA Ellipse Areas by Correlation

Now it is possible to tie geometry, error correlation, accuracy, and uncertainty together. Clearly, the T/FDOA solution dominates in accuracy; however it tends to have a larger spread of uncertainty with regards to its results. Yet, comparing the median and inter-quartile ranges of the uncertainty ellipse sizes for the two solutions, they are very similar. Thus, the mixed T/FDOA solution is able to transcend errors induced by geometry and measurement errors, possibly induced by correlation, and, thus, provide more accurate fixes—especially in the upper quantiles of the accuracy distributions. The price for such accuracy is reflected in the uncertainty of the estimate. This should not be upsetting, and, in fact, proves the robust nature of the Square Root Information Filter. Since the SRIF reports each solution with no idea with regard to its accuracy (accuracy requires knowledge of the true target location), it can only rate each fix by the solution estimate covariance. Therefore, even though the SRIF provides a more accurate fix, it correctly reports that measurement errors, error correlation, or geometry are degrading its confidence in the solution that it has provided.

C. THREE DIMENSIONAL GEO-LOCATION SCENARIO RESULTS

The three dimensional scenarios included a base line “good” geometry scenario, to show the effects of error correlation, and the comparison of a “good” and “bad” geometry cases to show the effects of sensor allocation on geometry. No dominance of either solution type for the three-dimensional case is shown.

Setting up scenarios to compute three dimensional fixes is very difficult. This difficulty is due mostly to the geometry of the scenario. A three dimensional fix requires four observers in order to form three differences for the evenly determined case. The addition of the height dimension, of course, expands both the partials matrix (from a 2×2 to a 3×3 matrix for the TDOA solution and from a 4×4 to a 6×6 matrix for the mixed T/FDOA solution) and the data vector (from 2×1 to 3×1 and from 4×1 to 6×1 for TDOA and T/FDOA formulations, respectively) in the linearized least squares formulation. As a result each difference pair between slave and master must allocate its position information from the partials matrix to its respective TDOA and/or FDOA measurement(s). The difficulty in geometry arises from the formulation of partial matrices from these difference pairs that are near singular. While this is straightforward in theory, it is difficult to explain concisely to a warrior allocating his or her assets to perform a passive geo-location. Further, the possibility of the construction of a near singular matrix is not as readily

apparent when viewing the relative three-dimensional geometry as compared to that of the two-dimensional geometry. Finally, and most profoundly for an operational system, this problem is further exacerbated when one considers that in practice, the warrior may have little information with regard to the target's true position and, thus, defining the geometry *a priori* becomes an even more difficult task. Yet, this does not mean three-dimensional fixes need be abandoned. The scenarios which depict "good geometry" provide excellent fixes—many with median miss distances well below 100 meters—that outperform poor geometry two-dimensional fixes. The main difficulty with a three-dimensional fix, then, may be providing the warrior with the means to optimally allocate his or her assets.

1. Good Geometry Results

The good geometry scenario consisted of a sensor network of two ships, an aircraft, and a fixed sensor targeting a ship. A visual depiction of the scenario is provided in figure 7-18. This scenario was run for 20 measurement error correlation values from -0.9 to 0.95. For the purposes of identifying the correlation combinations, a simulation run labeled with a negative correlation value actually means that within the three TDOA measurements *and* within the three FDOA measurements, two measurements are correlated negatively by a magnitude equal to the positive correlation of the other pair of measurements. For example, if measurements 1 and 2 were negatively correlated, then measurements 1 and 3 would be positively correlated while measurements 2 and 3 would be negatively correlated.

The results of this scenario are multifaceted. First, restricting the sensors and the target into very tight boxes ensured that the geometry of the TDOA measurements would be almost always perfect. Thus, the TDOA measurements dominated the solution with regard to the position of the target. Therefore, the identical results of both the TDOA and T/FDOA solutions proves the stability and accuracy of the mixed solution's square root information filter—a particularly gratifying result given the formulation, scaling, and un-scaling of the linearized least squares equation as described in Chapter IV and Appendix B.

The surprising result, as depicted in Figure 7-19, is the improvement in the accuracy of the solution as the correlation between measurement errors increases. However, upon inspecting Figure 7-20, the opposite is true of the distribution of the volume of the uncertainty ellipses. Given the results from the two-dimensional case

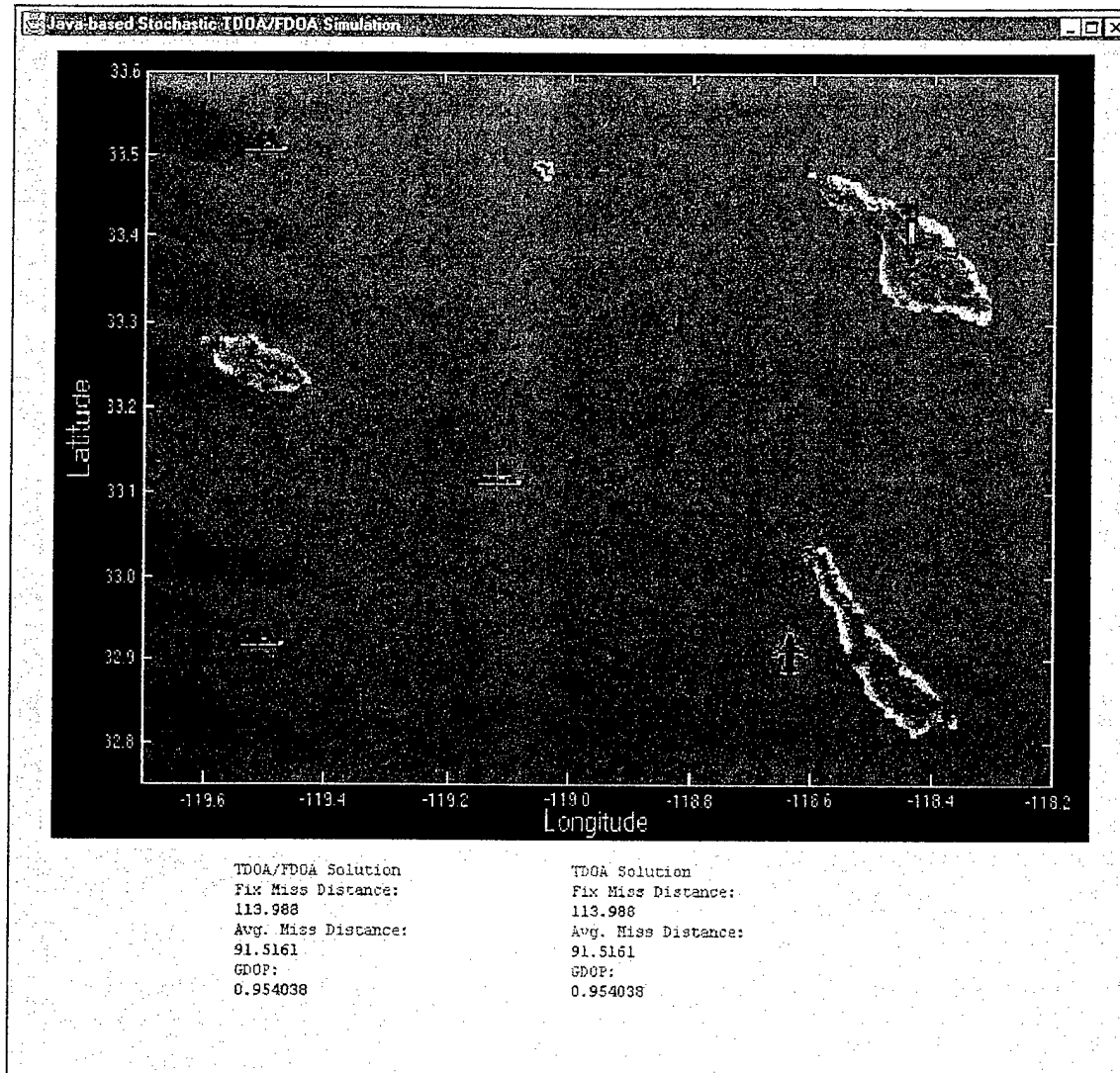


Figure 7-18 Geometry of Basic Scenario

discussed above, this is no longer a surprise. While the SRIF has no idea that it is producing more accurate results in the highly correlated noise environment, it is robust enough to realize that the measurement errors which it is encountering are deviating from what the weighting matrix had told it to expect. The SRIF produces the best fix it can; yet, it honestly reports, in the uncertainty of the fix, that the measurement errors are not indicative of what it had expected.

TDOA and T/FDOA Miss Distance Distributions by Meas. Error Correlation

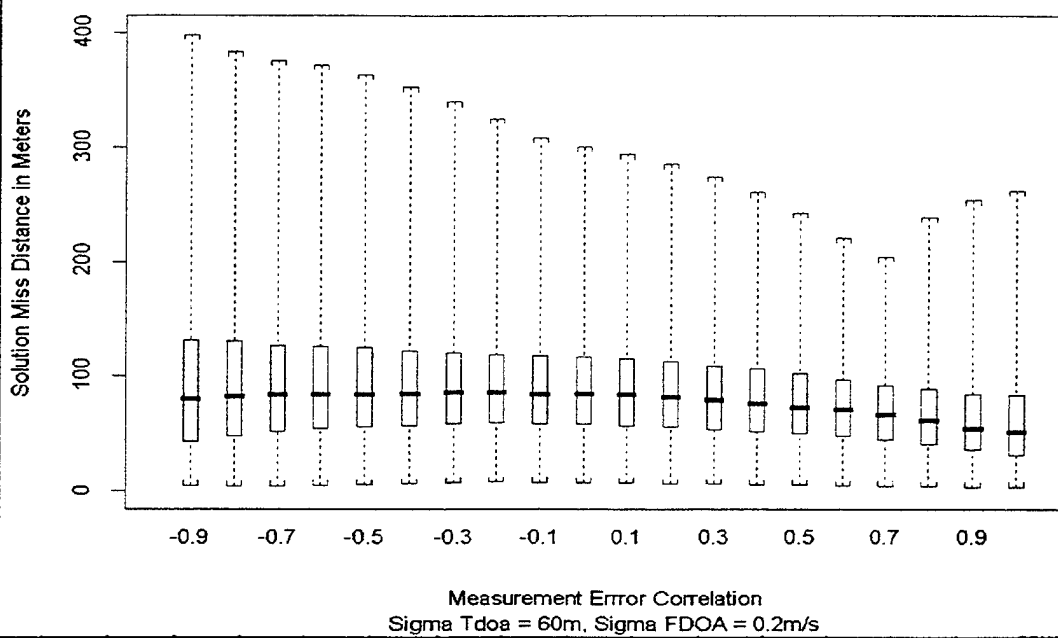


Figure 7-19 Comparison of Miss Distance Distributions by Correlation

TDOA and T/FDOA 2-Sigma Ellipse Volume Distns. by Meas. Error Corr.

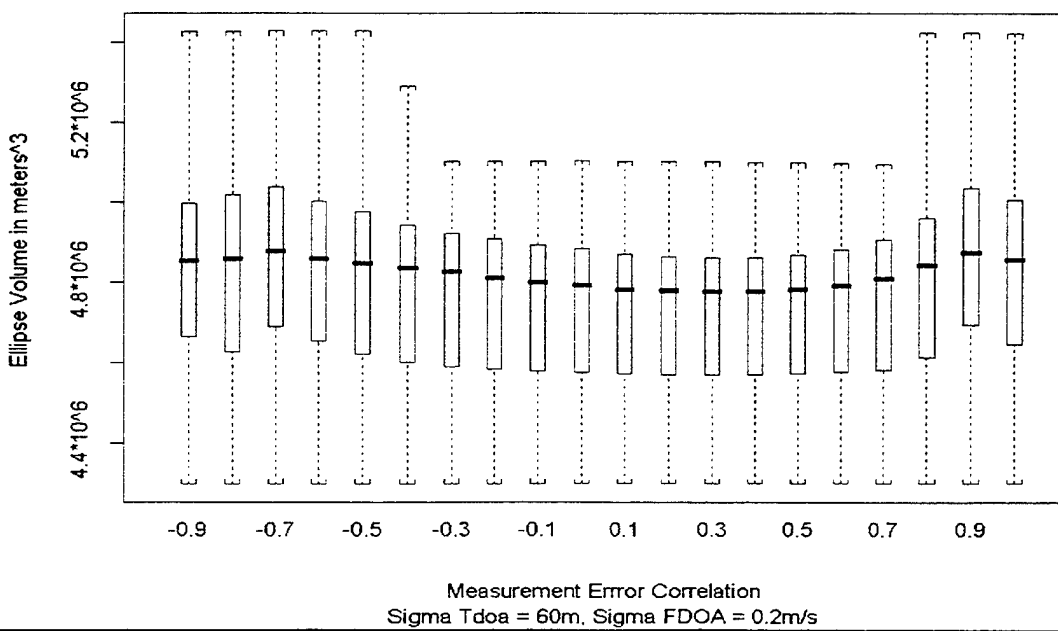


Figure 7-20 Comparison of Ellipse Volumes by Correlation

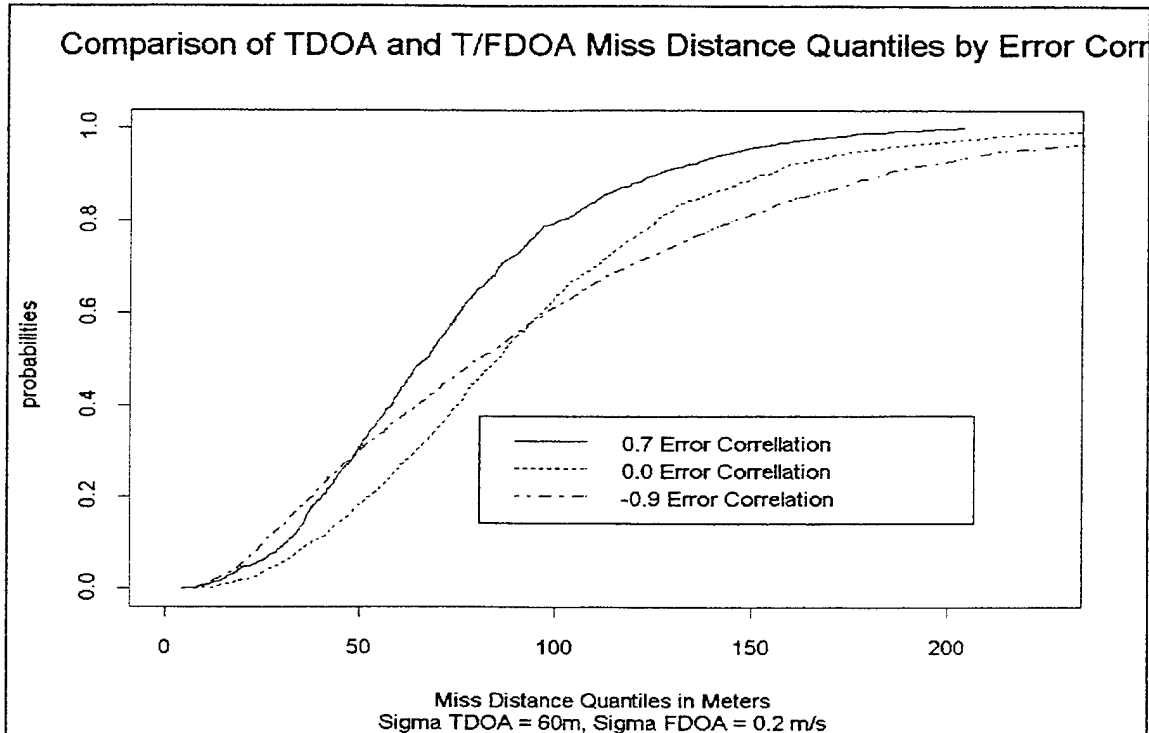


Figure 7-21 Comparison of Miss Distance Distributions by Correlation

2. Comparison of Good and Bad Geometry Scenarios

As described in the introduction to this section, the geometry of the observers relative to their target is crucial for an accurate three-dimensional solution. Figures 7-22 and 7-23 show the configurations of the “bad geometry” and “good geometry” scenarios for this illustration, respectively. Figures 7-24 and 7-25 show the quantile distributions of these two scenarios.

Examining the distribution of sensor platforms in Figure 7-22, it is not clear—even with the position of the target known—that this allocation of sensor assets would lead to a “bad geometry” scenario; yet, the GDOP in this scenario averaged 222 with minimum and maximum values of 149 and 1472, respectively. Compare this to the “good geometry” scenario in Figure 7-23 whose GDOP averaged 0.8962 with minimum and maximum values of 0.8874 and 0.91277, respectively. Without this data from the simulation runs, it would have been impossible to predict these results. Neither case appears exceptionally threatening from the geometry standpoint; yet, it will be the scenario’s geometry that directly impacts the accuracy of the geo-location solution.

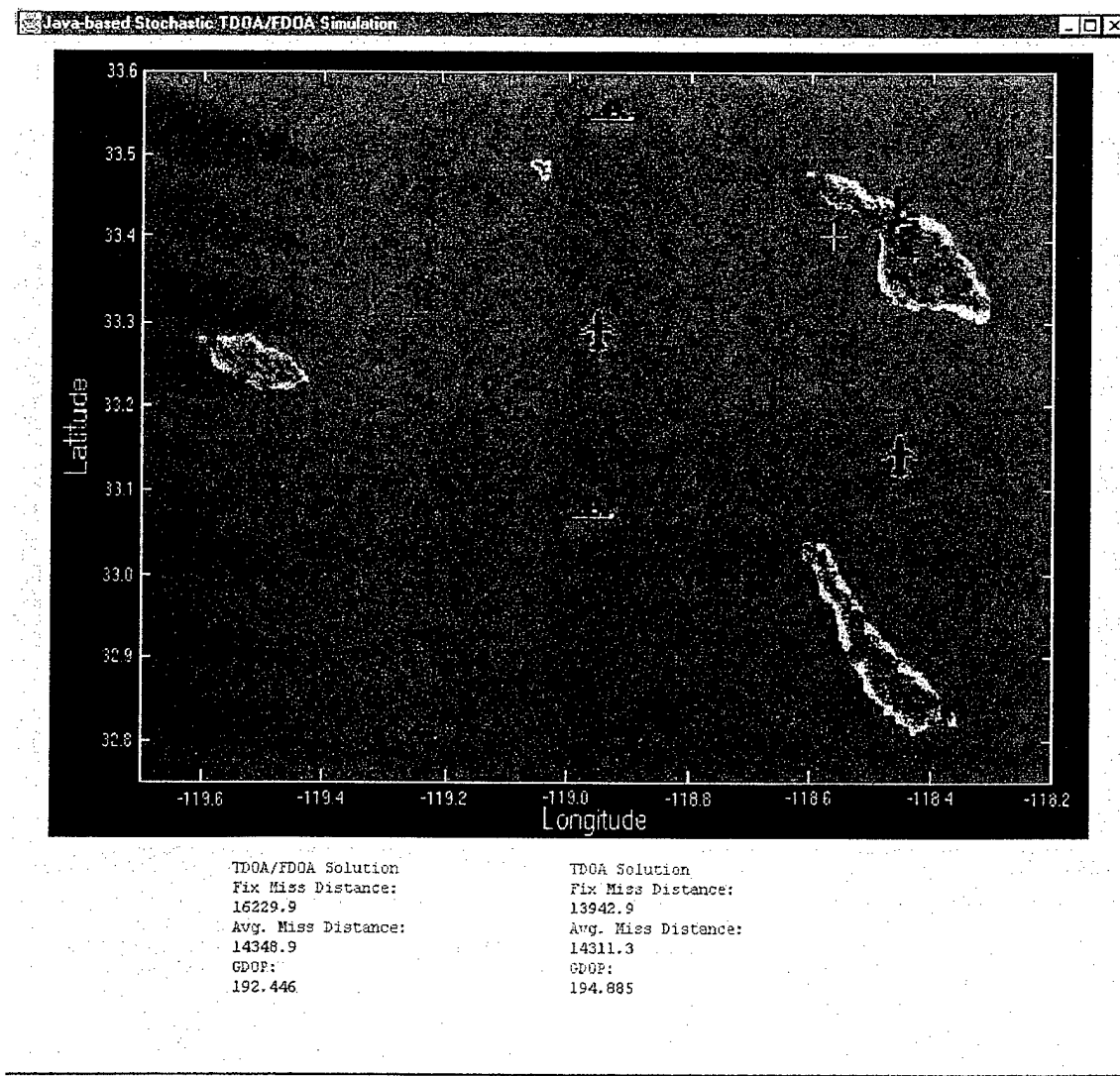


Figure 7-22 Bad Geometry Case

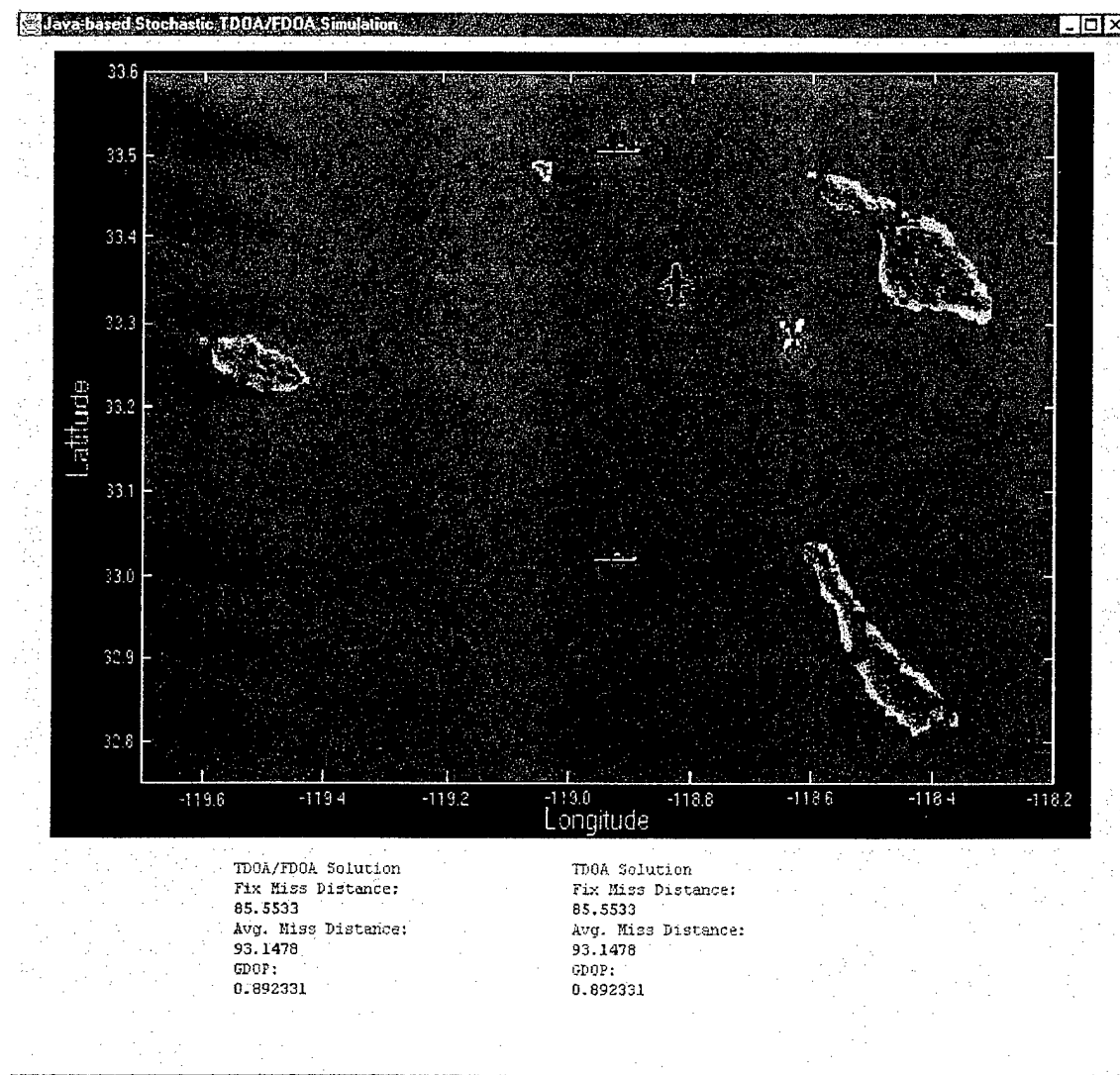


Figure 7-23 Good Geometry Case

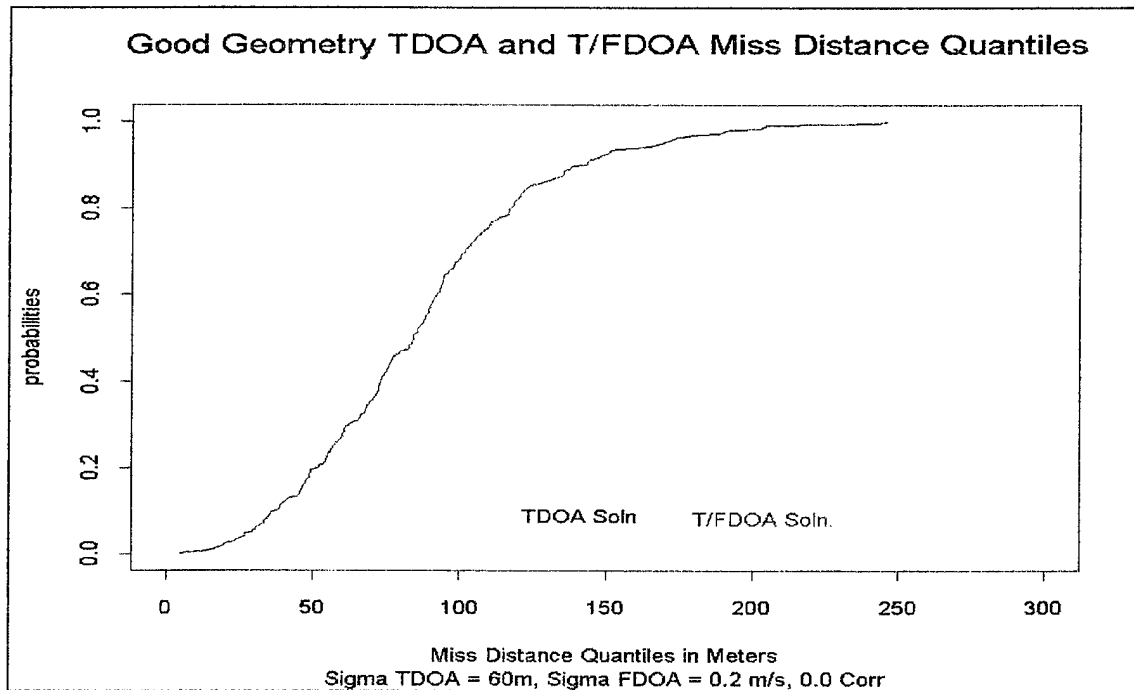


Figure 7-24 Good Geometry Miss Distance Distribution

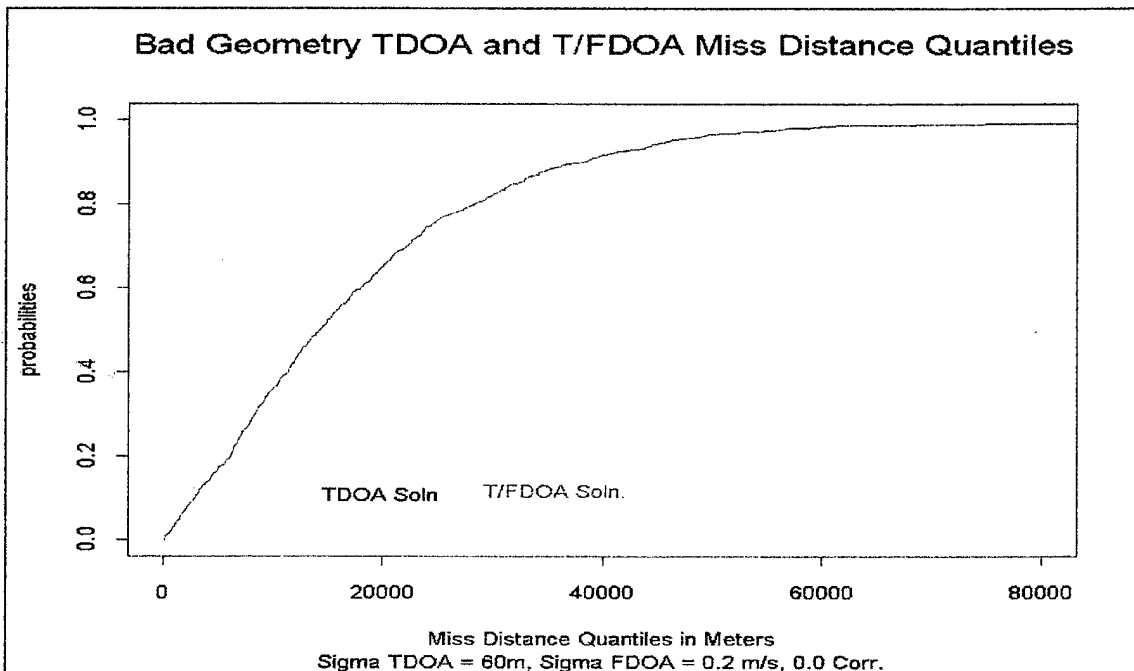


Figure 7-25 Bad Geometry Miss Distance Distribution

Upon examining Figures 7-24 and 7-25, the possible impact of poor geometry on the accuracy of the three-dimensional solution becomes clear. An explanation of what

makes the “good geometry” case “good” is required. In terms of sensors, the difference between the cases is the replacement of one of the aircraft observers from the “bad” case with a satellite in the “good” case. Given its altitude, the satellite is able to create a better three-dimensional surface when its position is differenced from that of the master. As a result, the satellite “sees” height better than that of the aircraft who may as well be on the surface of the earth in comparison to the satellite’s height. The partials matrix, then, contains more useful information with regard to the third dimension. Thus, the surface defined by the difference of the satellite’s and the master’s information is better suited to complement the other surfaces formed by the other observers and, therefore, can provide a more accurate fix with this “good geometry” of measurement surfaces.

The second obvious feature when examining Figures 7-24 and 7-25, is that, like the first good geometry case in the previous section, both the TDOA and T/FDOA miss distance distributions are identical. In this analysis, the author was not able to produce a case where the T/FDOA solution stochastically dominated the TDOA solution. While the construction of such a case may be possible, performance of both solutions would most likely be highly dominated by the quality of sensor geometry versus that of sensor measurements. Further, while individual cases can be shown where a single TDOA or mixed T/FDOA solution was obviously better than that of the other, the author was not able to show that this lead to the stochastic dominance of either solution type. Thus, the solution to improving three-dimensional fixes does not appear to be in the augmentation of FDOA information; however, FDOA information did not on the whole appear to degrade the distribution of the three-dimensional solution either. The consequences from these results lead to two avenues of discussion: solution formulation and sensor selection.

A solution to improving the three-dimensional fix may be simply collapsing to two-dimensions. This analysis has limited itself to the exploration of solutions in the evenly determined case. Yet, it is likely that most overdetermined two-dimensional solutions will dominate or at least do as well as those in the evenly determined case. In the overdetermined case, it has not been shown to what extent FDOA information could improve or degrade the solution. Likewise, the quality of a three-dimensional fix from an overdetermined sensor network with more than four observers has not been shown. Yet, having a plethora of sensors to distribute at will seems overly optimistic and would not suit the warrior who desires to know a lower bound on the performance of his or her equipment. Yet, these are both important analyses which should be performed to understand the operational capabilities of the true system.

On the other hand, if the utility for a three-dimensional fix is high, then the warrior who needs such high quality information should be concerned with the selection of robust three-dimensional assets. In particular, in this analysis it has been shown that the satellite is an excellent sensor to assist in observing height. Yet, it was also seen in two-dimensional simulation runs that in the rare case when a satellite passes directly overhead the target, it can say little about the target's two dimensional location since the satellite only "sees" height. Again, the proper allocation of assets sometimes may be out of the warrior's control. Given that satellite coverage may not always be available, another three-dimensionally robust sensor might be one of the prototype unmanned aerial vehicles (UAV's) that is designed to operate at very high altitudes for long periods of time—for example, the Tier II+ Conventional High Altitude Endurance (HAE) UAV (Global Hawk) or Tier III-Low Observable HAE UAV (Dark Star) both of which advertise surveillance altitudes greater than 18 kilometers and 12 kilometers, respectively. Note that the first three-dimensional "good geometry" scenario only used one aircraft. Further, both UAV's and satellites may be less obtrusive ways of improving the sensor to target geometry when airspace restrictions or the requirement for the concealment of sensors dictate that the traditional sensors would not suffice.

Like most decisions a military commander must make, the selection and allocation of sensors to perform passive geo-location is not a straightforward choice. Yet, further analyses of like those suggested above could assist the warrior in this decision process. Again, a good tool for exploring any of these issues would be a slightly modified version of JBSTAFSim.

VIII. CONCLUSIONS AND RECOMMENDATIONS

A. CONCLUSIONS

A simulation based methodology was used to explore the differences between geolocation solutions computed using both time-difference-of-arrival (TDOA) and mixed TDOA and frequency-difference-of-arrival (FDOA) techniques using a Multi-platform, GPS-assisted architecture. This methodology assumed no one method to measure either the TDOA or FDOA; yet, allowed for the stochastic modeling of the errors in such measurements in such a general way that they could apply to any TDOA or FDOA measurement process. Likewise, the platforms which measure such quantities were modeled in abstract ways, yet retained each platform's most basic behavior. In addition, the simulation portrayed joint platforms operating together in a joint operating environment. To enhance the numerical veracity of the solutions, the simulation implemented a numerically stable Square Root Information Filter (SRIF) which received initial target estimates based on a numerically stable direct solution implementing the Singular Value Decomposition routine. These numerically robust methods were used to provide the most numerically stable and accurate solutions possible in the face of poor sensor geometry and computer round-off error. Data taken during the simulation included: the solution miss distance from truth, the area or volume of the 2-sigma ellipse centered around the solution, and the geometric dilution of precision (GDOP). The analysis focused on the accuracy of the solutions represented by the fix miss distance, and the solution uncertainty, represented by the volume or area of the 2-sigma ellipse around the fix.

1. Two Dimensional Conclusions

In the two-dimensional problem, it was shown that a mixed T/FDOA solution maintains first order stochastic dominance over the TDOA solution in mediocre geometry. The price the mixed solution pays for this increased accuracy is a large increase in the spread of its fix uncertainty; however, both solutions maintained roughly the same partitioning of fix uncertainty around the center of their respective uncertainty distributions. Therefore, increasing the spread of the uncertainty distribution remains a small price to pay for the increased accuracy of the solution. The largest difference

between fix accuracy was seen in the upper quantiles of miss distances where the mixed T/FDOA solution significantly improved the solution fix accuracy over that of the TDOA solution. Thus, the FDOA surfaces appear to substantially improve the solution accuracy, especially when the TDOA surfaces would lead to poor fixes.

In addition to the contrasts between solution types, it was also shown that while the direct solution prevents the linearized least squares solution from diverging, the amount to which the SRIF was updated by the direct solution significantly impacted the accuracy of both solution types. In particular, solutions which used the direct solution as an initial estimate for every fix were so poor, their results were disregarded.

2. Three Dimensional Conclusions

As an exploration into the impact of correlated errors, measurement error correlation was varied across 20 values in a good geometry scenario. While both solutions produced more accurate results in the higher, positively correlated cases, the solutions also indicated more uncertainty in these fixes. Again, this confirmed the robust nature of the SRIF formulation. These results are useful since the actual system would implement sensors taking measurements in a common operating environment with common noise characteristics, thus, most likely creating similar measurement errors.

The three-dimensional simulations did not show stochastic dominance of either solution type. While some simulations showed differences in the accuracy of individual solution type fixes, neither solution type was shown to stochastically dominate the other. Results which produced identical accuracy distributions for both the TDOA and mixed T/FDOA solutions across several scenarios proved the stability of the algorithm which solves the mixed T/FDOA solution. The inference drawn from these simulations was that geometry, more than solution and measurement type, impacts the accuracy of the three-dimensional fix solution. Therefore, the choice of sensors which can more optimally measure three-dimensional information should be the first concern for those who require such fixes. In particular, it was shown that sensors with high altitude characteristics are well-suited for this task.

B. RECOMMENDATIONS

1. System Use and Design

The Multi-Platform, GPS-Assisted TDOA Geo-location System as designed by the Applied Research Laboratories, University of Texas, Austin is a robust and potentially highly functional passive geo-location system for both the Navy and the Department of Defense. FDOA information can be safely added to the geo-location formulation to augment the TDOA information for the solution of the target's location. In the two-dimensional solution case, the FDOA information can significantly improve the accuracy of the geo-location. In the three dimensional case, the additional information does not appear to degrade the system's performance in any significant manner.

The linearized least squares formulation in the SRIF appears to be a very stable and robust formulation for solving the geo-location problem. The system which implements this formulation should implement some direct solution or other means to provide an roughly accurate estimate of the target's location to start the SRIF's solution iterations. While the actual system would not be computing the large number of fixes for one target that were required in this stochastic analysis, a means to periodically update the SRIF with a new target estimate should be implemented. Further, the actual system would need to request this information based on signal characteristics, computation of the dimensionless shock, or some combination of both solver and signal properties. In addition, such an algorithm might be able to re-weight the partials matrix in the presence of correlated noise. The ability to chose a more optimal measurement covariance matrix would significantly improve the fix estimate covariance and, thus, decrease the uncertainty of the estimate of the target's location.

An avenue to improving three-dimensional fixes was shown to be through the use of platforms which can measure height information more reliably. This consequence leads to two recommendations. First, the ARL:UT system should be incorporated and tested on satellite systems and as a potential payload for prototype UAV platforms. Second, since this matter is at its crux a geometry issue, a new method to rate the geometry of the sensor network, other than GDOP, should be pursued. For the warrior, in particular, such a method should be able to assist in rating the sensor network's geometry *given possible locations* of the target. Such a method would allow the commander to allocate his or her

assets in an pseudo-optimal way given either possible locations of the target or given no *a priori* information with regard to the target's location.

2. Java-Based Stochastic TDOA and FDOA Simulation

JBSTAFSim proved itself as a robust stochastic simulation for the analyses presented in Chapter VII. In order to study any of the proposed areas above, modified versions of JBSTAFSim would provide the perfect tool for the analysis of any of these issues. In addition, JBSTAFSim could be modified so that specific platforms or platform characteristics, for example a particular type of satellite orbit, could be evaluated for its ability to contribute to the geo-location solution. In addition, due to time and scope limitations, JBSTAFSim's "batch mode" option for its solver was never stochastically tested with a static target. JBSTAFSim requires more programming so that it can make qualitative decisions with regard to the frequency with which it resets its batch mode solver.

Investigating solution types in both the overdetermined two-dimensional and three-dimensional cases should be undertaken. While it is likely that these solutions would dominate the evenly determined ones, it is not clear to what extent FDOA information might affect these solutions. This would be a particularly interesting study given that overdetermined, "bad geometry" three-dimensional fixes could potentially be collapsed to more accurate overdetermined two-dimensional fixes. With some effort JBSTAFSim could be modified to analyze this issues.

Next, JBSTAFSim has modeled both the TDOA and FDOA measurement errors as Normally distributed random variables. The Normal distribution was implemented for its ease in the ability to generate correlated random variables on a computer and, as presented in Chapter III, due to the fact that any measurement error distribution is in itself a function of many random variables which change over a variety of system configurations and environmental characteristics. Quite simply, the true distribution is neither known nor can it be known; yet it can be modeled. To that end, modeling the measurement errors with another distribution would prove an interesting test for the SRIF and would be relatively straightforward to implement in JBSTAFSim. Investigating the solution accuracy and uncertainty using either distributions that are either "heavy tailed" or skewed would be worthy endeavors. Likewise, extending JBSTAFSim's solver to create a non-diagonal measurement error covariance matrix might prove useful in any of these analyses.

Of the many possibilities that exist for the extension of JBSTAFSim, one final possibility could be of particular interest. Given its design and network aware capabilities, JBSTAFSim's existing modular design could be modified so that it receives *actual* TDOA and FDOA measurements and sensor information via a network. JBSTAFSim's solver would then compute the geo-location and display the results on a local computer *or* back to the network to be displayed on another host's computer using only a Web browser. While achieving this vision requires the resolution of *many* security issues, Public Key Encryption and secure sockets capabilities within the Java language itself are already being implemented in the latest version of Java. Further, this concept again shows the "flat" architecture that is innate in models created in Java. With very little cost to the user or developer, rich capabilities are immediately available to the model which can function across many platforms in a very robust nature.

APPENDIX A. SEQUENTIAL SQUARE ROOT DATA PROCESSING ALGORITHM AND THEORY

The purpose of this appendix is to describe both the underlying theory behind the square root information filter (SRIF) and the sequential data processing algorithm which exploits this theory. A basic understanding of solving linear least squares problems is assumed, but is not essential. The primary reference of this section is Reference 16 thus, notation will be presented as similarly as possible. In essence this section will provide a quick summary reference of the SRIF algorithm as described in detail in Reference 16. For the most part, all applicable ideas and examples presented here will be identical to those in Reference 16.

A. CONTEXT OF THE PROBLEM AND REVIEW OF LEAST SQUARES [REF. 16, 14-16]

With regard to geolocation in a F/TDOA problem, the most basic sequential linear least squares system of equations is defined as:

$$\left[\frac{\partial F}{\partial X} \right]_{x_0} \cdot (x - x_0) \cong \vec{z} - F(x_0) \quad \text{A-A1}$$

Where $\frac{\partial F}{\partial X}$ represents the TDOA partials or mixed F/TDOA partials evaluated at the state update x_0 . This $M \times N$ matrix is multiplied by the state step N vector $(x - x_0)$ which is approximately equal to the M data vector z minus the TDOA or F/TDOA functional M vector evaluated at x_0 .

From Chapter IV and for reference, the TDOA/FDOA equations are provided below.

Observation equations:

$$c \cdot TDOA_{ij}(\vec{r}) = R^{(i)} - R^{(j)}$$

$$f_T^{-1} \cdot FDOA_{ij}(\vec{r}, \vec{v}) = \frac{\Delta \vec{v}_{\varphi}^{(i)}}{c} - \frac{\Delta \vec{v}_{\varphi}^{(j)}}{c}$$

Measurement covariance matrix:

$$M = \begin{bmatrix} c^2 \sigma_{TDOA}^2 & 0 \\ 0 & f_T^{-2} c^2 \sigma_{FDOA}^2 \end{bmatrix}$$

Linearized least squares equation:

$$\begin{bmatrix} (\alpha^{(j)} - \alpha^{(i)}) & 0 \\ \left(\frac{\Delta \vec{v}_{\perp}^{(j)}}{R^{(j)}} - \frac{\Delta \vec{v}_{\perp}^{(i)}}{R^{(i)}} \right) & (\alpha^{(j)} - \alpha^{(i)}) \end{bmatrix}_{X_0} \begin{bmatrix} d\vec{x} \\ d\vec{v} \end{bmatrix} = \begin{bmatrix} c \cdot TDOA_{ij} \\ \frac{c}{f_T} \cdot FDOA_{ij} \end{bmatrix} - \begin{bmatrix} R^{(i)} - R^{(j)} \\ \Delta \vec{v}_{\varphi}^{(i)} - \Delta \vec{v}_{\varphi}^{(j)} \end{bmatrix}_{X_0}$$

Direction cosines are denoted by α , and R is the observer-target separation. In the state vector, $d\vec{x}$ and $d\vec{v}$ refer to the offset from the position and velocity, respectively, of the nominal state, and the subscripts φ and \perp refer to components parallel and perpendicular, respectively, to the line of sight. The symbols c and f_T refer to the speed of light and the frequency of the transmitter. Of course, the dimension of the state here is 6, not 2 as it appears, because all the elements on the left side of the equation are vectors.[Ref. 19]

For simplicity, let us now consider A-A1 as the set of equations:

$$A\vec{x} + \nu = \vec{z} \quad \text{A-A2}$$

Here the partials matrix in A-A1 is represented by the $M \times N$ matrix A ; the state step by the vector x ; and the functional and data difference by is represented by the vector z . We also introduce v to represent the M vector of observation errors. The least squares solution to minimize the mean square observation error is defined as:

$$J = \sum_{j=1}^m v(j)^2 = v^T v \quad \text{A-A3}$$

Or, in terms of x :

$$J(x) = (z - Ax)^T (z - Ax) \quad \text{A-A4}$$

Thus, $J(x)$ is non-negative and quadratic in the components of x so that the necessary and sufficient conditions for a minimum require that x satisfy the normal equations:

$$A^T Ax = A^T z \quad \text{A-A5}$$

A-A5 leads to the well-known least-squares solution x_{ls} :

$$x_{ls} = (A^T A)^{-1} A^T z \quad \text{A-A6}$$

Statistically, if we assume, for now, that the observation errors, v , are random variables that have been normalized so that:

$$E(v) = 0 \text{ and } E(v^T v) = I_M \quad \text{A-A7}$$

A-A5 then becomes:

$$A^T Ax_{ls} = A^T z = A^T Ax + A^T v \quad \text{A-A8}$$

A-A8 allows us to make two important conclusions about our least squares solution. First, that $E(x_{ls}) = x$; thus it x_{ls} is an unbiased estimate. Second, the estimate error covariance can be evaluated by:

$$(A^T A) E[(x_{ls} - x)(x_{ls} - x)^T] (A^T A) = A^T E(VV^T) A \quad \text{A-A9}$$

A-A9 simplifies so that we get a recognizable estimate for $P_{x_{ls}}$, defined as estimate error covariance:

$$P_{x_{ls}} = E[(x_{ls} - x)(x_{ls} - x)^T] = (A^T A)^{-1} \quad \text{A-A10}$$

Where $P_{x_{ls}}^{-1} = A^T A$ is defined as the information matrix, Λ_x .

B. A PRIORI INFORMATION [REF. 16, 16-17]

Now suppose that in addition to the linear system A-A2, there exists an *a priori* unbiased estimate of x and Λ , defined as \tilde{x} and $\tilde{\Lambda}$. This information can be included in the least squares solution by changing A-A4 to:

$$J_1(x) = (x - \tilde{x})^T \tilde{\Lambda} (x - \tilde{x}) + (z - Ax)^T (z - Ax) \quad \text{A-B1}$$

Again, like A-A5, the minimizing argument for $J_1(x)$, now define as \hat{x}_{ls} , is defined by satisfying the normal equations:

$$(\tilde{\Lambda} + A^T A) \hat{x}_{ls} = \tilde{\Lambda} \tilde{x} + A^T z \quad \text{A-B2}$$

From A-B2 and being reminded that $(x - \tilde{x})$ and V both have mean zero, a similar construct to A-A8 can be written to prove that \hat{x}_{ls} is unbiased. Further, assuming that the observation “noise” and the *a priori* estimate errors are independent ($E[(x - \tilde{x})V^T] = 0$), then like A-A9 and A-A10 we obtain the estimate error covariance:

$$P_{\hat{x}_{ls}} = E[(x - \hat{x}_{ls})(x - \hat{x}_{ls})^T] = (\tilde{\Lambda} + A^T A)^{-1} \quad \text{A-B3}$$

Notice how A-B2 and A-B3 reduce to A-A5 and A-A10 when $\tilde{\Lambda} = 0$, i.e. there is no *a priori* information.

C. A PRIORI INFORMATION AS ADDITIONAL OBSERVATIONS [REF. 16, 17-18]

Given that factorization of a positive semi-definite matrix is always possible, factor $\tilde{\Lambda}$ so that $\tilde{\Lambda} = \tilde{R}^T \tilde{R}$. \tilde{R}^T is called the square root of $\tilde{\Lambda}$. Square root matrices are not unique, but are related by orthogonal transformations. For example, if S_1 and S_2 are square roots of a positive semi-definite matrix, then $P = S_1 S_1^T = S_2 S_2^T$, there exists a matrix T such that $S_2 = S_1 T$ and $TT^T = T^T T = I$.

With this factorization in mind, let $\tilde{z} = \tilde{R}\tilde{x}$ and write:

$$(\tilde{x} - x)^T \tilde{\Lambda} (\tilde{x} - x) = (\tilde{z} - \tilde{R}x)^T (\tilde{z} - \tilde{R}x) \quad \text{A-C1}$$

Compare these results to $J(x)$ in A-A4 and one can glean that *a priori* estimate-covariance information can be interpreted as additional observations in the least squares solution. Therefore, $J_1(x)$ in A-B1 can be viewed as simply applying the least squares functional $J(x)$ to the augmented system:

$$\begin{bmatrix} \tilde{z} \\ z \end{bmatrix} = \begin{bmatrix} \tilde{R} \\ A \end{bmatrix} x + \begin{bmatrix} \tilde{v} \\ v \end{bmatrix} \quad \text{A-C2}$$

A-C2 is a recursive result since the previous estimate and covariance are combined with the new data to form an updated estimate and covariance. Numerically significant is that the estimate covariance results do not depend on which square root was used—allowing the selection of square root matrices that are simple to compute and enhance numerical accuracy.

D. HOUSEHOLDER ORTHOGONAL TRANSFORMATIONS [REF. 16, 57-62]

In section C, we made a brief reference to orthogonal transformations. SRIF depends on the Householder orthogonal transformation. An understanding of this transformation is *vital* in order to understand the SRIF mechanization.

First, a review of orthogonal matrices. A matrix T is orthogonal if $TT^T = I$. Four properties useful to know about orthogonal transformations are:

- A. If T_1 and T_2 are orthogonal, so is $T_1 T_2$.
- B. $T^{-1} = T^T$ and $T^T T = I$.
- C. For any M vector y , $\|Ty\| = \|y\|$ where $\|\cdot\|$ is the Euclidean norm.
- D. If v is an M vector of random variables with $E(v) = 0$ and $E(vv^T) = I$, then $\bar{v} = Tv$ has the same properties as v , namely: $E(\bar{v}) = 0$ and $E(\bar{v}\bar{v}^T) = I$.

Recall from A-A4 that for $M \times N A$, $J(x) = (z - Ax)^T(z - Ax) = \|z - Ax\|^2$. Define T to be a $M \times M$ orthogonal matrix and, using Property C from above, we have:

$$J(x) = \|T(z - Ax)\|^2 = \|(Tz) - (TA)x\|^2 \quad \text{A-D1}$$

Since, x_{ls} is independent of T , T can be chosen so that (TA) has a computationally attractive form such as:

$$TA = \begin{bmatrix} R \\ 0 \end{bmatrix} \begin{cases} n \\ m-n \end{cases} \quad \text{A-D2}$$

Where R is an upper triangular matrix. If Tz is partitioned,

$$Tz = \begin{bmatrix} z_1 \\ z_2 \end{bmatrix} \begin{cases} n \\ m-n \end{cases} \quad \text{A-D3}$$

then $J(x)$ can be written as:

$$J(x) = \|z_1 - Rx\|^2 + \|z_2\|^2 \quad \text{A-D4}$$

From A-D4, one can see that the minimizing x_{ls} must satisfy $Rx = z_1$ and that $J(x_{ls}) = \|z_2\|^2$. These results have been proved to be less susceptible to errors due to computer round-off in References 17 and 18. From above, we see the applicability of orthogonal transformations to the least squares problem. Let us now focus on an orthogonal transformation that will assist us in the results from section C.

Householder transformations are matrix representations corresponding to the geometric notion of a reflection. Let u be a nonzero vector and let U_{\perp} be the plane perpendicular to u . If y is an arbitrary vector,

$$y = (y^T \hat{u}) \hat{u} + v \quad \text{A-D5}$$

then the reflection of y in the plane U_{\perp} is equal to:

$$y_r = -(y^T \hat{u}) \hat{u} + v \quad \text{A-D6}$$

where \hat{u} is a unit vector in the direction of u and v is that part of y that is orthogonal to u . See Figure A-C1. Eliminating v from both equations gives:

$$y_r = y - 2(y^T \hat{u}) \hat{u} = (I - \beta uu^T)y \quad \text{A-D7}$$

where $\beta = \frac{2}{\|u\|^2}$. The matrix $T_u = I - \beta uu^T$ is the elementary Householder transformation.

Figure A-C1 shows the geometry of the Householder transformation.

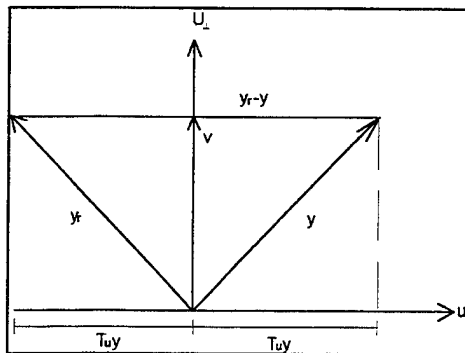


Figure A-C1

Five properties of this Householder transformation, T_u , are important to us.

1. $T_u = T_u^T$, T_u is symmetric.
2. $T_u^2 = I$, T_u is idempotent. (Combined with Property 1 shows that T_u is orthogonal.)

3. If $u(j) = 0$ then $(T_u y)(j) = y(j)$, rather, if the j th component of u is zero, then T_u leaves the j th component of y unchanged.
4. If $u \perp y$ then $T_u y = y$.
5. $T_u y = y - \gamma u$, where $\gamma = 2y^T u / u^T u$. This is practically a time and storage saver since forming and storing T_u prior to computing $T_u y$ requires more computation than the direct evaluation using this property. If M is large this could be particularly helpful.
6. Let $\sigma = \text{sgn}(y(1)) \cdot (y^T y)^{1/2}$ and define $u(1) = y(1) + \sigma e_1$, $u(j) = y(j), j > 1$. Then $T_u y = -\sigma e_1$ and $2/u^T u = 1/(\sigma u(1))$.

Property 6 allows us to choose a direction of u so that $y_r = T_u y$ lies along e_1 which gives $T_u y = (\sigma, 0, \dots, 0)^T$. This is the first step in matrix triangularization. Since Property C in our orthogonal transformation review assures us that the length of y is invariant, therefore $\|T_u y\| = |\sigma| = (y^T y)^{1/2}$. The direction of u can be obtained from Property 5 above: $u = \text{const}(y - \sigma e_1)$, which explains Property 6 again— $u^T u = 2\sigma u(1)$. Refer back to Figure A-C1; note $y_r - y$ is orthogonal to U^\perp and so is parallel to u . Also note, in Property 6, that the sign of σ is chosen to maximize $|u(1)|$ this assists in reducing numerical problems when T_u is applied to the columns of A as $1/\sigma u(1)$.

If Property 6 is applied to an $M \times N$ matrix A (with y as its first column) the first step of a matrix triangularization results.

$$T_u A = \begin{cases} 1 \\ m-1 \end{cases} \left\{ \begin{array}{c|cc} \begin{matrix} 1 \\ s \\ 0 \end{matrix} & \xrightarrow{\sim} & \tilde{A} \\ \hline 0 & & \end{array} \right\} \quad \text{A-D8}$$

Note that via Property 6, s and \tilde{A} are computed directly from A and the matrix T_u is implicit—never calculated. Repeated application of Property 6 and the results of A-C8 to the columns of A results in a series of orthogonal transformations which combine into one orthogonal transformation, T (by Property A of orthogonal transformations) and can be written as:

$$TA = \begin{bmatrix} s_1 & a_1^T \\ s_2 & a_2^T \\ \ddots & \vdots \\ 0 & s_k \frac{a_k^T}{A_{k+1}} \end{bmatrix} \quad \text{A-D9}$$

E. THE SRIF DATA PROCESSING ALGORITHM [REF. 16, 69-72]

The last four sections now culminate into the SRIF Data Processing Algorithm. This method is reputed to be more accurate (less susceptible to the effects of computer round-off errors) and stable (accumulated round-off errors will not cause the algorithm to diverge) than other conventional non-square root methods.

Begin by supposing that we have an *a priori* array from A-C1 $[\tilde{R}\tilde{z}]$ corresponding to the equation $\tilde{z} = \tilde{R}x + \tilde{v}$ where \tilde{v} has zero mean and unity covariance and \tilde{R} is $N \times N$. We are interested in constructing the least squares solution to the *a priori* data equation and the new measurements $z = Ax + v$. In section C equation A-C2, the least squares solution was described as:

$$\begin{bmatrix} \tilde{z} \\ z \end{bmatrix} = \begin{bmatrix} \tilde{R} \\ A \end{bmatrix} x + \begin{bmatrix} \tilde{v} \\ v \end{bmatrix} \quad \text{A-E1}$$

In section D, this was seen to be equivalent to finding the least squares solution to:

$$T \begin{bmatrix} \tilde{R} \\ A \end{bmatrix} x = T \begin{bmatrix} \tilde{z} \\ z \end{bmatrix} - T \begin{bmatrix} \tilde{v} \\ v \end{bmatrix} \quad \text{A-E2}$$

Further, section D showed that T can be chosen so that:

$$T \begin{bmatrix} \tilde{R} \\ A \end{bmatrix} = \begin{bmatrix} \hat{R} \\ 0 \end{bmatrix} \quad \text{A-E3}$$

where \hat{R} is an upper triangular matrix and we set:

$$T \begin{bmatrix} \tilde{z} \\ z \end{bmatrix} = \begin{bmatrix} \hat{z} \\ e \end{bmatrix} \text{ and } T \begin{bmatrix} \tilde{v} \\ v \end{bmatrix} = \begin{bmatrix} \hat{v} \\ v_e \end{bmatrix}$$

Then A-E2 becomes:

$$\hat{R}\hat{x} = \hat{z} - \hat{v} \quad \text{A-E4}$$

and

$$0 = e - v_e \quad \text{A-E5}$$

A-E4 is in the form of a data equation and can now act as the *a priori* data equation that will be combined with the next set of observations. The e in A-E5 is the error in the least squares fit; recall from A-D4:

$$J(x) = \|\hat{R}\hat{x} - \hat{z}\|^2 + \|e\|^2 \quad \text{A-E6}$$

Thus, $\|e\|^2$ is the sum of squares residual error corresponding to the least squares solution.

The algorithm then requires the construction of the augmented information array $\begin{bmatrix} \tilde{R} & \tilde{z} \\ A & z \end{bmatrix}$ and then can be expressed as follows (letting the *a priori* information array equal to $\begin{bmatrix} \hat{R}_0 \tilde{z}_0 \end{bmatrix}$):

$$T_j \begin{bmatrix} \hat{R}_{j-1} & \hat{z}_{j-1} \\ A_j & z_j \end{bmatrix} = \begin{bmatrix} \hat{R}_j & \hat{z}_j \\ 0 & e_j \end{bmatrix}, j = 1, \dots, m \quad \text{A-E7}$$

where $\begin{bmatrix} \hat{R}_0 \hat{z}_0 \end{bmatrix} = \begin{bmatrix} \tilde{R}_0 \tilde{z}_0 \end{bmatrix}$ and T_j orthogonal to triangularize the matrix $\begin{bmatrix} \hat{R}_{j-1} \\ A_j \end{bmatrix}$. Thus, $\hat{x}_j = \hat{R}_j^{-1} z_j$ is the least squares estimate corresponding to the a priori information and the measurement set, and $\hat{P}_j = \hat{R}_j^{-1} \hat{R}_j^{-T}$ is the covariance of this estimate. Note that because \hat{R}_j is triangular, the calculation of these two estimates can be easily accomplished using back substitution methods.

F. WHITENING OBSERVATION ERRORS [REF. 16, 47-49]

Early in section A, equation A-A7 asserted that $E(\nu^T \nu) = I_M$. We now consider the case where $E(\nu^T \nu) = P_\nu$ where P_ν is positive definite. We know, then, that we can write this matrix as:

$$P_\nu = L_\nu L_\nu^T \quad \text{A-F1}$$

where L_ν is a lower triangular square root of P_ν . Now we can multiply the observations by L_ν^{-1} and the observation set will have unit covariance observation error. Thus the familiar $Ax + \nu = z$ is transformed to $\bar{A}x + \bar{\nu} = \bar{z}$ with:

$$\bar{z} = L_\nu^{-1}z, \quad \bar{A} = L_\nu^{-1}A, \quad \bar{\nu} = L_\nu^{-1}\nu$$

In the TDOA and TDOA/FDOA case we assume that the observations are uncorrelated, but the i th observation error has variance σ_i^2 . Thus, $L_\nu^{-1} = \text{Diag}(1/\sigma_1, \dots, 1/\sigma_m)$. Therefore, our augmented matrix takes on the form:

$$\begin{bmatrix} \tilde{R} & \tilde{z} \\ L_\nu^{-1}A & L_\nu^{-1}z \end{bmatrix} \quad \text{A-F1}$$

As a side note, Reference 16 includes a description of the case where observations are correlated.

APPENDIX B. MIXED TDOA/FDOA SCALING

The purpose of this appendix is to discuss the scaling of mixed TDOA and FDOA partials, covariance and data in the linear least squares formulation. What follows is a summary of and the examples *directly* from an unpublished work by Dr. Brian Tolman at ARL:UT, Reference 19.

First, consider the usual linear least squares formulation with measurement covariance M as described in Ref. 19:

$$AX = B \quad \text{B-1}$$

$$X = (A^T M^{-1} A)^{-1} A^T M^{-1} B \quad \text{B-2}$$

$$C = (A^T M^{-1} A)^{-1} \quad \text{B-3}$$

where,

$$A = \left. \frac{\partial F}{\partial X} \right|_{X_0} \quad \text{B-4}$$

B-5

$$B = D - F(X_0)$$

Dr. Tolman then considers two arbitrary diagonal matrices to re-scale the problem.

$$S_1 = \text{diagonal}(m \times m) \quad \text{B-6}$$

$$S_2 = \text{diagonal}(n \times n) \quad \text{B-7}$$

$$\tilde{A} = S_1 A S_2 \quad \text{B-8}$$

$$\tilde{X} = S_2^{-1} X \quad \text{B-9}$$

$$\tilde{B} = S_1 B \quad \text{B-10}$$

$$\tilde{M} = S_1 M S_1 \quad \text{B-11}$$

The problem and its solution then become

$$\tilde{A}\tilde{X} = \tilde{B} \quad \text{B-12}$$

$$\tilde{X} = (\tilde{A}^T \tilde{M}^{-1} \tilde{A})^{-1} \tilde{A}^T \tilde{M}^{-1} \tilde{B} = S_2^{-1} (A^T M^{-1} A)^{-1} A^T M^{-1} B = S_2^{-1} X \quad \text{B-13}$$

$$\tilde{C} = (\tilde{A}^T \tilde{M}^{-1} \tilde{A})^{-1} = S_2^{-1} (A^T M^{-1} A)^{-1} S_2^{-1} = S_2^{-1} C S_2^{-1} \quad \text{B-14}$$

[Note that if S is diagonal, the effect of multiplying on the left (SA) is to multiply row (i) by S(i,i), and the effect of multiplying on the right is to multiply column (j) by S(j,j).]

The scaling by S_1 can be thought of as multiplying each observation equation by a separate constant, as when, for example, the units of the TDOA equation are changed from seconds to meters. The scaling by S_2 can be thought of as changing the units of the elements of the state vector (which of course also changes the solution covariance). The consistency of the above equations shows that the linear problem may be arbitrarily scaled without modifying the solution. In non-linear problems as well, the scaling by S_1 clearly acts in the same way, effectively multiplying each observation equation by a (perhaps different) constant. However, the scaling by S_2 cannot work for non-linear problems, except in special cases, because there the matrix A is in fact a matrix of partial derivatives

$$\tilde{A} = \frac{\partial F(\tilde{X})}{\partial \tilde{X}} = \frac{\partial F(X)}{\partial X} S_2^{-1} \quad \text{B-15}$$

and the second equality here would hold only if F(X) were linear in X. The TDOA equations, however, *are* a special case (see below), and the state vector can be scaled, with one important caveat.[Ref. 19]

Numerical analysis indicates that the ideal situation is to have a matrix A which is “equilibrated,” meaning that

$$\sum_j |A_{kj}| \approx \sum_i |A_{ik}| \approx \text{const. } \forall k \quad \text{B-16}$$

That is, minimizing the numerical error incurred while solving the least squares equation requires that the sum of absolute values along every row and every column has about the same magnitude. While this is possible in principle, in practice it is very difficult to find scaling matrices which will do this in the general case.[Ref. 19]

Consider in detail the scaling of the mixed F/TDOA problem as described in Reference 19.

Observation equations:

$$c \cdot TDOA_{ij}(\vec{r}) = R^{(i)} - R^{(j)} \quad B-17$$

$$f_T^{-1} \cdot FDOA_{ij}(\vec{r}, \vec{v}) = \frac{\Delta \vec{v}_{\varphi}^{(i)}}{c} - \frac{\Delta \vec{v}_{\varphi}^{(j)}}{c} \quad B-18$$

Measurement covariance matrix:

$$M = \begin{bmatrix} c^2 \sigma_{TDOA}^2 & 0 \\ 0 & f_T^{-2} c^2 \sigma_{FDOA}^2 \end{bmatrix} \quad B-19$$

Linearized least squares equation:

$$\begin{bmatrix} (\alpha^{(j)} - \alpha^{(i)}) & 0 \\ \left(\frac{\Delta \vec{v}_{\perp}^{(j)}}{R^{(j)}} - \frac{\Delta \vec{v}_{\perp}^{(i)}}{R^{(i)}} \right) & (\alpha^{(j)} - \alpha^{(i)}) \end{bmatrix}_{X_0} \begin{pmatrix} dx \\ dv \end{pmatrix} = \begin{pmatrix} c \cdot TDOA_{ij} \\ \frac{c}{f_T} \cdot FDOA_{ij} \end{pmatrix} - \begin{pmatrix} R^{(i)} - R^{(j)} \\ \Delta \vec{v}_{\varphi}^{(i)} - \Delta \vec{v}_{\varphi}^{(j)} \end{pmatrix}_{X_0} \quad B-20$$

Direction cosines are denoted by α , and R is the observer-target separation. In the state vector, dx and dv refer to the offset from the position and velocity, respectively, of the nominal state, and the subscripts φ and \perp refer to components parallel and perpendicular, respectively, to the line of sight. Note the scaling of these equations. The TDOA equation has units (meters) and typically these values are of order 10^5 or more. The FDOA equation has units (m/s) and typical values are of order 1. Therefore the relative scaling is of order 10^{-5} , and may approach much smaller values. This is particularly true when the problem begins to approach singularity. Thus there is a significant difference of scale within the mixed TDOA/FDOA problem. Also note that the TDOA, FDOA and mixed problems, although non-linear, can be scaled in the sense of scaling the state vector, as long as *all three components of position and all three components of velocity are scaled alike*. To see this it is enough to note that changing the scale of the three position (velocity) components, uniformly, does not change the physics of the problem, it simply changes the units of length (or time or both). [Ref. 19]

Thus the F/TDOA problem may be scaled in the following way. Choose to scale the problem with 4 constants, one each for the three position coordinates together, the three velocity components, the TDOA data and the FDOA data. The scaling matrices are

$$S_1 = \begin{pmatrix} L^{-1} & 0 \\ 0 & V^{-1} \end{pmatrix} \quad \text{B-21}$$

$$S_2 = \begin{pmatrix} l & 0 \\ 0 & v \end{pmatrix} \quad \text{B-22}$$

where each element represents a diagonal block with constant elements; the blocks in S_2 have dimension 3, and the blocks in S_1 cover the TDOA data (L) and FDOA data (V). Then the least squares equation becomes

$$\left[\begin{array}{cc} \left(\alpha^{(j)} - \alpha^{(i)} \right) \frac{l}{L} & 0 \\ \left(\frac{\Delta \vec{v}_\perp^{(j)}}{R^{(j)}} - \frac{\Delta \vec{v}_\perp^{(i)}}{R^{(i)}} \right) \frac{l}{V} & \left(\alpha^{(j)} - \alpha^{(i)} \right) \frac{v}{V} \end{array} \right]_{X_0} \begin{pmatrix} l^{-1} \vec{dx} \\ v^{-1} \vec{dv} \end{pmatrix} = \left[\begin{array}{c} \frac{c}{L} \cdot TDOA_{ij} \\ \frac{FDOA_{ij}}{f_T V / c} \end{array} \right] - \left[\begin{array}{c} \left(R^{(i)} - R^{(j)} \right) / L \\ \frac{\Delta \vec{v}_\phi^{(i)}}{V} - \frac{\Delta \vec{v}_\phi^{(j)}}{V} \end{array} \right]_{X_0} \quad \text{B-23}$$

with measurement covariance

$$M = \begin{bmatrix} \frac{c^2 \sigma_{TDOA}^2}{L^2} & 0 \\ 0 & \frac{\sigma_{FDOA}^2}{f_T^2 V^2 / c^2} \end{bmatrix} \quad \text{B-24}$$

Examination of these equations allows one to identify an appropriate value for each scaling constant so as to make the terms of order unity, as much as is possible. The length scale L should be the scale of the TDOA data, which is of order the typical observer-observer separation distance. The other length scale, l , is of order R , the observer-target separation. If these length scales are equal the TDOA problem is well conditioned and the partials matrix has all terms of order unity. If they are not, the TDOA problem is difficult to solve (the geometry is poor), but this is a problem which scaling is not going to address anyway. In any case it is probably simplest and best just to choose $L = l =$ an average or other compromise of the two length scales [Ref. 19]

In the FDOA portion, V apparently needs to be equal to two velocity scales, both the scale of the FDOA data (right hand side of the equation), which has the scale of the typical observer-observer relative velocity along the target line-of-sight, and also the scale of the typical observer-target relative velocity perpendicular to the line-of-sight (left hand side). Again, if these scales are equal the problem is well conditioned, and if they are not, there is nothing to do about it. The second velocity scale is arbitrary, since it appears only once, in the partials matrix; it is probably best used to cancel the scaling of the direction cosines, i.e. $v = V$. With this scaling in place, clearly every equation is dimensionless, and every term has a magnitude of the order of unity (or at least close). Of particular importance is the partials matrix, which is nicely "equilibrated". This should have a direct effect on the numerical stability and accuracy of the estimation process.[Ref. 19]

APPENDIX C. RELATIVE PRECISION

Relative precision provides a precise estimate of the mean when the sample size of the data is unknown. Relative precision requires that we continue to sample our simulation results until we are certain, at some level of confidence, α , that the current estimate has a given relative error, γ . Another way of saying this would be that we are $(1 - \alpha)\%$ confident that the percentage error in our estimate, the empirical mean, is 100γ percent. From Reference 23, this probabilistic relationship is defined as:

$$P\left(\frac{|\bar{X} - \mu|}{\mu} \leq \gamma\right) = (1 - \alpha) \quad \text{C-1}$$

In order to satisfy this relationship, JBSTAFSim samples the miss distance until there have been at least 30 observations and the confidence interval half-width of the estimate divided by the empirical mean is less than or equal the percentage error in our estimate. Rather, calling the empirical variance S^2 and Z_k the $100k$ th quantile for a standard Normal random variable, this terminating condition is defined as:

$$\left(\frac{Z_{1-\alpha/2} \cdot \sqrt{\frac{S^2}{n}}}{\bar{X}} \right) \leq \frac{\gamma}{1 + \gamma} \quad \text{C-2}$$

Thus, the left hand side of C-2 represents an estimate of the actual relative error. Once γ is set, the simulation continues until this estimate satisfies the above inequality which means the point estimate \bar{X} has a relative error of at most $\gamma/(1 - \gamma)$ with probability of approximately $(1 - \alpha)$. The derivation of C-1 and C-2 can be found in Reference 23.

Finally, it should be noted that our estimate, \bar{X} , is actually distributed with a Student- t distribution with n degrees of freedom; however since n will be very large (greater than 1000), the quantile from the standard Normal distribution is more than adequate to calculate the estimate confidence interval half-width.

LIST OF REFERENCES

1. Streight, David A., "Application of Cyclostationary Signal Selectivity to the Carry-On Multi-Platform GPS Assisted Time Difference of Arrival System, Master's Thesis, Naval Postgraduate School, Monterey, California, March 1997.
2. Feuerstein, D., Julianelli, L., and Caldwell, O., "TDOA Sensor Study", Applied Research Laboratories: The University of Texas at Austin, Space and Geophysics Group, Geomatics systems Division, 6 December 1996.
3. Waltz, E., and Llinas, J., *Multisensor Data Fusion*, Artech House Publishers, Inc., Norwood, MA, 1990.
4. Azaira, M., and Hertz, D., "Time Delay Estimation by Generalized Cross Correlation Methods", *IEEE Transactions on Acoustics, Speech and Signal Processing*, Vol. ASSP-32, No. 2, April 1984.
5. Stein, Seymour, "Algorithms for Ambiguity Function Processing", *IEEE Transactions on Acoustics, Speech and Signal Processing*, Vol. ASSP-29, No. 3, June 1981.
6. Knapp, C., and Carter, G.C., "The Generalized Correlation Method for Estimation of Time Delay", *IEEE Transactions of Acoustics, Speech, and Signal Processing*, Vol. ASSP-24, No. 4, August 1976.
7. Rusu, P., and Julianelli, L., "Covariance of Time-Difference-Of-Arrival Residuals Among Pairs of Observers for RF Emitter Location Systems", *Proceedings of the 1997 AOC Western Region IW Technical Symposium*, pp. 331-337, 1997.
8. Rusu, P., and Julianelli, L., "A Stochastic Model for Time Difference of Arrival Error Estimation", Applied Research Laboratories Interoffice Memorandum, Appendix A, Austin, TX, November 1995.
9. Bancroft, Stephen, "An Algebraic Solution of the GPS Equations", *IEEE Transactions on Aerospace and Electronic Systems*, Vol. AES-21, No. 7, January 1985.
10. Rusu Petre, "TOA-FOA Approach to find the Status of RF Transmitters", Unpublished work, Applied Research Laboratory: The University of Texas at Austin, Austin, TX, 1995.
11. Rusu, Petre, "The Equivalence of TOA and TDOA RF Transmitter Location", Unpublished work, Applied Research Laboratory: The University of Texas at Austin, Austin, TX, 1997.

12. Schau, H.C., and Robinson, A.Z., "Passive Source Location Employing Spherical Surfaces from Time-of-Arrival Differences", *IEEE Transactions on Acoustics, Speech and Signal Processing*, Vol. ASSP-35, No. 8, August 1987.
13. Chaffee, J., and Abel, J., "On the Exact Solutions of Pseudorange Equations", *IEEE Transactions on Aerospace and Electronic Systems*, Vol. 30, no. 4, October 1994.
14. Tolman, Brian, "Review and Clarification of three TDOA Solution Algorithms", Applied Research Laboratories Interoffice Memorandum, Austin, TX, 1996.
15. Rusu, Petre, "On the Dilution of Precision Factors in TDOA Computations", Applied Research Laboratories Interoffice Memorandum, Austin, TX, 1995.
16. Bierman, Gerald J., *Factorization Methods for Discrete Sequential Estimation*, Mathematics in Science and Engineering, Volume 128, Academic Press, New York, 1977.
17. Lawson, C.L. and Hanson, R.J., *Solving Least Squares Problems*, Prentice-Hall, New Jersey, 1974
18. Wilkinson, J., "Error Analysis of Transformations base on the Use of Matrices of the Form $I-2ww^T$ ", *Errors in Digital Computation*, Vol.II, pp.77-101, Wiley New York, 1965.
19. Tolman, Brian, "Scaling of Least Squares Problems, Specifically F/TDOA", Applied Research Laboratories Interoffice Memorandum, Austin, TX, 1997.
20. Leach, M., and Feuerstein, D., "Preliminary Test Results from a Carry-On Multi-Platform GPS-Assisted Time Difference of Arrival System", *Proceedings of the Symposium on Radiolocation and Direction Finding*, San Antonio, TX, June 1995.
21. Press, W., Teukolsky, S., Vetterling, W., Flannery, B., *Numerical Recipes in C*, Second Edition, Cambridge University Press, NY, 1992.
22. Cornell, G. and Horstmann, C., *Core Java*, Sunsoft Press-Prentice Hall, Mountain View CA, 1996.
23. Law, A. M. and Kelton W. D., *Simulation Modeling and Analysis*, McGraw-Hill, NY, 1991.
24. Furgason, Shawn, Applied Research Laboratories, Electronic Mail Correspondence, 4 August 1997.

INITIAL DISTRIBUTION LIST

1. Defense Technical Information Center.....2
8725 John J. Kingman Rd., STE 0944
Ft. Belvoir, Virginia 22060-6218
2. Dudley Knox Library.....2
Naval Postgraduate School
411 Dyer Rd.
Monterey, California 93943-5101
3. Chairman, Code OR.....1
Department of Operations Research
Naval Postgraduate School
Monterey, California 93942-5101
4. Prof. Arnold H. Buss, Code OR/Bu.....1
Department of Operations Research
Naval Postgraduate School
Monterey, California 93942-5101
5. Prof. Gus K. Lott, Code EC/Lt.....1
Department of Electrical and Computer Engineering
Naval Postgraduate School
Monterey, California 93942-5101
6. Prof. Carl R. Jones, Code SM/Js.....1
Department of Systems Administration
Naval Postgraduate School
Monterey, California 93942-5101
7. Applied Research Laboratories.....3
The University of Texas at Austin
Attn: Dr. Mark Leach
P. O. Box 8029
Austin, Texas 78713-8029
8. Commanding Officer.....2
Attn: Code 40
Naval Information Warfare Activity
9800 Savage Rd.
Ft. Meade, Maryland 20755-6000